Molecular expression associated with vibrissa follicle development and differentiation

Hammond, Nigel L.

Abstract

The hair follicle is a complex mini-organ formed as a result of epithelial-mesenchymal interactions, provided by three different stem cell sources: epithelial, neural crest and mesenchymal. Hair follicle morphogenesis is directed by a distinct set of molecular signals which are unique to each stage of development. These interactions continue into the adult cycle, represented by periods of rapid growth (anagen), apoptosis driven regression (catagen), a period of relative quiescence (telogen) and shedding of the club hair (exogen). Many of the molecules involved have been elucidated such as Wnts, Bmps, Fgfs, TGF-βs and Shh amongst others. However, the nature of their regulation and effect on gene expression is still unclear.

Id proteins are emerging as powerful players in the transcriptional control of many fundamental biological processes, such as the cell cycle, proliferation and differentiation, apoptosis and lineage commitment. As a result, the expression patterns of Id2 and Id3 were investigated by immunocytochemistry in developing and adult vibrissae. Wistar rats aged E14 to P4 were used to cover all stages of vibrissae development (stages 0-6+) and 3 - 6 month old rats for the adult stages. This thesis reports that high Id2 expression was seen in specialised neuroendocrine cells (Merkel cells) of the hair follicle and basal epidermis, confirmed by co-expression of the Merkel cell marker, cytokeratin-20. This post-mitotic Id2 expression continued through postnatal ages and into the adult follicle.

Staining with Id3 was characterised by cytoplasmic, basally polarised expression in the epithelia of stage 1-4 follicles. After this stage, expression switched to being nuclear with high levels in many different cell types including the dermal papilla, dermal sheath and outer root sheath. Id2 and Id3 expression was also investigated in retinoic acid induced differentiation of E13.5 and E14 mystacial pads, studying the glandular morphogenesis of vibrissae and the effect on Id protein expression. Id2 and Id3 immunoreactivity was cytoplasmic and polarised but no evidence of nuclear staining was seen.

Id2 and Id3 expression in developing vibrissae is reported here for the first time, describing the profiles of these proteins during hair follicle development and differentiation. These findings highlight an important cytoplasmic role for Id proteins in development and may have implications for reciprocal epithelial-mesenchymal interactions, pattern formation and stem cells in the hair follicle.

Acknowledgements

I would like to thank my supervisor, Dr. Colin Jahoda, for his constant support, encouragement and inspiration during the past 18 months.

Many thanks to all members of Lab 8, in particular those of the Animal Cell Biology Group. Thanks to Dr. Jenna Whitehouse for her technical assistance, Dr. Gavin Richardson, Dr. Amanda Lee, Beth Arnott, Heather Crawford and Claire Higgins for their assistance throughout the course and making my time in the lab so enjoyable.

Finally, a special thanks to my family for their support throughout my time at Durham.

MOLECULAR EXPRESSION ASSOCIATED WITH VIBRISSA FOLLICLE DEVELOPMENT AND DIFFERENTIATION

NIGEL L HAMMOND

MSc THESIS

ANIMAL CELL BIOLOGY RESEARCH GROUP
DEPARTMENT OF BIOLOGICAL & BIOMEDICAL SCIENCES
UNIVERSITY OF DURHAM
DURHAM

2006

List of Figures

List of Tables

Declaration

I confirm that no part of the material offered has previously been submitted by me for a degree in this or any other University. Material generated through joint work has been acknowledged and the appropriate publications cited. In all other cases material for the work of others has been acknowledged and quotations and paraphrases suitably indicated.

Copyright

Publications

Hammond N.L., Jahoda C.A.B. Expression of Id proteins during hair follicle development. (*in preparation*).

Abbreviations

ABC	ATP-binding cassette
BCRP	breast cancer resistance protein
bHLH	basic helix-loop-helix
BMP	bone morphogenetic protein
BrdU	bromodeoxyuridine
CC	collagen capsule
cDNA	complimentary deoxyribonucleic acid
CF	club fibre
CSR	class switch recombination
CTS	connective tissue sheath
DEPC	diethylpyrocarbonate
DNA	deoxyribonucleic acid
dNTP	deoxynucleoside triphosphate
DP	dermal papilla
DS	dermal sheath
DTT	dithiothreitol
DVN	deep vibrissal nerve
EA	early-anagen
EB	end bulb
EMT	epithelial-mesenchymal transition
ES	embryonic stem cell
FITC	fluorescein isothiocyanate
FGF	fibroblast growth factor
F-SC	follicle sinus-complex
FSG	fish skin gelatin
GF	growing fibre
H&E	hematoxylin and eosin
HGF	hepatocyte growth factor
HLH	helix-loop-helix
HSC	Hematopoietic stem cell
^{3}H-T	tritiated thymidine
Id	inhibitor of DNA-binding/differentiation
IRS	inner root sheath
LA	late anagen
MA	mid-anagen

MC	merkel cell
MCC	merkel cell carcinoma
MDR	multidrug resistance protein
MEM	minimal essential medium
mRNA	messenger ribonucleic acid
MRP	multidrug resistance-associated protein
NES	nuclear export signal
NK	natural killer cell
NLS	nuclear localisation signal
OD	optical density
OLP	oligodendrocyte precursor
ORS	outer root sheath
PBS	phosphate buffered saline
PDGF	platelet-derived growth factor
PTC	patched
RA	retinoic acid
Rb	retinoblastoma
RNA	ribonucleic acid
RT	reverse transcription
RT-PCR	reverse transcriptase-polymerase chain reaction
SG	sebaceous gland
SHH	sonic hedgehog
SP	side-population
SVN	superficial vibrissal nerve
TA	transit-amplifying
TGF-β	transforming growth factor-beta
TM	trans-membrane
TMD	trans-membrane domain
tRA	all-trans retinoic acid
TRITC	tetramethyl rhodamine isothiocyanate
WNT	wingless and int family

1.0 Introduction

1.1 The Hair Follicle

The hair follicle is a very complex, highly sensitive mini-organ capable of cyclic regression and physiological regeneration (Stenn and Paus, 2001), a feature which is unique to hair follicles and occurs over the lifetime of the mammal. The production of a hair shaft is the most obvious function of the hair follicle and this fibre is involved in many different roles both in humans and other mammals. These range from providing insulation and mechanisms of skin cleansing to sensory roles and as a medium of social communication, the latter being particularly important in humans. This variety is achieved by follicles differing from site to site, producing hair shafts of different sizes, shapes and colours, for example the large specialised sinus follicles (whiskers/vibrissae) and the smaller pelage follicles (body hairs) (Stenn and Paus, 2001).

The formation of hair follicles occurs during embryogenesis and as a result of signals being sent between the dermal cells and overlying epithelial cells. This interaction results in the development of an epidermal downgrowth, forming a peg where further differentiation gives rise to the different epithelial layers of the follicle (Hardy, 1992). The dermal cells form a condensation and interact with the epidermal peg to eventually give rise to the dermal papilla (DP). Signalling between these discreet cell populations continues whilst the follicle is maturing and throughout the postnatal adult cycle. All hairs share the same basic structure but some have different structure

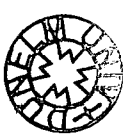

not present in all hair types, such as the arrector pili muscle in human follicles and the mesenchymal capsule in vibrissae.

Hair follicle morphogenesis generally occurs once in the lifetime of an individual but the follicle cycles and regenerates throughout its adult life (Stenn and Paus, 2001). This growth cycle consists of periods of growth (anagen), regression (catagen), rest (telogen) (Dry, 1926) and shedding (exogen). During the cycle the inferior follicle undergoes dramatic reformation whilst the upper, permanent follicle is subject to substantial remodelling (Lindner *et al*, 2000). The permanent portion of the human follicle includes the sebaceous gland and the region of the follicle above the muscle insertion, including the so-called bulge region (Stenn and Paus, 2001).

1.2 Anatomy of the Hair Follicle

Although hair follicles differ from site to site and some have specialised functions, the general structure is common to all. The hair follicle can be split into four regions, the bulb (the lower segment containing the dermal papilla and matrix cells), suprabulbar area (area above the bulb extending to the site of insertion of the arrector pili muscle), isthmus (from the erector pili muscle to the entrance of the sebaceous gland) and infundibulum (comprising the upper quarter from the sebaceous gland to the follicular orifice) (Sperling, 1991) (Figure 1.1).

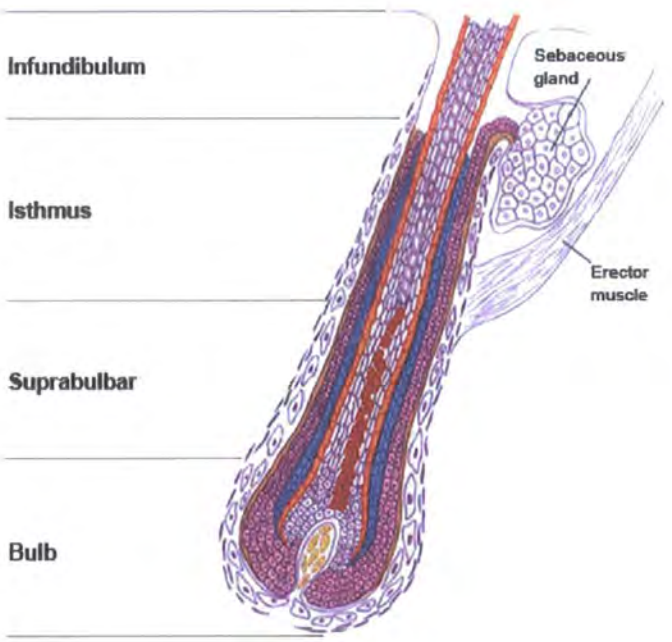

Figure 1.1. Hair follicle anatomy

The hair follicle (human) is divided into four regions named the bulb, suprabulbar, isthmus and infundibulum regions. The diagram shows the follicle in its growing phase (modified from Whiting & Howsden, 1998).

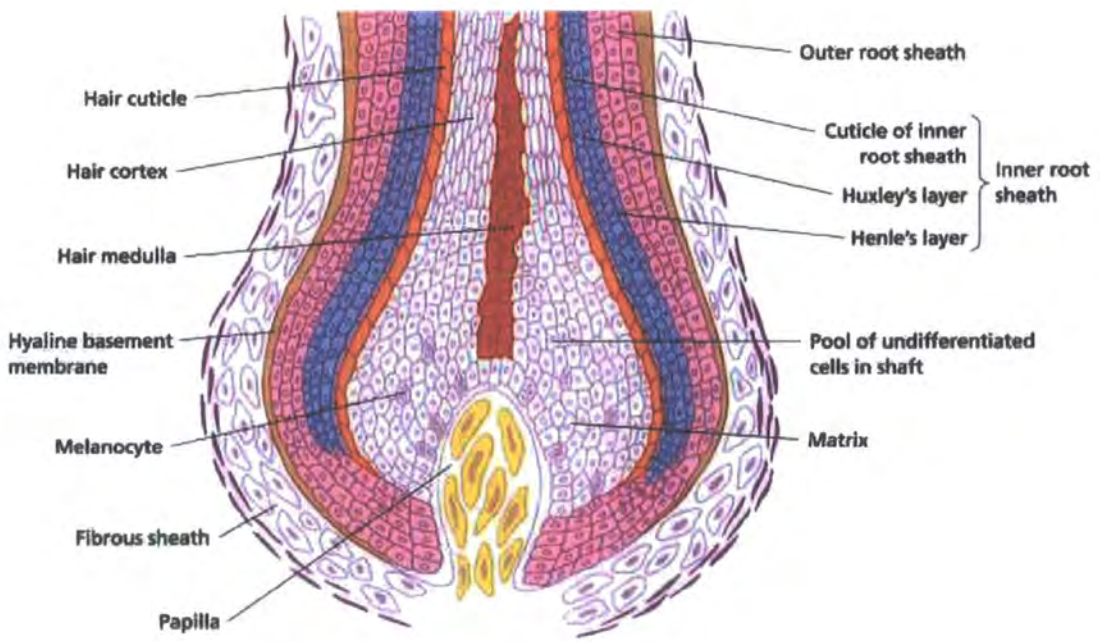

Figure 1.2. The hair bulb

The structure of the hair bulb showing the diversity of cell lineages (modified from Whiting & Howsden, 1998).

During hair follicle morphogenesis, the epidermal peg differentiates into three enclosed epithelial cylinders. The central cylinder forms the hair shaft, the outer cylinder the outer root sheath (ORS) and the middle cylinder the inner root sheath (IRS). The dermal papilla (DP), derived from mesenchymal cells sits at the base of the follicle protruding into the hair bulb, and is held close to the base of the epidermal derived cells by the dermal sheath (DS) which runs the length of the follicle. Surrounding the DP in the hair bulb is the epidermal hair matrix. This region consists of actively proliferating and differentiating epithelial cells, which under the influence of the DP give rise to six different types of cells that make up the layers of the hair shaft and IRS. In pigmented hair, it is in the matrix cells that active melanocytes are primarily located. These cells produce pigment molecules, melanin, which is incorporated into the growing hair shaft in the form of melanosomes.

Separating the epithelial derived cells (ORS) from the mesenchymal cells (DP) is a thin layer called the basement membrane. Above the bulb this layer thickens and is known as the glassy membrane (Figure 1.2). Acting as a barrier between the two cell lineages it plays an important role in immunological protection (Stenn and Paus, 2001).

1.2.1 Dermal Papilla

The DP is formed from the recruitment and condensation of mesenchymal cells early in hair follicle morphogenesis and plays a crucial role in inducing follicle development from the epidermis and production of the hair fibre.

Early studies by Oliver *et al* revealed that removal of the DP stops hair growth. However, follicle regrowth was possible due to the lower third of the DS supplying new cells for regeneration of a new DP at the site of the original (Oliver, 1966a, 1966b, 1966c; Jahoda, 1992). However, when more than the lower third of DS was removed, regeneration of the DP did not occur. Both the DS and DP cells develop from the mesenchymal condensation in embryonic skin. This common origin is believed to account for the similarities in characteristics between the two populations.

Many studies have shown that a hair follicle must have extensive epithelial-epithelial and epithelial-mesenchymal interactions in order for it to grow and form properly. The hair follicle is unique in that this epithelial-mesenchymal crosstalk persists from embryonic development into the adult cycle (Fuchs *et al,* 2001). The powerful ability of the DP to induce follicular growth was demonstrated when a whisker follicle DP was transplanted into the upper dermis of a rat ear, resulting in not only growth of a follicle in this region but also showing characteristics from where the DP originated, eg a whisker (Jahoda, 1992). This inductive capacity is even retained in low passage DP cells *in vitro* where the cells show aggregative properties, a feature essential for formation of the DP. When implanted *in vivo* the cells retained this behaviour and induced follicle formation (Jahoda *et al,* 1984, Jahoda and Oliver, 1984).

More recently these inductive properties have been demonstrated in humans. When a scalp DP was transplanted from an adult male to the forearm of an adult female, a follicle was induced producing a scalp hair shaft (Reynolds *et al,* 1999). Central to

all these studies it is apparent that the characteristics of a follicle reflect the properties of its papilla (Van Scott *et al*, 1963). Various studies have revealed clues to the molecular pathways active in the DP and how these change over development and cycling. These molecules include WNTs, Fibroblast growth factors (FGFs), Bone morphogenetic proteins (BMPs), SHH (Sonic hedgehog), Hepatocyte growth factor (HGF) and Platelet-derived growth factor (PDGF) amongst others (Stenn and Paus, 2001).

1.2.2 Hair Matrix and Fibre

The hair fibre or shaft is composed of three layers all of which differentiate from the highly proliferative hair matrix cells surrounding the DP. This region in the bulb where keratinocytes proliferate rapidly is called the critical region or hair matrix zone (Auber, 1950, Orwin, 1979). The outer layer is the cuticle and is composed of matrix cells outside the centre of the hair follicle. Just above the bulb, these cells are not fully keratinised and arrange themselves in an overlapping tiled orientation but in the middle follicle they are fully keratinised. Cells in the centre of the matrix differentiate to become the cortex, the middle layer of the hair shaft. This layer forms the majority of the hair. As these cells move upwards, they differentiate into cortical cells changing in appearance from round into flattened cells. These cells are then squeezed together to form the lamellae of the cortex and gradually become keratinised and harden. The innermost layer is the medulla, forming a tube at the centre of the hair fibre and consists of a central strand of cells that are loosely organised. The medulla is not present in every type of hair but where present it is more prominent in rodents (Chase, 1954).

In pigmented hair, melanocytes produce the pigment molecule melanin which is incorporated into the cortex of the developing hair fibre in the bulb region. These dendritic cells are essential for pigmentation and are neural-crest derived (Rawles, 1947). The body of the melanocytes lies on the basement membrane at the apex of the DP, surrounding it whilst their dendrites extend to the precortical keratinocytes, defining the hair melanin unit. Melanin granules are found mostly within the cortex and medulla cells in the hair follicle with few found outside these compartments (Chase, 1954).

1.2.3 Inner Root Sheath

The IRS consists of three layers, all formed from the matrix cells of the hair bulb in the critical region. Adjacent to the hair fibre cuticle is the IRS cuticle which is a single cell thick. Next is the Huxley layer, consisting of up to four cells thick in human follicles, and outermost the Henle layer running adjacent to the ORS (Chase, 1954, Sengel, 1976) (Figure 1.2). The cells destined to become IRS gradually become differentiated and keratinised as they are pushed further away from the bulb region. The differentiation process has been suggested to begin earlier in the IRS progenitor cells as these cells have begun to keratinise by forming trichohyalin granules in the upper bulb region, whereas the hair shaft progenitor cells are still dividing at the same level (Hashimoto and Shibazaki, 1976). Pinkus also observed formation of the IRS first then the cortex (Pinkus, 1978). This is consistent with Chase's observations decades earlier, remarking on how the IRS keratinises forming a hollow cone of cells above the matrix bulb, with the hair shaft being formed and moulded inside later (Chase, 1954).

The pattern of keratinisation in the IRS cuticle is such that it compliments that of the hair shaft cuticle. The scales of the IRS are flared downwards and those of the hair shaft are flared upwards, resulting in interlocking of the two cuticles. The IRS grows at the same rate as the hair shaft moving upwards together, but the IRS is broken down at the level of the sebaceous gland and does not protrude from the follicle like the hair shaft (Chase, 1954). This region is known as the zone of sloughing and is where the IRS debris is mixed with products of the sebaceous gland to form sebum. The sebaceous gland is known to play an important role in the process of breaking down the IRS. When follicles were grown in culture without such a gland or with the gland ablated, both resulting hairs retained their sheath (Williams and Stenn, 1994, Philpott *et al*, 1994).

1.2.4 Outer Root Sheath and Bulge

The ORS is continuous with the epidermis, the only follicular component to do so. This sheath surrounds the IRS extending down to the hair bulb to the base of the dermal papilla, but not enclosing it (Chase, 1954). The ORS is at its thinnest around the bulb but thickens significantly in the isthmus region. In human follicles, it is in the ORS of the isthmus that the bulge resides, below the sebaceous gland where the erector pili muscle is attached. The bulge consists of a cluster of cells which are biochemically distinct expressing several distinct markers including cytokeratin 15 (Lyle *et al*, 1998) and have properties characteristic of epithelial stem cells (Paus and Cotsarelis, 1999).

Hair follicle stem cells are thought to be slow-cycling cells with a superior clonogenicity and proliferative capacity, and are also able to effect this over a long

period of time (Lavker and Sun, 1982, 2000). The current understanding of stem cells are they divide rarely, giving rise to a stem cell and a transient amplifying (TA) cell. The TA cells have a limited proliferative potential and once this has been exhausted, the highly proliferative TA cells undergo terminal differentiation (Ma *et al* 2004). This TA population is thought to be responsible for increasing the number of differentiated cells produced by each stem cell division (Watt and Hogan, 2000).

The lack of specific stem cell markers has made locating these stem cells very difficult. Taking advantage of the cells slow-cycling nature, studies were done investigating the label retention of tritiated thymidine (^{3}H-T) and bromodeoxyuridine (BrdU) (Morris and Potten, 1999, Taylor *et al*, 2000), realising that only cells that rarely divide and persist for a long time will retain these labels . Early work by Cotsarelis and colleagues found label-retaining cells (LRCs) exclusively in the bulge of the mouse hair follicle (Cotsarelis *et al*, 1990). Further work by Kobayashi and colleagues on rat vibrissa follicles found that the cells of the bulge had the greatest colony-forming capacity *in vitro* (Kobayashi *et al*, 1993) and paved the way for further research into these poorly understood cells.

Tumbar and colleagues developed a strategy to fluorescently label the slow cycling cells of the bulge by engineering mice to express a fluorescent histone protein. This method was used to purify the LRCs based on their label-retaining properties (Tumbar *et al*, 2004). Other strategies included utilising the bulge-preferred promoter activity of the Keratin 15 (K15) gene to fluorescently label bulge cells and fluorescence-activated cell sorting (FACS) to isolate the cells (Morris *et al*, 2004). Both of these research groups demonstrated *in vivo* labelling and multipotency of

hair follicle bulge cells. These strategies allowed transcriptional profiling of LRCs to be undertaken revealing a unique set of expressed genes defining the stem cell niche (Morris *et al, 2004;* Tumbar *et al*, 2004). Furthermore, it has been demonstrated that there are two distinct populations of cells within the bulge (Blanpain *et al*, 2004). These cells are growth inhibited in the bulge but can self renew *in vitro* and make epidermis and hair when grafted, suggesting that the niche microenvironment imposes features of 'stemness' on this cell population (Blanpain *et al*, 2004). It has also been demonstrated that stem cells in the bulge region also form the secondary germ in the cycling hair follicle. Furthermore, these progenitor cells have been shown to dedifferentiate and repopulate the bulge following injury due to hair depilation (Ito *et al*, 2004).

The ORS is also host to a number of other specialised cells; melanocytes which can be activated and repopulate the skin (Staricco, 1963), Langerhans' cells involved in activating the immune system (Gilliam *et al*, 1998) and Merkel cells (Kim and Holbrook, 1995), specialised mechano-receptors whose function in the hair follicle is the subject of much discussion. Just like the IRS, the ORS is also subject to keratinisation but only above the level of the isthmus. In this region trichilemmal keratinisation takes place up until the level of the infundibulum where the ORS changes to normal epidermal keratinisation (Sperling, 1991).

1.3 Hair Follicle Morphogenesis

At the heart of formation of the hair follicle is a complex communication between the ectoderm and underlying mesoderm, which later give rise to the epidermis and dermis respectively. These signals are inherent to the embryonic epithelium and

mesenchyme and do not need intact neural or hormonal signals, as both pelage and vibrissa follicles can form *de novo* from organ cultured fragments of embryonic skin (Hardy, 1969). The following description of hair follicle morphogenesis is based on the pelage follicle but all other mammalian types exhibit the same basic principles of development (Paus *et al*, 1999).

1.3.1 The Stages of Morphogenesis

The process of morphogenesis is divided into nine specific stages after Hardy (1949, 1951, 1992), stages 0 to 8 showing the key developmental changes throughout the process (Figure 1.3). The first stage of development (stage 0) was originally described as the pregerm stage (Pinkus, 1958) and refers to the morphologically homogenous epidermis. During stage 1, the pregerm develops into an epidermal thickening in the basal epidermis, recognised as the epidermal placode (Hardy and Vielkind, 1996), in response to the initial signal arising in the dermis known as the first dermal message (Hardy, 1992). These cells display a vertically polarised orientation in contrast to the adjacent epidermal keratinocytes. Below this thickening the dermal fibroblasts increase in number and change their orientation (Paus, 1999), thought to be in response to an epithelial signal arising from the placode (Hardy, 1992).

Stage 2 is characterised by the hair germ developing into a broad column of epidermal keratinocytes (Pinkus, 1958) with a convex proximal end covered by a mesenchymal 'cap', the whole structure is described as the hair plug (Hardy, 1949). This downgrowth is a result of massive epithelial cell proliferation (Pinkus, 1958). The hair plug also starts to show an anterior-posterior orientation during stage 2

(Paus *et al* 1999). By stage 3 the hair peg has started to surround the dermal fibroblasts, which have now condensed into a ball to form the DP. This is where the second dermal message is reported to be transmitted to the adjacent epidermal cells of the hair plug instructing them to make a hair follicle (Hardy, 1992).

During stage 4 of morphogenesis, the elongated hair peg develops a bulb-like thickening of its proximal portion and elongation of the DP cavity resulting in most of the DP being enclosed by the hair peg (Paus *et al*, 1999). Also differentiation of Henle's layer begins to form the IRS-cone, described earlier as the hair cone stage by Hardy (Hardy, 1949). At stage 5 or the bulbus peg stage (Pinkus 1958), the IRS-cone has developed halfway up the follicle, the bulge region is visible and the first sebocytes are evident at the neck of the hair peg (Paus *et al*, 1999). By stage 6, the hair follicle has reached the subcutis level of the skin. The hair canal has started to develop and the IRS has differentiated into its three layers complete with growing hair shaft up to the level of the hair canal. Also the sebocytes, first seen at stage 5, begin to form the sebaceous gland (Paus *et al*, 1999). Hardy previously characterised this as the hair formation stage (Hardy, 1949).

Stage 7 is characterised by the hair shaft entering the hair canal at the level of the fully developed sebaceous gland and the DP narrowing, now almost completely enclosed by the bulb. At the final stage, the hair follicle reaches its final length at the subcutaneous muscle layer with a hair shaft now visible through the epidermis (Paus *et al*, 1999). The hair follicle in this stage now resembles a mature anagen morphologically (Parakkal, 1969)

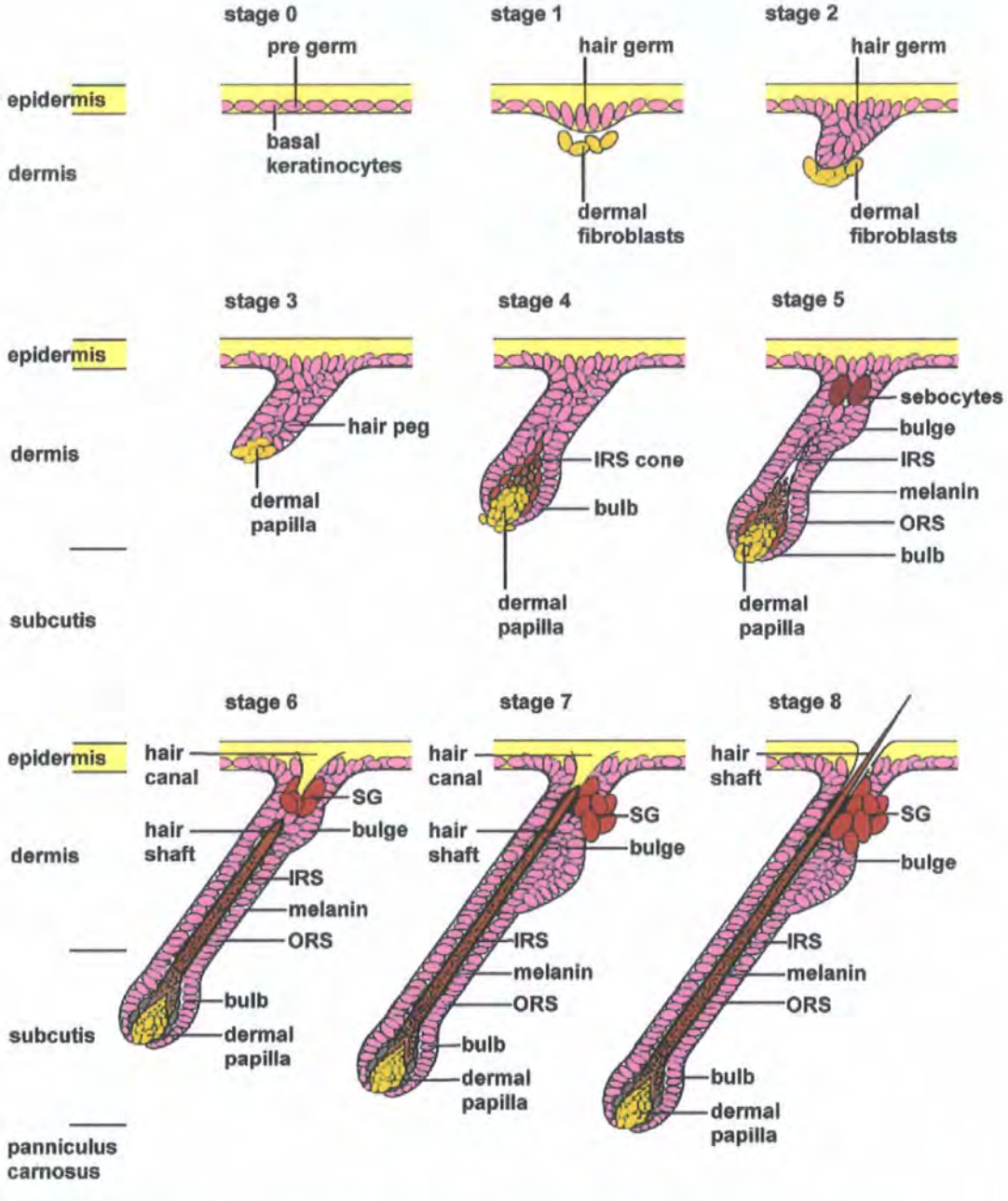

Figure 1.3. Hair follicle morphogenesis classification.

Stage 0: Uniform epidermis with no visible hair follicles. **Stage 1**: Visible hair germ morphogenesis with the development of an epidermal thickening and aggregation of mesenchymal cells in the dermis below. **Stage 2**: Elongation of the hair germ with a convex proximal end and adjacent dermal fibroblast condensate. **Stage 3**: Hair peg with formation of the keratinocytes into a column around the follicular axis and a concave proximal end with a closely associated DP cell condensate. **Stage 4**: First development of the bulb region and visible IRS cone, enclosure of the DP cells. **Stage 5**: Elongation of the bulbous hair peg and IRS, first recognition of the bulge region, sebocytes, and melanin granules. **Stage 6**: Hair fibre shaft with melanin granules visible within the IRS, DP cells almost completely surrounded by keratinocytes. **Stage 7**: Hair fibre shaft leaves the IRS and enters the hair canal. **Stage 8**: Mature first anagen stage. Hair fibre emerges from the epidermis (modified after McElwee and Hoffmann, 2000).

1.3.2 Nature of the Signals

The epithelial-mesenchymal interactions of the hair follicle have been fascinating developmental biologists for over 50 years when the first recombination experiments were performed. It was found that the process of development of the hair follicle was very similar to that of feathers and scales in the embryonic skin of birds and lizards, even in culture (Sengel, 1975). When dermis from the back of a mouse (capable of interacting with epidermis to form pelage follicles in that region) was separated and recombined with mouse epidermis from a hair-free region, hair follicle formation would result (Hardy, 1992). Indeed further experiments by Dhouailly (1973, 1975, 1978) on recombinations using mouse, chick and lizard skin tissues gave consistent results, indicating the formation of appendage is epidermis dependant whereas the initiation and patterning of the appendage is dermis dependant (Olivera-Martinez *et al,* 2004). A classic example of this was when mouse upper lip dermis (vibrissa-forming) was recombined with lizard embryo dorsal epidermis, with the result of formation of large scale buds arranged in a whisker pattern (Dhouailly, 1975). These experiments revealed the existence of developmental signals which are only now beginning to be elucidated at the molecular level. The developmental pathways at the heart of hair follicle formation include WNTs, BMPs, SHH, TGFß and others (Figure 1.4).

Early experiments with tissue recombinations between reptiles, birds and mammals (Sengel, 1971, 1976; Dhouailly, 1973) revealed that skin appendages are initiated by a series of three tissue interactions. These interactions relate to specific stages in morphogenesis and were found that this sequence of events could be interrupted by addition of above physiological levels of retinol or retinyl acetate (Hardy *et al*,

1990). Further experiments revealed pelage follicles treated with excess retinoids regressed at the point where they should be receiving the second dermal message (stage 3c). Likewise vibrissae were also arrested around stage 3c, but many developed lateral buds that grew into branching, mucous-secreting glands leading to speculation the epithelium was responding to a new and different second dermal signal from the general dermis (Hardy, 1968; Bellows and Hardy, 1977). Active metabolites in vitamin A were found to be all-*trans* retinoic acid (tRA) and 9-*cis* retinoic acid (9cRA) with two receptor families subsequently identified, RAR and RXR, each with three isotypes α, β and γ. Together members of these families form RAR/RXR heterodimers to the polymorphic *cis*-acting response elements of RA target genes (RAREs) (Chambon, 1996). Most RAREs that have been identified consist of a direct repetition (DR) of two core hexameric motifs separated by a spacer of several nucleotides, -($^{A}/_{G}$)G($^{G}/_{T}$)TCA- n -($^{A}/_{G}$)G($^{G}/_{T}$)TCA- , however there are many subtle variations of these motifs (Balmer and Blomhoff, 2005). Owing to the diversity of RAREs and the complexity of direct or indirect targets of RA, there is still much to be learned from these powerful morphogens.

An initial signal arising in the dermis, known as the first dermal message, was found to initiate placode formation in the overlying epidermis. Mouse dermis was capable of initiating feather buds from chick foot epidermis and scale placodes from lizard epidermis, indicating the dermis was instructing the epidermis to make an appendage appropriate to its class of origin (Hardy, 1992). On formation of the placode, an epithelial signal from the placode is thought to instruct the mesenchymal cells below to from the dermal condensation (Millar, 2002), which eventually will become the DP. There is then a second dermal message from this condensation to the adjacent

proliferating hair peg stimulating these cells to further proliferate and grow downwards eventually interacting with the DP and differentiating into the hair follicle structures (Hardy, 1992).

The first dermal signal, known to arise from the dermis and act on undifferentiated epithelium, has currently not been elucidated and its mode of action is still poorly understood (Millar, 2002). So far the most credible theory is that the dermal signal occurs uniformly rather than a periodic signal, and triggers the activation of follicle promoters and repressors to produce a regular pattern of follicles (Slack 1991; Barsh 1999). Studies into β-catenin expression by Noramly and colleagues have highlighted this molecule as playing a significant role, not just in the first dermal signal but also in the formation of placodes. Transient nuclear β-catenin (active) was found uniformly within the dermis and 1 day later appeared in the overlying epithelium in the chick, suggesting activation of the WNT signalling pathway. Also nuclear β-catenin becomes elevated in regions destined to become placodes, as does the expression of specific WNTs (Noramly *et al*, 1999). Placode formation has been shown to be a competition between promoters and repressors. Activation of ectodysplasin (EDA) and its receptor (EDAR) signalling in the epithelium followed by WNT and FGF signalling strive to promote placode formation, whereas subsequent activation of the bone morphogenetic protein (BMP) signalling pathway represses placode formation in adjacent skin (Millar, 2002).

The first epithelial signal, which induces formation of the dermal condensation, has been reported as most likely to be as a result of WNT signalling, as the dermal condensation fails to develop in the absence of epithelial β-catenin (Huelsken *et al*,

2001). Work by Chuong and colleagues on feather placode formation greatly increased knowledge of the key morphogenetic molecules involved in placode formation (Chuong *et al*, 1996). Further evidence was provided when DasGupta and Fuchs generated transgenic mice with a TOPGAL reporter gene which indicated which cells had active WNT signalling. The results showed expression in both the dermal condensation and follicular epithelium (DasGupta and Fuchs, 1999). Karlsson *et al* also found that platelet-derived growth factor-A (PDGF-A) was present in the placode, whereas its receptor was present in the dermal condensation, indicating signalling between the two tissues. Gene knockout studies on PDGF-A in mice supported this (Karlsson *et al*, 1999). Another major secreted protein involved in epithelial-mesenchymal signalling is sonic hedgehog (SHH) (Bitgood and McMahon, 1995). Although it is not an element of the first epithelial signal, its signalling from the epithelium is essential in regulating proliferation of the hair peg development of the DP (Karlsson *et al*, 1999). SHH expression is dependent on WNT signalling, and like PDGF-A, its receptor Patched1 (PTC1) and transcription effector GLI1, are both found in the epithelium and dermal condensation indicating SHH signalling is necessary in both tissues (Dahmane *et al*, 1997; Miller, 2002).

The second dermal signal, which regulates the proliferation and downgrowth of the hair peg is also as yet unknown, but has been reported to be likely to be activated by SHH (Millar, 2002). St-Jacques *et al* found that SHH signalling was essential for proliferation of the epidermal downgrowth as morphogenesis was arrested in SHH-null mice at this stage. It also indicated SHH was not required for initiating hair follicle development (St-Jacques *et al*, 1998).

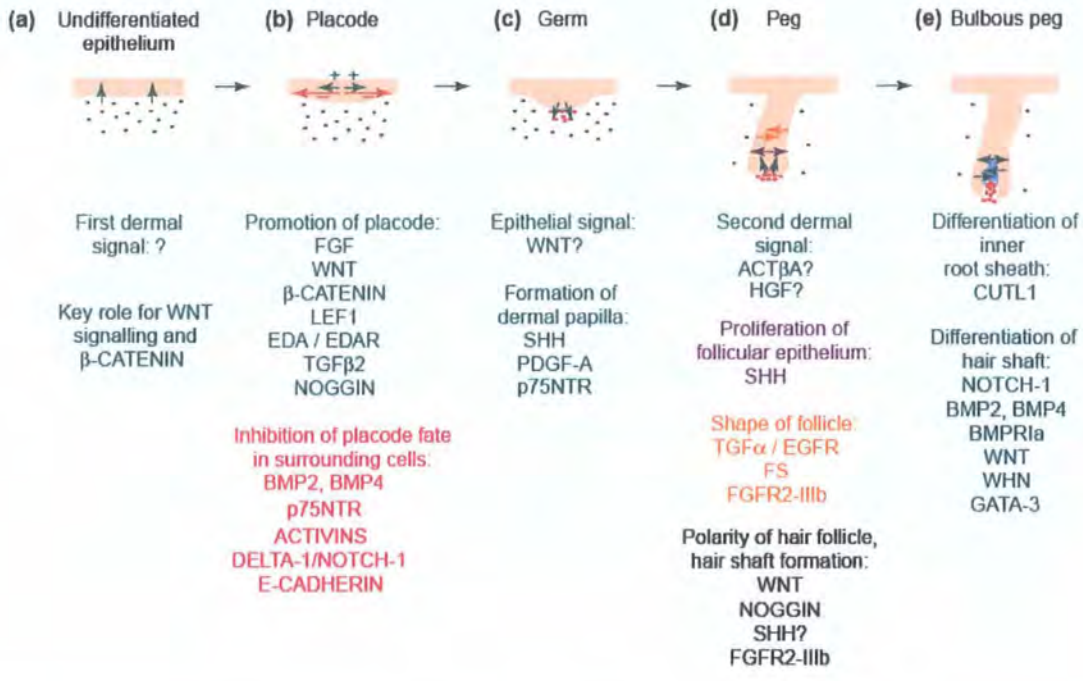

Figure 1.4. Intercellular signals in hair follicle morphogenesis

(a) Formation of hair follicle placodes is initiated by an unknown signal (green arrows) from the dermis (black dots) to the surface epithelium (pink). (b) Hair follicle placode formation is promoted by fibroblast growth factor (FGF); WNT, acting via its effectors β-catenin and lymphocyte enhancer factor 1 (LEF1); ectodysplasin (EDA) and ectodysplasin receptor (EDAR); transforming growth factor β2 (TGFβ2); and Noggin (green arrows with 'plus' signs). Placode formation is inhibited by bone morphogenic proteins (BMPs) (dark pink arrows with 'minus' signs). For simplicity, placode promoting and repressing signals are diagrammed only in the epithelium. In reality, however, noggin and BMP4 are expressed in follicular mesenchyme, and β-catenin, LEF1, TGFβ2 and BMP2 are expressed in both epithelium and mesenchyme. (c) Formation of the dermal condensate, shown as red dots, is induced by an epithelial signal (green arrows), possibly including a WNT. Development of the dermal condensate into a dermal papilla requires the activity of sonic hedgehog (SHH) and platelet derived growth factor-A (PDGF-A). (d) A second dermal signal, possibly including activin βA (ACTβA) or Hepatocyte growth factor (HGF) (green arrows), instructs the follicular epithelium to grow down into the dermis. Proliferation of the follicular epithelial cells is regulated in part by SHH (blue arrows). Transforming growth factor α (TGFα), epidermal growth factor receptor (EGFR), follistatin (FS) and FGFR2-IIIb are required for normal follicle architecture (orange arrows). (e) Differentiation of inner root sheath precursor cells (pale blue) is regulated by unknown signals (green arrows). (modified from Cotsarelis and Miller, 2001; Schmidt-Ullrich and Paus, 2005)

Other molecules have been highlighted as possible candidates, such as activin βA (ActβA) and its regulator, follistatin (FS) which have been found in the dermal condensation and follicular epithelium respectively. Mice lacking this activin displayed defective morphogenesis of vibrissae (Roberts and Barth 1994; Matzuk *et al*, 1995). Hepatocyte growth factor (HGF) and its receptor, Met, have similar expression patterns with HGF present in the dermal condensation and Met in the follicular epithelium. Overexpression studies have revealed a possible role in morphogenesis in signalling between the two tissues (Lindner *et al*, 2000). Recently the discovery of a novel protein, MAEG, was found expressed in the mesenchyme at the basement membrane of developing hair follicles but diminished towards the tip of the hair peg. The adhesion receptor α8β1 integrin was found to be a possible target of MAEG through the common RGD-motif, which was expressed in the placode but later restricted to the tip of the hair peg (Osada *et al*, 2005). MAEG is structurally and functionally similar to nephronectin, which is known to play a crucial role in kidney morphogenesis (Miner, 2001) and has been speculated that MAEG may be important in hair follicle morphogenesis (Osada *et al*, 2005).

1.4 The Adult Hair Cycle

One of the most unique features of the hair follicle is its ability to cycle throughout its adult life. The reasons for cycling are speculated as allowing animals to control the length of body hair from site to site, to expand and grow, to change its body cover in response to environmental stimuli and to protect against improper or malignant follicle formation (Stenn and Paus, 2001). In most rodents, pelage follicles develop as a wave sweeping posteriorly and dorsally in a synchronised manner, ensuring hairs in the same region are in the same phase of growth. A

striking example of this was when Durward and Rudall (1949) rotated a piece of skin 180 degrees showing the wave of follicle growth continued as it would have done in the original position, also indicating the factors responsible are intrinsic to the follicles. In humans and guinea pig follicle growth is asynchronous with each follicle having its own innate rhythm (Chase, 1954). The molecular nature of this rhythm is one of the key questions being asked in hair follicle biology but is as yet elusive. Once understood it could have profound clinical implications (Paus and Foitzik, 2004).

The adult hair follicle undergoes successive cyclical transformations from stages of rapid growth (anagen) to apoptosis driven regression (catagen), a period of relative quiescence (telogen), shedding of the club hair (exogen) and back to anagen (Dry, 1926) (Figure 1.5). The first spontaneous adult cycle has been recognised as beginning with catagen after the development of the first anagen follicle during morphogenesis (Paus and Cotsarelis, 1999). Although these stages of the cycle have been devised it is important to remember that these are dynamic, flowing processes (Chase, 1954).

1.4.1 Anagen

The anagen stage involves the complete regeneration of the lower cycling part of the follicle, known as the region below the bulge. This period of active growth has been divided into six stages, anagen I-VI (Chase *et al*, 1951). In the early stages of anagen (I-II) the secondary germ (a cluster of epithelial cells at the base of the telogen follicle) (Silver and Chase, 1970) undergoes a burst of mitotic activity and subsequently grows down around the papilla, resulting in elongation and thickening

of the keratinocyte strand. During anagen III the follicle reaches its maximum length, extending deep into the subcutis. The hair bulb also has reached its maximum size. The cells of the secondary germ proliferate rapidly due to continued mitotic activity and form the IRS, moulding the developing hair shaft as it extends up to the level of the permanent sebaceous gland and capsule of the club hair (Chase, 1954; Müller-Röver *et al*, 2001). By anagen IV the hair shaft is still being formed but emerges into the hair canal by stage V and subsequently emerges through the epidermis in anagen VI. It is in this final stage which is the substantial growth phase of anagen, spending some 8-9 days growing for mouse and two or more years for humans (Chase, 1954). The length of the growing hair is determined by the proliferative capacity of the matrix cells, whilst the thickness of the hair shaft corresponds to the size of the DP (Auber, 1952).

1.4.2 Catagen

Catagen is a highly controlled stage involving very precise cell differentiation and apoptosis resulting in substantial remodelling of the cycling portion of the follicle and shrinkage towards the bulge region (Stenn and Paus, 2001). The whole process has been divided into eight sub-stages, termed catagen I-VIII (Müller-Röver *et al*, 2001). Catagen I is morphologically identical to anagen VI. During catagen II-IV the DP withdraws its fibroblast projections from the basement membrane (De Weert *et al*, 1982) and the papilla narrows and shrinks to a compact ball shape, due to loss of its extracellular matrix (Stenn and Paus, 2001). Between stages IV-VI the hair follicle begins to regress with formation of the club hair surrounded by the germ capsule (originally the ORS), and thickening of the glassy membrane enclosing the elongating epithelial strand (Müller-Röver *et al*, 2001). By catagen VII the club hair

has a characteristic brush-like appearance and has regressed distally to the level of dermis/subcutis border, whilst the epithelial strand followed by the DP and trailing connective tissue sheath (CTS) follow suit. In the final stage, the epithelial strand undergoes programmed cell death (Weedon *et al*, 1979; Lindner *et al*, 1997) and the DP resides at the border of the dermis/subcutis with the relatively long CTS trailing behind (Müller-Röver *et al*, 2001).

1.4.3 Telogen

In the telogen phase the trailing CTS seen in catagen VIII is absent and the regressing IRS has completely disappeared. The compact ball-shaped DP is now closely attached to the small cap of the secondary hair germ which has a flattened appearance (Müller-Röver *et al*, 2001). This secondary hair germ consists of relatively quiescent cells (Wilson *et al*, 1994) and is separated from the DP by the basement membrane which is relatively thick and multilayered (Jahoda *et al*, 1992). After telogen the hair follicle progresses into anagen I. Morphologically these stages are distinct in with the elongation of the keratinocyte strand in anagen I. Although the phase of telogen is widely seen as a "resting" phase, it is still debated whether this is really the case with some taking the view of Chase (1954) that telogen is an anagen brake, implying the cells must be actively inhibiting anagen although evidence of this has not been found (Stenn and Paus, 2001). Despite this uncertainty no stages of telogen have yet been proposed (Müller-Röver *et al*, 2001).

1.4.4 Exogen

Exogen is a very poorly understood stage given to the process of shedding of the club hair which usually occurs sometime between telogen and anagen (Stenn *et al*, 1998).

It was initially suggested that the new growing hair in the anagen phase mechanically pushes the club hair out (Kligman, 1961) but this alone cannot account for this process as it is known that rodent follicles can contain two or three hairs whilst one is still growing (Chase *et al*, 1953). As the shedding phase is recognised to be separate from telogen and anagen it is thought that the process is also under a different set of controls (Stenn and Paus, 2001).

At the end of telogen, the club hair is held in place by trichilemmal keratinisation of the ORS cells surrounding it. Studies of desmosomes on transgenic mice have indicated that desmoglein 3 null mice have inadequately secured club hairs, indicating a possible role for these molecules. Recently proteolytic pathways have been implicated in the control of exogen with the discovery that stratum corneum chymotryptic enzyme (SCCE) is expressed in the sebaceous gland and keratinised ORS cells (Ekholm and Egelrud, 1998) whilst another protease, plasminogen activator-inhibitor type 2 (PAI-2) has been found expressed in the ORS cells surrounding the pelage club hair (Lavker *et al*, 1998).

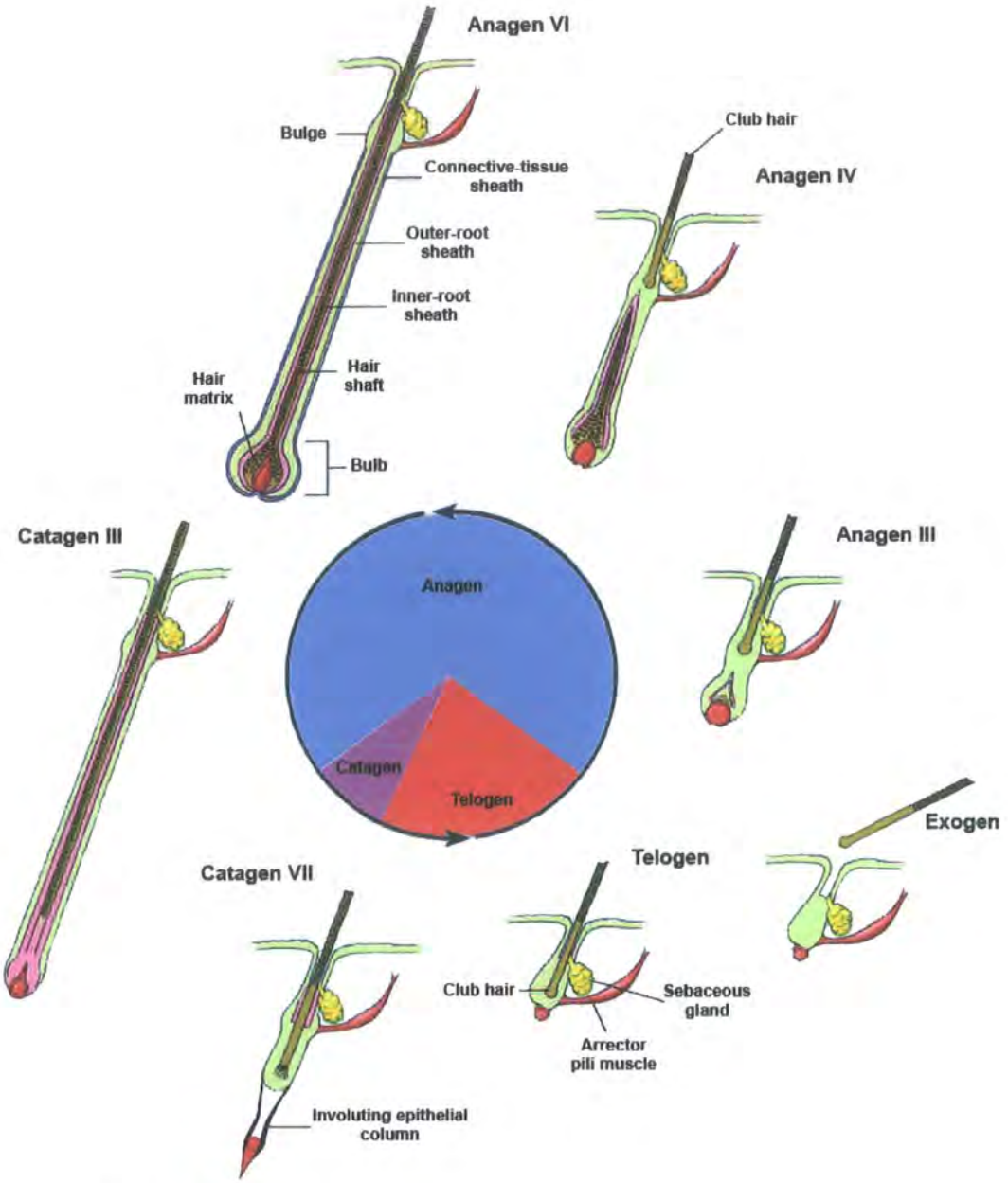

Figure 1.5. The adult hair cycle

The diagram shows the three stages of follicular cycling in a human hair (anagen, catagen, telogen and exogen). The roman numerals indicate morphologic substages of anagen and catagen. The pie chart shows the proportion of time the hair follicle spends in each stage (modified after Paus and Cotsarelis, 1999).

1.5 Vibrissa Follicles

Vibrissa follicles are found in rodents on the mystacial pad and represent the largest of the hair producing organs, reflected in the size of the hair shafts produced. Whereas pelage follicles develop as a wave, vibrissae have a well defined pattern of development. They are arranged in ventro-dorsal and anterior-posterior rows on the mystacial pad (Oliver, 1969) with each follicle labelled accordingly (Figure 1.6). The size of each follicle is also predictable with the largest follicle at A1 down to the small ones at F5. The patterning of vibrissae is mirrored in the opposite mystacial pad, even down to follicle length and stage of cycling making vibrissae an excellent experimental model (Oliver, 1969).

Whilst the cycles of both pelage and vibrissae undergo the same stages proposed by Chase (1965), the vibrissal cycle is both distinctive and different in many ways (Figure 1.7). The anagen phase is very similar to the pelage cycle, producing a growing hair at its maximum rate until there is a decrease in the volume of the matrix and a decline in the proliferation of the matrix cells (Young and Oliver, 1976). During catagen, there is no epidermal shortening and the basic structure of the follicle remains the same. The production of the club hair is distinctive in that it has a very pointed tip and is asymmetrical in relation to the nerve entry (Jahoda and Oliver, 1984). Once the club hair has been released from the DP, the DP shrinks to resemble that of a pelage telogen stage. Unique to vibrissae, the club hair is still maturing during the relatively short telogen and into the next anagen. Whilst the club is still moving distally towards the sebaceous gland the next anagen cycle begins and it is not until anagen V that the club hair has fully matured (Young and Oliver, 1976). This is in contrast to the pelage cycle where telogen marks the end of

formation of the club. The shedding of the club hair in vibrissae is a predictable event where it is released when the growing hair nears its full length. Comparing this to the pelage cycle, exogen is random and is thought to be independent of the hair cycle (Stenn and Paus, 2001).

Anatomically, vibrissae are different from pelage in that they possess an outer collagen capsule containing ring and cavernous sinuses surrounding the central follicular core (Young and Oliver, 1976) (Figure 1.8). These follicles are richly innervated and have a specialised sensory function. Two main nerves innervate the follicle and these are the deep vibrissal nerve (DVN) and superficial vibrissal nerve (SVN). The DVN enters below the mid-follicle and innervates the sinus whilst the SVN supplies innervation to the epidermal rete ridge collar and the inner conical body at the neck of the follicle (Rice *et al*, 1986).

1.6 Innervation of Vibrissa Follicles

Vibrissae are a unique sensory system of mammals that are characterised by a rich and diverse innervation involved in numerous sensory tasks (Maklad *et al*, 2004). The vibrissa follicle, termed follicle-sinus complex (F-SC), has sensory endings distributed to as many as six distinct locales within each F-SC. These are (1) the epidermal rete ridge collar, (2) the inner conical body, (3) the mesenchymal sheath at the level of the ring sinus, (4) the ORS at the level of the ring sinus, (5) the mesenchymal sheath and trabeculae at the level of the cavernous sinus, and (6) the DP of the bulb. The innervation to both sinuses is provided by a large deep vibrissal

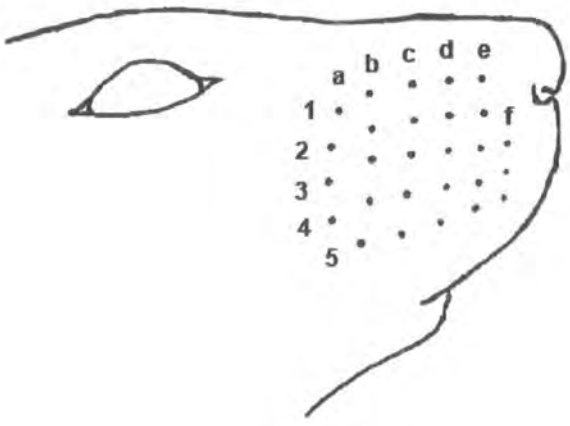

Figure 1.6. Rat vibrissae patterning.
Sketch showing the position and labelling of vibrissae on the rat mystacial pad (from Oliver, 1969)

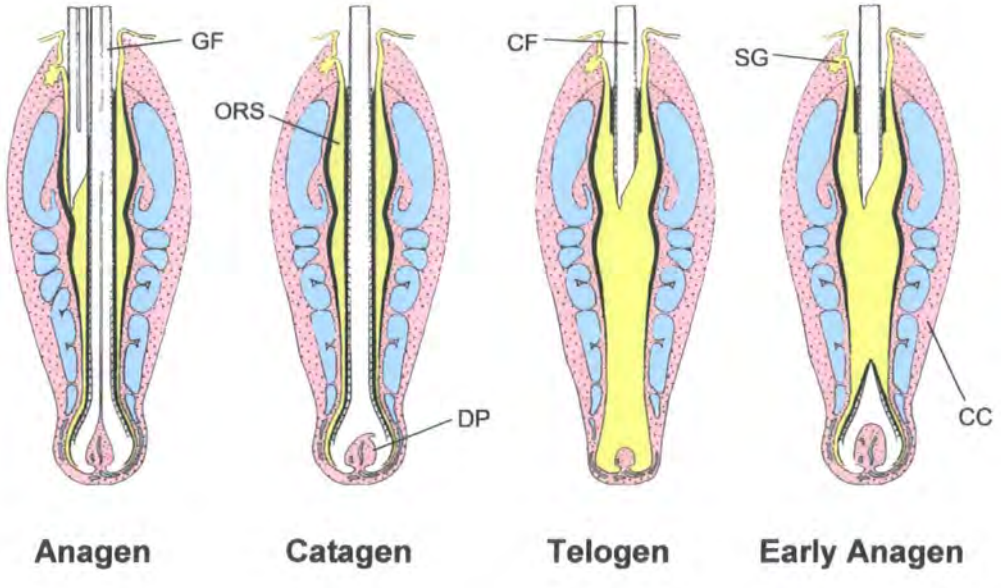

Figure 1.7. The vibrissa follicle cycle.
Diagram showing vibrissal follicle growth. In the vibrissa follicle, shape of the dermal papilla (DP) and the position of the growing (GF) and club fibres (CF) are indicators of cycle stage. Outer root sheath (ORS), Sebaceous gland (SG), Collagen capsule (CC) (adapted from Oliver 1966).

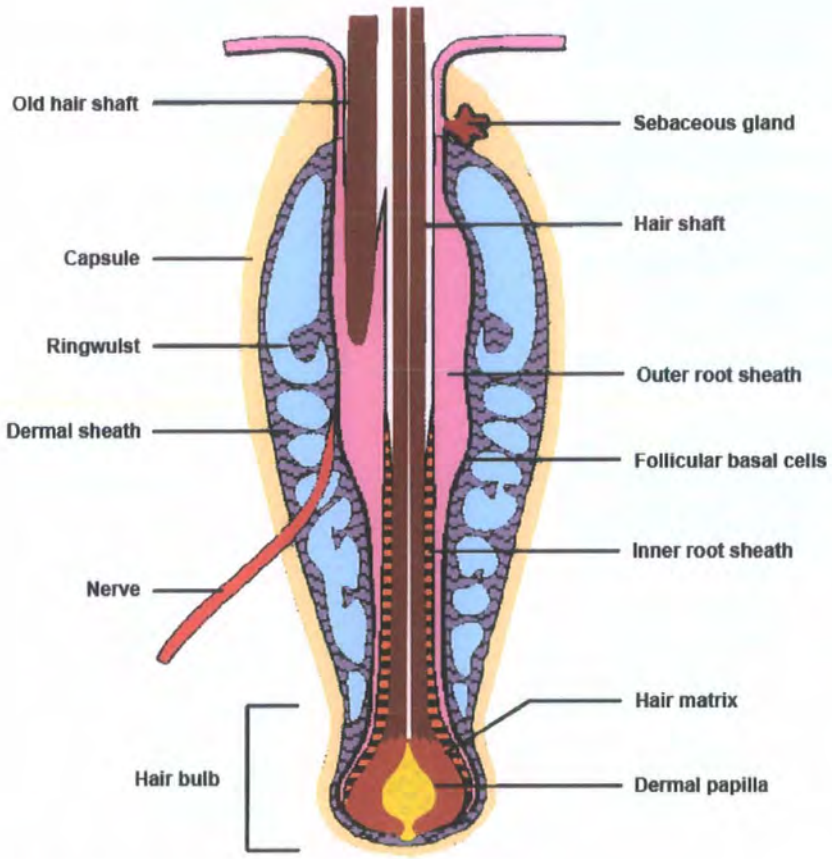

Figure 1.8. The rat vibrissa follicle.

Diagram showing the rat vibrissa follicle (modified from Matsuzaki and Yoshizato, 1998)

nerve (DVN). The innervation to the inner conical body and rete ridge collar is provided by several smaller superficial vibrissal nerves (SVN) (Rice *et al*, 1986) (Figure 1.9).

1.6.1 Deep Vibrissal Nerve

Each F-SC is innervated by a single DVN that is a unique branch from a major fascicle of the intraorbital nerve (Dörfl, 1985). These fascicles lie in the dermis between each row of F-SCs and supply DVNs to the adjacent ventral row of F-SCs. The posterodorsal aspect of the sinus capsule is penetrated by the DVN at the level of the cavernous sinus (Rice *et al*, 1986). As it ascends and traverses this sinus, it breaks into smaller bundles of axons that become distributed around the follicle.

Occasionally some axons leave these bundles and innervate the cavernous sinus but most go on to innervate at the level of the ring sinus (Rice *et al*, 1986). At the ring sinus, the axons branch and form sensory endings at various levels, becoming distributed separately in the mesenchymal sheath around the follicle (Rice *et al*, 1986). Innervation at the level of the ring sinus is consistently the densest in many species. The mesenchymal sheath, between the ringwulst and conus, is innervated by lanceolate endings (rapidly adapting mechanoreceptors). These are characterised by their flat, blade-like appearance and may be branched or unbranched. The lanceolate endings are orientated longitudinally and parallel to the hair shaft completely surrounding the follicle. There are also numerous Merkel endings (slowly adapting mechanoreceptors) located between the ringwulst and the conus (Rice *et al*, 1986).

1.6.2 Superficial Vibrissal Nerve

The fascicles or row nerves, which branch from the major infraorbital nerve, also give rise to smaller superficial skin nerves (Dörfl, 1985). These ascend in the dermis both dorsal and ventral in close proximity to each F-SC and branch just deep to the epidermis. These skin nerves provide SVNs to the F-SCs in addition to supplying nerves that form a superficial plexus innervating the intervibrissal fur (Munger and Rice, 1986). As many as six SVNs converge upon each F-SC, but depending on the species these nerves may send ascending branches to the rete ridge collar, and descending branches to the inner conical body (Rice *et al*, 1986).

The rete ridge is innervated in most mammals but not in Rabbit. This innervation consists of scattered Merkel endings that completely surround the mouth of the vibrissal follicles. SVNs almost exclusively innervate the inner conical body, and compared to other locales has the greatest interspecies variation. Studies by Andres in the rat revealed Ruffini (low threshold mechanoreceptors) and free nerve endings as well as long thin lanceolate endings in this locale (Andres, 1966). The ORS at the level of the ring sinus is also innervated by Merkel endings that traverse the glassy membrane to terminate among specialised sensory mechanoreceptors, Merkel cells. The Merkel endings are supplied by axons which ascend in the mesenchymal sheath with branches that are orientated circumferentially around the follicle and perpendicularly to lanceolate endings. Interestingly in Rabbit, the SVNs are poorly developed and the F-SCs lack a rete ridge collar and associated Merkel cells (Rice *et al*, 1986).

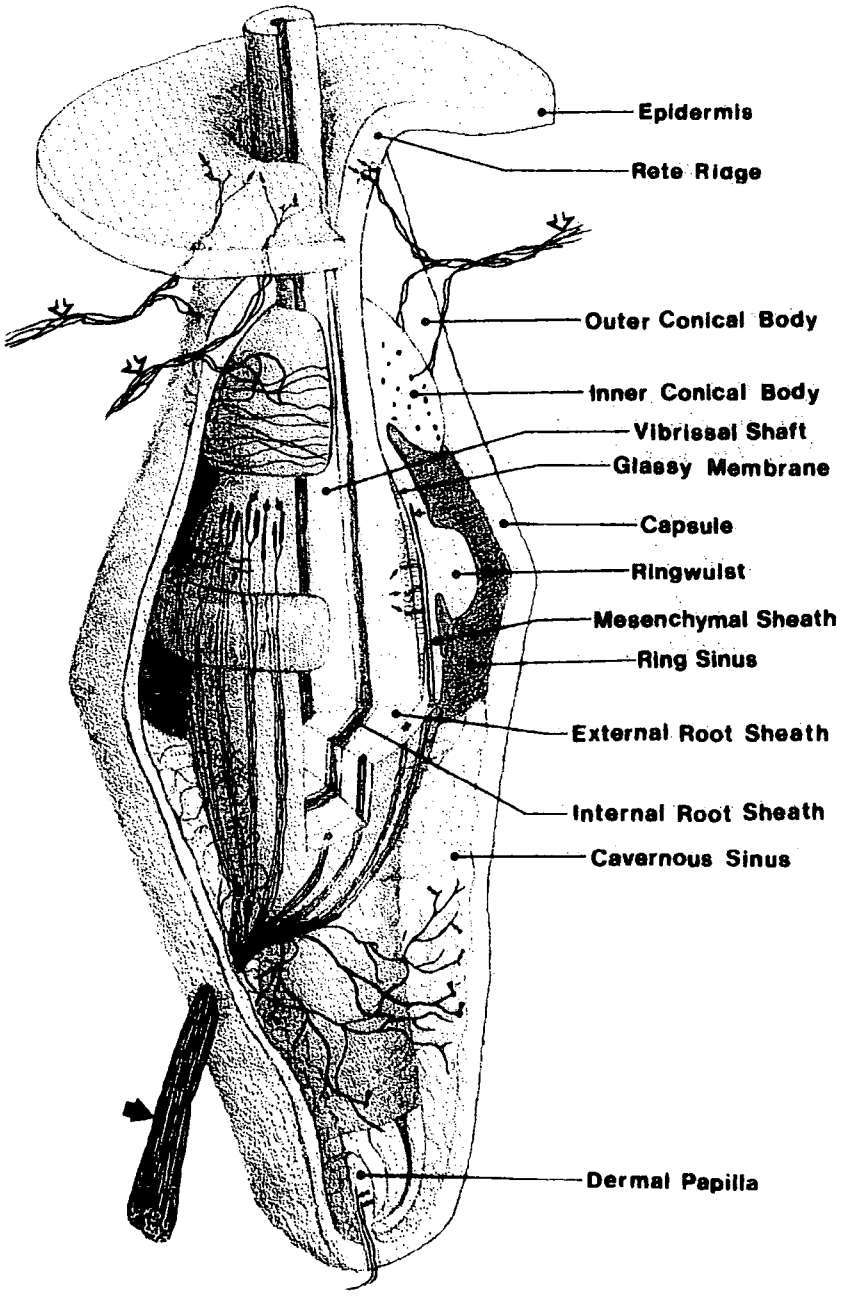

Figure 1.9. Innervation of vibrissal follicle sinus-complex (F-SC)

A schematic, three dimensional view of a vibrissal follicle sinus-complex (F-SC). On the left side only the capsule has been cut away to demonstrate the three-dimensional distribution of the innervation supplied by several superficial vibrissal nerves (SVN) (large open arrows) and one large deep vibrissal nerve (DVN) (large solid arrow). On the ride side, several components have been cut away to illustrate detailed relationships of the innervation. Some specific types of sensory terminals are indicated: Merkel endings (small solid arrows), lanceolate endings (small open arrows), encapsulated endings (small solid arrowheads) and Ruffini endings and free nerve endings (small double arrowheads). The SVNs branch to innervate the rete ridge collar and inner conical body. The rete ridge contains Merkel endings. The inner conical body contains a circular array of axons, lanceolate terminals, Ruffini terminals and free nerve endings. The main DVN branches inside the capsule to innervate structures at the level of the cavernous sinus and ring sinus. At the level of the ring sinus, Merkel terminals penetrate the glassy membrane to end within the external root sheath. (from Rice *et al*, 1986)

1.6.3 Merkel Cells

Merkel cells were first discovered in 1875 by Friedrich Sigmund Merkel. He noticed these cells were in close contact with nerve fibres in the hair follicle and glaborous skin and called them 'Tastzellen' (Merkel, 1875). These cells have now been renamed as Merkel cells (MCs). MCs are predominantly located in sensitive skin areas and oral mucosa, in particular basal epidermis, the touch dome, hair follicle, vermillion border of the lip, and palate (Winkelmann and Breathnach, 1973; Breathnach, 1980; Hartschuh *et al*, 1986; Whitear, 1989; Tachibana, 1995). In contrast, MCs in birds are found in the dermis (Halata *et al*, 2003). These cells are characterised by dense-cored osmophilic granules (MC granules), microvilli-like projections which protrude from the cell surface, intermediate filaments, small desmosomes connecting them to keratinocytes and a pale lobular nucleus containing few nucleoli. Most MCs also form a synaptic contact with a sensory axon terminal (Tachibana and Nawa, 2002). This complex of MC and a synaptic contact have been given many titles, Merkel's corpuscle (Cauna, 1962), Merkel cell-neurite complex (Munger, 1965) and most recently, Merkel ending (Halata, 1975).

In vibrissae, MCs can be found in two prominent locations: superficially near the rete-ridge collar, close to where the hair shaft penetrates through the epidermis and in the epithelial thickening of the hair follicle below the sebaceous gland (Halata and Sames, 2002). Much larger numbers of MCs (up to 2000) are found basally in this location and are oval in shape, orientated with a long axis perpendicular to the hair shaft. The nerve endings associated with MCs are located on the IRS aspect of MCs, with its cytoplasmic protrusions extending between neighbouring keratinocytes or

through the glassy membrane into the blood sinus (Halata and Sames, 2002) (Figure 1.10).

The function of MCs is thought to act as slowly adapting type I mechanoreceptors transducing steady indentation in hairy and glabrous skin (Iggo and Findlater, 1984; Ogawa, 1996; Szeder *et al*, 2003). However, it is still debated whether it is MCs or their afferents acting as mechanical transducers as removing MCs by enzymatic treatment, photoablation or genetic modification abolished the responses of slowly adapting afferents in some studies (Mills and Diamond, 1995; Kinkelin *et al*, 1999), but not in others (Ikeda *et al*, 1994). If indeed MCs are sensory receptor cells then signals must be transmitted through synaptic contacts with somatosensory neurons (Haeberle *et al*, 2004). In keeping with this MCs contain dense-core vesicles that resemble neurosecretory vesicles (Hartschuh *et al*, 1990). Various studies have confirmed the presence of many neuropeptides such as vasoactive intestinal peptide (VIP), calcitonin gene-related peptide (CGRP), peptide histidine isoleucine (PHI), synaptophysin and substance P, with some of these detected in the MC granules themselves (Hartschuh and Weihe, 1988; Weihe *et al*, 1991; Cheng-Chew and Leung, 1991, 1994, 1996; Tachibana, 1995).

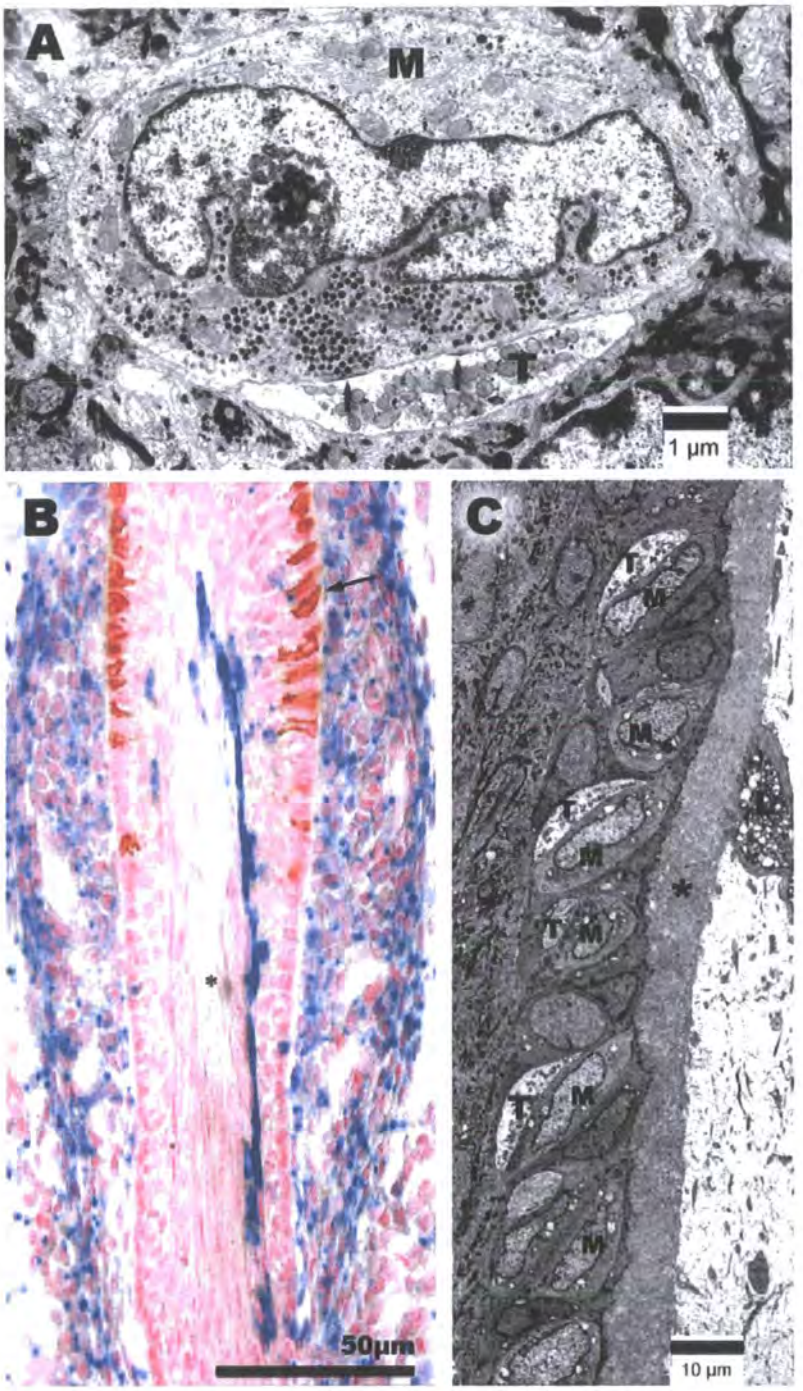

Figure 1.10. Ultrastructure and location of Merkel cells.

(A) High power electron microscopy of a Merkel cell (M) with nerve terminal (T) from the rete pig skin of the cat nose. Synapse-like contacts can be seen between Merkel cell and nerve terminal (arrow). The Merkel cell is characterised by a lobular nucleus and an accumulation of dense-cored granules in the synaptic cytoplasm (from Halata *et al*, 2003). (B) Xgal-reaction product in a tangential section through an adult Wnt1-cre/R26R whisker follicle. The bulge area is characterised by the presence of Merkel cells (cytokeratin-18 peroxidase reaction product; arrow). Blue Xgal-positive cells show cells of neural-crest in origin (from Sieber-Blum and Grim, 2004). (C) Ultrathin longitudinal section from a rhesus monkey sinus hair, through the thickened portion of the follicle below the sebaceous gland. Merkel cells (M) and nerve terminals (T) are arranged obliquely to the glassy membrane (*) like the scales of a pine cone, with the Merkel cells always directed towards the glassy membrane. A lanceolate nerve terminal (L) in close contact with the glassy membrane (*) is seen on the outer side (Halata *et al*, 2003).

Recently, microarray work by Haeberle and colleagues highlighted over 300 MC-enriched transcripts including neuronal transcription factors, presynaptic molecules and ion-channel subunits. Further analysis revealed that MCs are poised to release glutamate and other neuropeptides and also possess voltage-gated Ca^{2+} channels. These have been shown to trigger release of synaptic vesicles, demonstrating that MCs express the molecular tools to send both excitatory and modulatory signals to sensory neurons (Haeberle *et al*, 2004). It should be noted however that there is evidence of heterogeneous subpopulations of MCs, some which are non-innervated but have secretory granules and cytoplasmic processes (Tachibana *et al*, 1997, 1998). These subpopulations of MCs have been shown to be irregular in shape, populating rodent oral mucosae (Tachibana *et al*, 1997). It has been postulated these irregularly shaped cells may have trophic roles for growing nerve fibres and keratinocytes (Tachibana and Nawa, 2002). Because the sensory role of MCs is still controversial, other possible functions have been proposed. Pasche and colleagues proposed that MCs may release neuromodulators to regulate the sensitivity of mechanoreceptive neurons (Pasche *et al*, 1990). MCs have also been implicated to influence the innervation or development of epithelia (Pasche *et al*, 1990; Cronk *et al*, 2002).

Until recently the origin of MCs was also highly contested with scientists opting for one of two explanations: (1) the neural crest origin hypothesis, and (2) the epidermal origin hypothesis (Tachibana, 1995). However, Szeder and colleagues have settled this by demonstrating the neural crest origin of MCs. This group used Wnt1-cre/R26R compound transgenic mice in which neural crest cells were permanently marked. They found that murine MCs both in vibrissae and interfollicular locations were neural crest in origin, displaying the β-galactosidase transgene (Szeder *et al*,

2003). This is particularly interesting given that a population of pluripotent neural crest stem cells, termed epidermal neural crest stem cells (eNCSC), has been found in the bulge region of adult mouse vibrissae (Sieber-Blum *et al*, 2004). It has been suggested that MCs can detach from the epithelium and migrate (Moll *et al*, 1986). It is tempting to speculate that MCs, with follicular stem cells, can migrate out of the follicle to populate interfollicular regions and may explain the prominent locations found in vibrissae. Given the location of MCs in the follicle, neural crest-derived melanocyte precursors (Peters *et al*, 2002; Mishimura *et al*, 2002) and pluripotent eNCSC in the bulge it is tempting to postulate a link between these stem cells and MC development.

1.7 Inhibitor of DNA-Binding (Id) Proteins

Since the discovery of Id proteins over a decade ago, extensive research has revealed information about their role in proliferation, differentiation, cell fate and lineage commitment, cell cycle control and tumourigenesis. To date four members of the Id family of proteins have been found in mammals, Id1-Id4, all displaying overlapping but distinct expression profiles in a variety of cell types and tissues (Jen *et al*, 1996).

Id proteins consist of a highly conserved helix-loop-helix (HLH) domain and less conserved N and C terminal regions. It is via this HLH domain that they exert their functions by dimerising with the basic helix-loop-helix (bHLH) family of proteins. These bHLH proteins can form transcriptionally active complexes of either hetero or homodimers initiating tissue-specific gene expression. The dimerisation of bHLH proteins allows DNA binding via the canonical 'E-box' or 'N-box' sequences allowing expression of genes containing these sequences. Id proteins, which lack a

basic region critical for DNA binding, can block this process by forming transcriptionally inactive heterodimers with bHLH proteins, suppressing gene expression (Figure 1.11). More than 350 bHLH proteins have been identified so far, some of which are ubiquitously expressed (eg. E12, E47) and others which are tissue-specific (eg. NeuroD, Mash1). The diversity of the bHLH family and the unique overlapping expressions of the Id proteins are thought to contribute to the specific differentiation process during development (Coppé *et al*, 2003).

1.7.1 Id2

The HLH protein Id2 has a much more restricted expression pattern compared to the ubiquitously expressed Id3 (Norton, 2000). During embryogenesis Id2 has been found to be specifically expressed in a sub-population of migrating neural crest cells (Martinsen and Bronner-Fraser, 1998). Ectopic expression and overexpression studies revealed that the neural crest specification is regulated by Id2, directing ectodermal precursors into neural rather than ectodermal lineages (Martinsen and Bronner-Fraser, 1998). Furthermore, Id2 has been found in cardiac neural crest cells of chick. Ablation of these cells led to an altered Id2 expression and abnormal heart development. The same phenotype was observed across species suggesting a conserved role for Id2 in cardiac neural crest cells and normal development (Martinsen *et al*, 2004). Studies by Samanta and Kessler revealed Id2 playing a role in lineage commitment of oligodendrocyte precursors (OLPs), whereby Id2 (and Id4) was able to bind the bHLH proteins responsible for oligodendrogenesis (Olig1/2) thereby inhibiting differentiation but instead promoting astrocyte differentiation (Samanta and Kessler, 2004). Similarly, Wang and colleagues also found Id2 overexpression blocked oligodendrocyte differentiation and enhanced proliferation.

The timing of this differentiation was found to coincide with Id2 translocating out of the nucleus (Wang *et al*, 2001). The ability of Id2 to control lineage commitment was also demonstrated in the foetal thymus of mice. T and natural killer (NK) cells develop from common progenitors but in $Id2^{-/-}$ mice, NK cell numbers were severely reduced. In addition to absence of NK cells, there was also a lack of Peyer's patches and peripheral lymph nodes (Yokota *et al*, 1999). It was found that in $Id2^{-/-}$ mice these progenitors could only form T cells, revealing that in wild type mice, Id2 restricts these bipotent progenitors to the NK lineage (Ikawa *et al*, 2001).

In B cell development Id2 has a highly specific role in keeping IgE levels low by inhibiting class switch recominations (CSR). This may be important during normal immune responses to prevent serious complications such as allergic hypersensitivity (Sugai *et al*, 2003). In addition to Id2's numerous roles in cell cycle control, proliferation, differentiation and lineage commitment, Id2 has also been linked with apoptosis. Alway and colleagues demonstrated a link between high Id2 expression and muscle atrophy via proteolytic caspases (Alway *et al*, 2003). Furthermore, other research has highlighted a role in neuronal apoptosis, whereby Id2 was induced during serum and potassium-induced apoptosis in cerebellar granule neurons. The cells were protected from apoptosis via targeted deletion of the Id2 gene in neurons (Gleichmann *et al*, 2002).

During the cell cycle, Ids are regulated at many levels; transcription regulation, protein stability and post-translational modification (Zebedee and Hara, 2001). In

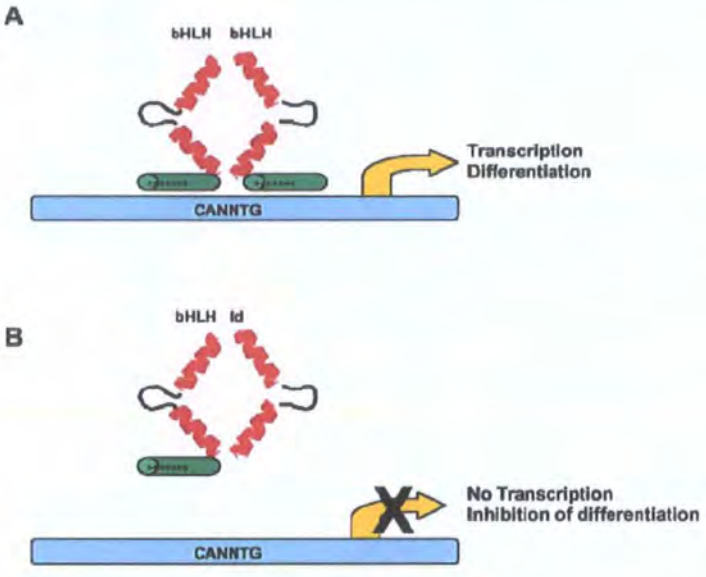

Figure 1.11. Model for Id effects on bHLH transcription.

(A) In the absence of Id proteins, dimers of bHLH proteins can bind DNA and activate transcription of differentiation-associated genes. (B) With expression of Id proteins, bHLH-Id dimers form which are unable to bind DNA and expression of differentiation-associated genes is inhibited (from Hashmat *et al*, 2003)

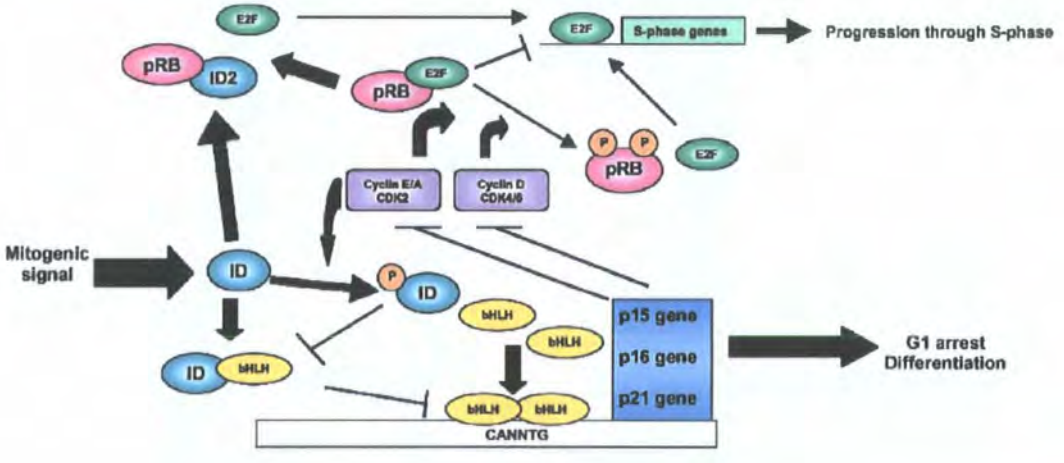

Figure 1.12. Model for Id gene function in cell cycle progression.

Common cell cycle regulatory pathways in which Id gene regulation has been implicated are shown above. Id phosphorylation by cyclin-dependent kinases in late G1 is shown. This modified Id protein inhibits Id-bHLH dimer formation as shown. bHLH-mediated activation of the cdk-inhibitory proteins p15, p16, and p21 is also shown. This activity is also inhibited by Id proteins. The particular function of Id2 and its association with the retinoblastoma family of proteins (pRB) is also noted. Id2 interactions with pRB allow for release of E2F, expression of S phase genes, and cell cycle progression. All Id interactions noted support the role of Id proteins in cell cycle progression (from Halata *et al*, 2003).

addition to binding members of the bHLH family, Id2 is the only Id protein to bind the 'pocket proteins' (Rb, p107, p130) (Lasorella *et al*, 1996). Toma and colleagues demonstrated this interaction by overexpression studies with Id2. The apoptotic phenotype was rescued by expression of a constitutively active, hyperphosphorylated form of retinoblastoma, pRb (Toma *et al*, 2000). Rb and its family members are key regulators of the cell cycle, involved in the G0 to S1 transition. Rb acts by sequestering Id2, providing a crucial checkpoint for proliferation (Weinberg, 1995) (Figure 1.12). Deregulated expression of Id2 is known to lead to inactivation of the Rb pathway leading to uncontrolled proliferation, a process which is a tell-tale sign of cancer (Iavarone *et al*, 1994; Lasorella *et al*, 1996). In addition to inactivation of Rb, Id2 is known to be a target of the β-catenin/TCF pathway in colon adenocarcinoma, leading to deregulation of Id2 (Rockman *et al*, 2001). Because of the potential role Id proteins play in development of cancer, Id genes and their proteins are excellent candidates for molecular targeted therapies (Fong *et al*, 2004) and represent an exciting new approach to cancer research.

Various signalling pathways have been implicated with Id2 transcription. One such pathway is the Transforming Growth Factor (TGF)-beta family and bone morphogenetic proteins (BMP). Valcourt and colleagues have shown that TGF-β and not BMP induces epithelial-mesenchymal transitions (EMT) in human and mouse epithelial cells, which is accompanied with downregulation of Id2 (Valcourt *et al*, 2005). Furthermore, studies by Kondo and colleagues found that Id2 interacted with E2A proteins prior to EMT. Upon TGF-β signalling Id2 levels were downregulated leaving E2A in molar excess and able to initiate EMT (Kondo *et al*, 2004). The type I insulin-like growth factor receptor (IGF-IR) has also been

implicated in controlling Id2, both positively and negatively regulating differentiation in a murine hematopoietic cell line (Bellati *et al*, 2001; Prisco *et al*, 2001; Navarro *et al*, 2001).

Recently, Id1 and Id2 have been found to be important retinoic acid responsive genes in acute promyelocytic leukaemia (APL). Id1 and Id2 were dramatically upregulated upon treatment with tRA, whereas Id3 and Id4 could not be detected (Nigten *et al*, 2005). Given the modulating effects retinoic acid treatment has on vibrissae and findings by Nigten and colleagues on APL cells, investigation into the expression of Id proteins on retinoic acid treated mystacial pads may further knowledge in this area. As a result of all these studies it is clear that Id2 can have many differing roles in the cell depending on the stimulus it receives and its cellular niche. There is still much to learn from these influential proteins and more studies are needed to elucidate their complex interactions at the molecular level.

According to the literature, no studies have been published on Id2 expression in the hair follicle, either during early development, the adult cycle or in response to retinoic acid treatment. Id proteins are widely accepted as keeping cells in a proliferative, undifferentiated state and needed for the timing of various cellular events. They confer stem-cell like qualities and as such have not been extensively investigated either in embryonic or adult stem cell populations. In light of this, the hair follicle is an attractive organ in which to study the expression of Id2 from a development perspective.

1.7.2 Id3

Id proteins traditionally have been viewed as negative regulators of differentiation, and Id3 is no exception. However, since the discovery of the proteins many studies have highlighted a much wider role for these proteins. In support of the traditional model, Id3 is known to negatively regulate muscle differentiation by inhibiting the DNA-binding activities of the myogenic regulatory factors (Melnikova and Christy, 1996). Furthermore, in adult epidermis Id3 is downregulated in differentiating keratinocytes cultured *in vitro*, and also within *in vivo* skin sections. In contrast, levels of Id3 are high in the proliferating basal layers of the epidermis (Langlands *et al*, 2000), agreeing with the established view of promoting proliferation and inhibiting differentiation. During embryogenesis and development Id1-2-3 display overlapping but distinct expression patterns whereas Id4 shows a unique expression pattern (Jen *et al*, 1996). Expression is stage-dependent and region-specific (Jen *et al*, 1996, 1997) reflecting the important roles of Id proteins in normal development and differentiation (Yokota, 2001).

As with Id2, Id3 is also involved in lineage commitment in the foetal thymus. Here the common progenitors of NK and T cells are also influenced by Id3, inhibiting T cells and promoting NK development. Constitutive expression of Id3 demonstrated this, conversely absence of Id3 lead to the default pathway of NK development (Heemskerk *et al*, 1997). Furthermore Spits and colleagues revealed both Id2 and Id3 inhibit development of $CD34^+$ stem cells into predendritic cells (pre-DC)2, favouring the NK lineage, supporting the idea that DC2 precursors, T and B cells are from a common origin (Spits *et al*, 2000). However, in cells that have already committed to T cell development, and initiated T cell receptor (TCR) gene

rearrangements (pre-T cells), overexpression of Id3 inhibits development into TCRalpha-beta but not gamma-delta T cells. Evidence was also found of cells displaying properties of NK and pre-T cells, highlighting the important role of Id3 and bHLH proteins in T cell development (Blom *et al*, 1999).

Significant advances in Id function have been realised through knockout studies in mice. Id1 and Id3 are co-expressed temporally and spatially during murine neurogenesis (Duncan *et al*, 1992; Ellmeier and Weith; 1995; Jen *et al*, 1997) and angiogenesis (Jen *et al*, 1997). Because of the overlapping expression of Id1 and Id3 during embryogenesis, it was suggested that redundant functions existed between these two members of the Id family. Indeed, mice null for both Id1 and Id3 were found to be embryonic lethal at mid-gestation, showing abnormal neurogenesis and angiogenesis (Lyden *et al*, 1999). Ids were investigated in tumour angiogenesis because of the similarities between brain and tumour invasion by vascular tissue. It was found that Id knockout mice (Id1+/-, Id3-/-) failed to support growth and/or metastasis of three different tumours, all showing poor vascularisation (Lyden *et al*, 1999). However, a single copy of Id1 or Id3 is sufficient to rescue embryonic angiogenesis in the brain but it appears not in neovascularisation of tumours (Benezra *et al*, 2001). Clearly further research is needed to understand the role Id1 and Id3 play in angiogenesis and tumourigenesis.

A number of studies have illustrated the pathways by which Id3 is regulated. A number of studies showed that both Id2 and Id3 are phosphorylated by cyclin-dependent kinase 2 (CDK2) in late G1 of the cell cycle (Hara *et al*, 1997; Deed *et al*, 1997). Indeed in vascular smooth muscle, Id3 has been shown to be phosphorylated

both *in vitro* and *in vivo*, providing a switch with which to control the regulation of the cell cycle inhibitor p21Cip1, and VSMC growth (Forrest *et al*, 2004). Id3 and the bHLH proteins E12 and E47 have also been found to play key roles in thymocyte development. Upon signalling via the TCR, it was shown that Id3 is rapidly induced and regulated in a dose dependent manner by the extracellular signal-regulated kinase (ERK) MAPK module. Such a pathway is involved in differentiation and proliferation in a wide variety of cell types (Bain *et al*, 2001). In addition to the ERK MAPK pathway, Id3 has also been shown to be regulated by BMP and TGF-β signalling pathways (Hollnagel *et al*, 1999; Kee *et al*, 2001). Hollnagel and colleagues demonstrated that expression of BMP-4 in ES cells resulted in induction of Id2 and Id3 expression (Hollnagel *et al*, 1999), whereas when cultured B-lymphocyte progenitors were treated with TGF-β, Id3 expression was also rapidly induced (Kee *et al*, 2001).

In the hair follicle during morphogenesis and during hair cycling there is complex cross-talk between various signalling pathways. During morphogenesis, BMP signalling has been shown to be important in inhibiting placodal fate of cells surrounding newly developing follicles and is also involved in the differentiation of the hair shaft. Signalling via the TGF-β pathway has been attributed to promotion of the placode and shape of the follicle (Schmidt-Ullrich and Paus, 2005). To date there has only been one report of Id3 in the hair follicle and this focussed on the role of BMP signalling in the control of Id3. O'Shaughnessy and colleagues reported that Id3 expression in the DP corresponded with BMP signalling during middle anagen of the adult cycle in both pelage and vibrissae, but interestingly during telogen when no BMP signalling is present, Id3 expression was found. This highlighted the

possibility that not only BMPs are involved in regulating Id3, but also cell-cell contacts (O'Shaughnessy *et al*, 2004). Cultured DP cells were found to lose Id3 expression through passages, but levels were restored on addition of BMP-4 (O'Shaughnessy *et al*, 2004).

Previous studies into Id proteins in the hair follicle by this lab (Whitehouse *et al*, 2002; O'Shaughnessy *et al*, 2004) have demonstrated much is still to be learned from their spatial and temporal expression patterns and how they are regulated during the complex epithelial-mesenchymal interactions during morphogenesis and adult cycling. Because of this, Id3 represents an ideal protein to study in greater depth in the hair follicle.

1.8 Multidrug Resistance Proteins

The ATP-binding cassette (ABC) superfamily comprise over fifty proteins that perform many and varied functions (Klein *et al*, 1999; Müller, 2001) and represent the largest family of transmembrane proteins (Müller, 2001). Some of these members mediate drug transport and as a result have been associated with drug resistance in cancer cell lines (Gottesman *et al*, 1996; Longley and Johnston; 2005). These drug efflux proteins fall into two main groups, termed the multidrug resistance (MDR) and multidrug resistance-associated protein (MRP) type transporters. The three major multidrug resistance ABC proteins are MDR1 (P-glycoprotein, ABCB1), multidrug resistance associated protein 1 (MRP1, ABCC1) and ABCG2 (BCRP/ABCP/MXR) (Sarkadi *et al*, 2004). These transporters are increasingly found overexpressed in tumours but their expression is widespread in normal tissues, particularly excretory tissues such as the liver, kidney and intestine (Chan *et al*,

2004). Recently, some of these transporters have been implicated with stem cell populations in many different tissues (Goodell *et al*, 1997; Storms *et al*, 2000; Zhou *et al*, 2001; Scharenberg *et al*, 2002; Martin *et al*, 2004;) and it is emerging as an important new field of stem cell biology (Bunting, 2002).

1.8.1 BCRP

Breast cancer resistance protein was originally isolated from human MCF-7 breast cancer cells (Doyle *et al*, 1998) and also human placenta (Allikmets *et al*, 1998) and given the variable names BCRP and ABCP respectively. To further confuse matters, Miyake and colleagues characterised the same transporter in mitoxantrone-resistant cell lines, giving it a third name, MXR (Miyake *et al*, 1999). Under the new nomenclature this protein is classified as ABCG2 (Parker *et al*, 1998).

BCRP is a half transporter consisting of 6 trans-membrane (TM) domains and an intracellular ATP-binding region located towards the N-terminus (Sarkadi *et al*, 2004), believed to be active as a homo-dimer (Litman *et al*, 2001) (Figure 1.13). Since the early studies isolating and cloning BCRP, it has been established that this protein functions as a high capacity drug transporter with wide substrate specificity. BCRP can transport large hydrophobic molecules including cytotoxic compounds (mitoxantrone, topotecan, flavopiridol, methotrexate), fluorescent dyes (e.g., Hoechst 33342) and even toxic compounds found in normal food (PhIP) (Sarkadi *et al*, 2004). Many ABC half-transporters are found in subcellular locations but BCRP has been found localised to the plasma membrane, consistent with its role as a drug export pump (Rocchi *et al*, 2000).

Hematopoietic stem cells (HSCs) have long been known to efflux certain fluorescent dyes such as rhodamine 123 and Hoechst 33342, routinely exploited for isolation of these cells by fluorescence-activated cell sorting (FACS) (Ploemacher and Brons, 1985; Pallavicini *et al*, 1985; Spangrude and Johnson, 1990). More recently this method has been developed to target a specific side population (SP) of progenitors (Goodell *et al*, 1996). Schlarenberg and colleagues found that BCRP was a potent Hoeschst efflux pump and the protein contributed significantly to the generation of the SP phenotype in HSCs (Schlarenberg *et al*, 2002). It was also found that BCRP was not just restricted to HSCs but was expressed in a wide variety of stem cells (Zhou *et al*, 2001). Furthermore, BCRP expression has been found to be exclusive to skeletal muscle SP cells (Meeson *et al*, 2004), present in neural stem cells (Cai *et al*, 2002, 2004) and carciac SP cells in the developing and adult heart (Martin *et al*, 2004). More recently, de Paiva and colleagues reported BCRP expression in human limbal epithelial stem cells and SP cells (de Paiva *et al*, 2005).

1.8.2 MRP1

Multidrug resistance-associated protein 1 (ABCC1) was originally cloned from a multidrug resistant human small cell lung cancer cell line that did not express P-gp (ABCB1) (Cole *et al*, 1992). In this subfamily of at least 9 members, MRP1 is the only known member to confer drug resistance, however the newest member (MRP7) has yet to be characterised (Borst *et al*, 2000). Each of these members falls into one of two categories depending on their trans-membrane domains (TMDs). MRP1 has an extra TMD, denoted by TMD_0, which consists of 5 helices linked to two other TMDs each containing an intracellular nucleotide-binding domain (NBD) (Figure 1.13).

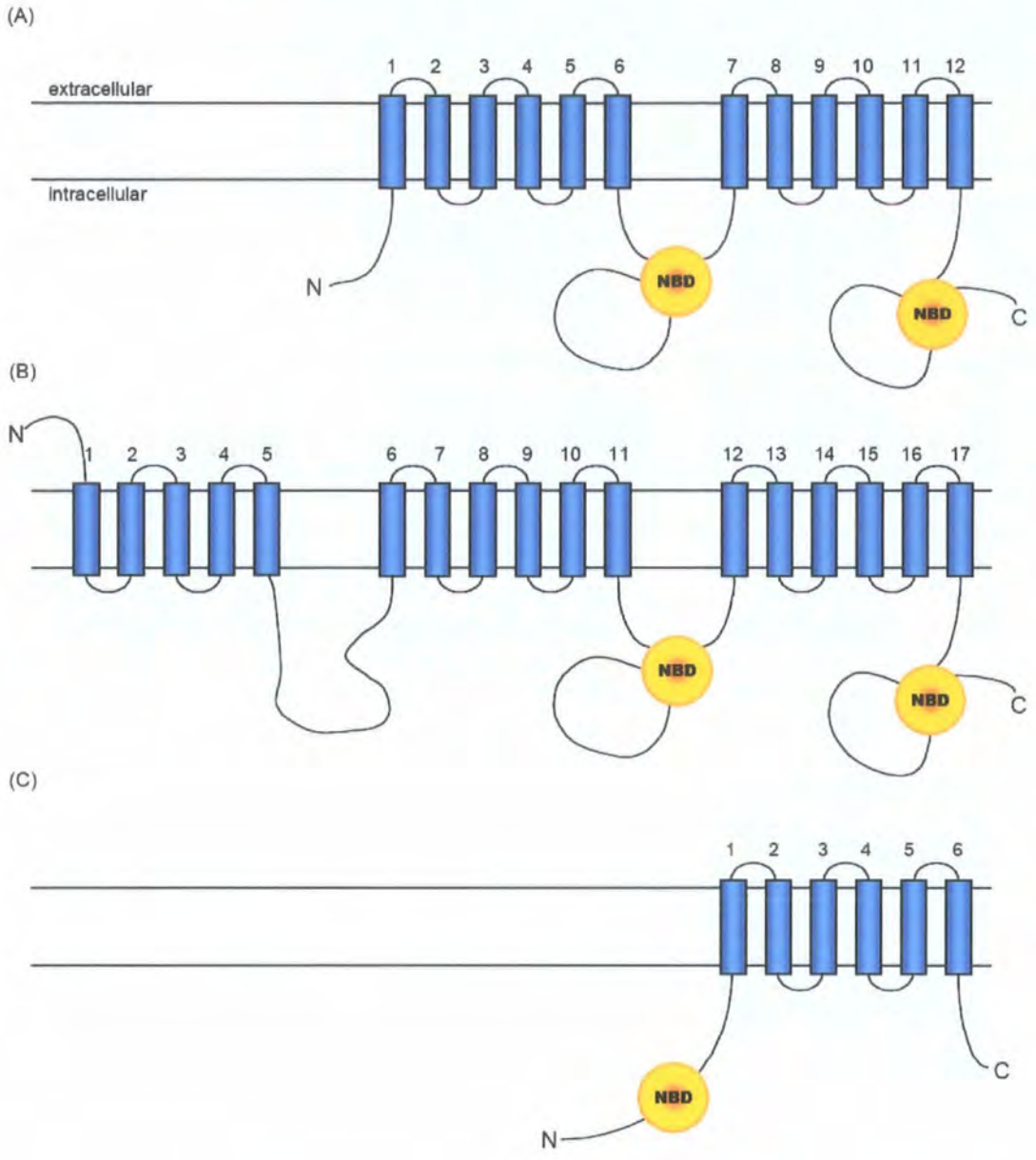

Figure 1.13. Transmembrane arrangement of ABC efflux proteins.

(A) Pgp (MDR1), MDR3, BSEP (SPgp), MRP4, MRP5, and MRP8, have 12 TM (transmembrane) regions and two NBDs (nucleotide binding domains). (B) Typical MRP transporters (MRP1-3 and 6–7) have five extra TM regions towards the N terminus. (C) 'Half-transporters' such as BCRP have just six TM regions and one NBD (from Chan *et al*, 2004).

Other members fall into this category, such as MRP2, MRP3 and MRP6, however the TMD_0 has been shown not to be essential for transport activity (Bakos *et al*, 1998). The role of MRP1 in SP and stem cells has been found to be very limited. Ros and colleagues reported that high expression of MRP1, along with MRP3 and MDR1 was seen in regenerating bile ductules in the hepatic progenitor cell compartment and was also upregulated in hepatocytes in severe human liver disease (Ros *et al*, 2003). A study on mouse ES cells showed MRP1 was absent, but when stimulated to differentiate along a hepatocyte lineage these differentiated cells expressed MRP1 (Tanaka *et al*, 2003). However, it has been suggested that MRP1 (and P-gp) may protect hematopoietic progenitor cells from chemotherapy-induced toxicity. Knockout mice against both these transporters revealed that bone marrow was up to 25-fold more sensitive to vincristine than wild-type bone marrow, and also that the presence of both transporters conveyed greater protection (van Tellingen *et al*, 2003).

1.9 Current Challenges in Hair Follicle Biology

Despite a resurgence of research into this fascinating appendage over the past decade, many critical questions remain unresolved that have implications for a broad range of biological disciplines. During hair follicle morphogenesis, it still remains a mystery where exactly the crucial follicle initiation signal arises. Follicle formation requires many different interacting signalling cascades which all need to be precisely timed. Many pathways have been discovered in the developing follicle, but exactly how all these molecules and pathways communicate is still unresolved and is a major challenge posed to hair follicle researchers, for example the molecular pathway

which favours the formation of a hair follicle instead of a sweat gland in a given location is unknown (Schmidt-Ullrich and Paus, 2005).

It has been known for some time that the bulge region of the hair follicle harbours slow-cycling, label-retaining cells with a high proliferative potential and clonogenicity. However, despite much research into this area the elucidation of a specific hair follicle stem cell marker has been unfruitful. Many candidates have been proposed but distinguishing stem cells from their transit-amplifying progeny has proved difficult, with conflicting reports (Ma *et al*, 2004). Elucidation of definitive hair follicle stem cell markers, coupled with a greater understanding of how the bulge cells relate to interfollicular keratinocyte stem cells, the DP mesenchymal cells and how this all fits into cycling (Ma *et al*, 2004) will yield exciting prospects for therapeutic treatments, notably in tissue and wound repair.

The search for the so-called 'Hair Cycle Clock' (HCC) is equally as elusive. It is undisputed that the biological "clock" that drives cycling of the hair follicle resides in the hair follicle itself, but the molecular nature of this system is unknown. Some have postulated that the heart of the hair follicle rests in the epithelial stem cell region while others have opted for the mesenchymal DP (Stenn *et al*, 1999). What is clear however is that elucidation of this mechanism will have a significant impact on other biological problems and have implications for clinical therapy since the vast majority of patients with hair growth disorders suffer from an undesired alteration of hair follicle cycling (Paus and Foitzik, 2004).

1.10 Aims of this Study

The Id protein family comprise a group of proteins which due to their function of regulating transcription are powerful players in the control of the cell cycle and differentiation. The hair follicle is a fascinating appendage and a great model to study from a developmental perspective. Id3 has not been extensively studied during hair follicle morphogenesis and Id2 has not been investigated at all in the hair follicle. This epithelial appendage is also the focus of much research into the multiple stem cell populations present in the follicle and the elucidation of specific stem cell markers. Multidrug resistance proteins represent potential novel markers of such populations, being recently implicated in some stem and SP cells (Cai *et al*, 2002, 2004, Meeson *et al*, 2004; Martin *et al*, 2004). Therefore the aims were:

1) To investigate the expression of Id2 and Id3, covering early follicle morphogenesis through to neonatal and the adult follicle cycle.

2) To investigate any relationship between Id expression and high proliferating cell populations, such as the putative stem cell bulge region.

3) To investigate the presence of multidrug resistance proteins in the hair follicle and their potential protective role in stem cell populations.

4) To study glandular morphogenesis of vibrissae treated with retinoic acid and how this affects Id protein expression.

2.0 Materials and Methods

2.1 Animals

Wistar rats (LSSU, Durham University) of either sex (3-12 months) were killed and tissue was obtained and frozen for subsequent immunocytochemistry. The same rats were also used for expression and culture studies.

2.1.1 Adult Vibrissa Follicles

An L-shaped incision was made postero-ventral to the mystacial pad, clamped at one end and then peeled back towards the snout using artery clamps (Figure 2.2). The connective tissue surrounding the vibrissa follicles was removed with fine forceps under a low-powered dissection microscope (Nikon SMZ-10, Japan) allowing the follicles to stand up on end. The follicles were pulled clean from the face by holding them where they meet the skin surface and pulling away, giving a clean vibrissa follicle, intact hair fibres and nerve. These individually isolated follicles were put into MEM (Sigma, UK) ready to be staged.

The isolated follicles were initially staged based on the number of hair fibres, length of the growing hair and follicle morphology; early anagen (EA) where a fine growing fibre is present above the neck of the follicle, with a length up to one quarter of the thick club fibre; mid-anagen (MA) where the growing fibre is between one quarter and three quarters the length of the club fibre; late anagen (LA) where the growing fibre is more than three quarters the length of the club fibre; and catagen / telogen where a single fibre is present (Figure 2.3). The follicle was further classified according to whether the end bulb was swollen indicating the start of catagen, or a narrowing of the end bulb region suggesting

the follicle was in telogen (Williams *et al,* 1994). The purpose was to give an indication of the growing cycle of the follicle as a guide for when sectioning using a cryostat.

Once staged each follicle was transectioned at the neck, mounted in plastic base moulds in TissueTek O.C.T (Agar Scientific) and orientated so that the nerve emerging from the follicle was on the right hand side and parallel to the bottom of the base mould. As with all samples, the follicle was pushed to the bottom of the mould to ensure it was orientated horizontally. The samples were then snap frozen in liquid nitrogen and stored at -80°C ready for sectioning.

2.1.2 Neonatal Mystacial Pads

Mystacial pads were taken from neonates ranging from new born to 4 day old rats. In each case, a rectangular sample of pad was taken making incisions parallel to the rows of follicles going as deep as the facial cavity. Once removed the pad was carefully trimmed to provide a straight edge for mounting ensuring the follicles are in line. The pads were mounted in plastic base moulds in TissueTek O.C.T at 90° to the base, snap frozen in liquid nitrogen and stored at -80°C. When preparing the 4 day pads, the whiskers were trimmed to allow for easier mounting.

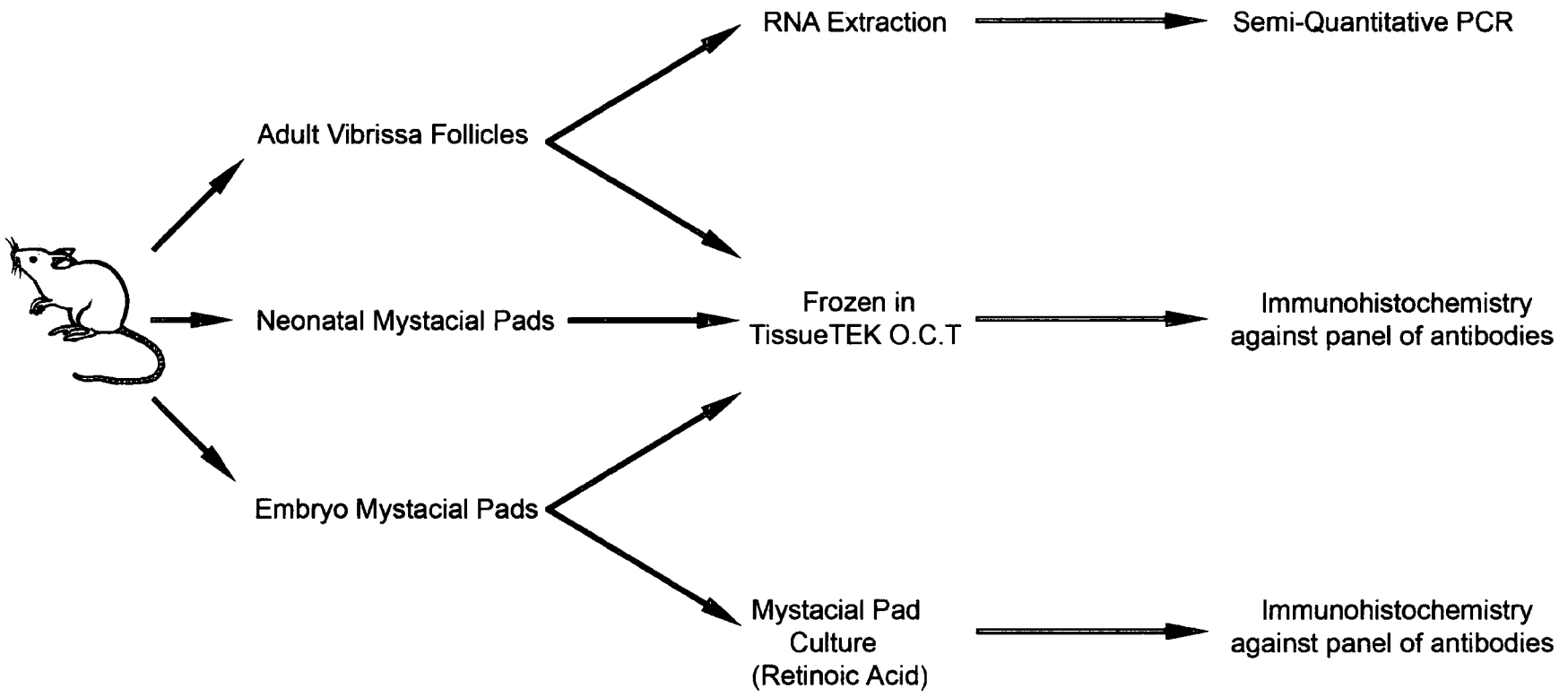

Figure 2.1 Diagram showing overview of methods used.

2.1.3 Embryo Heads and Snouts

Embryos ranging in age from E14 to E20 were taken, and depending on their size their heads or snouts were removed and embedded. For all embryos, an incision was made using a scalpel with a flat blade at the opening of the mouth below the upper lip and running back towards the top of the head. The embryo heads were placed on the cut edge, with E14 and E16 being mounted as so. E18 and E20 heads had a further incision made vertically down leaving the snout. These were orientated as for E14 and E16 samples but were mounted in foil boats and snap frozen as previously.

2.1.4 Embryo Mystacial Pads for Culture

All procedures were carried out under strict aseptic techniques. Mystacial pads were dissected from embryos aged E13.5 and E14 into a culture dish spotted with MEM (Sigma, UK). The pads were dissected by cutting round all four sides using a pair of fine dissection scissors being careful not to take too much dermis below the pad. Dissected pads of same aged embryos were stock piled in spots of MEM ready for culturing.

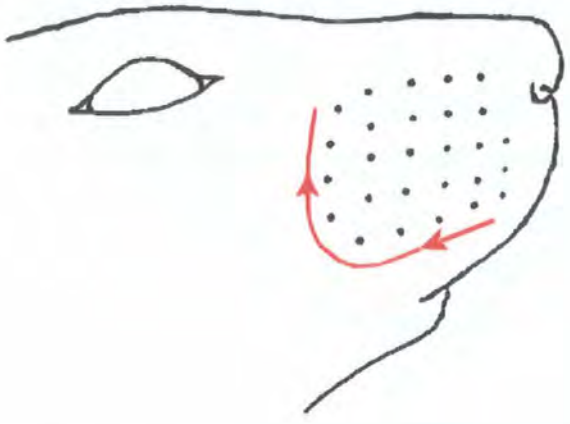

Figure 2.2. Mystacial pad dissection
Sketch showing the rat mystacial pad with arrowed line (red) showing where to make incisions. The pad was clamped along the newly made flap and rolled back towards the snout, revealing the vibrissae and intact nerves (modified from Oliver 1969).

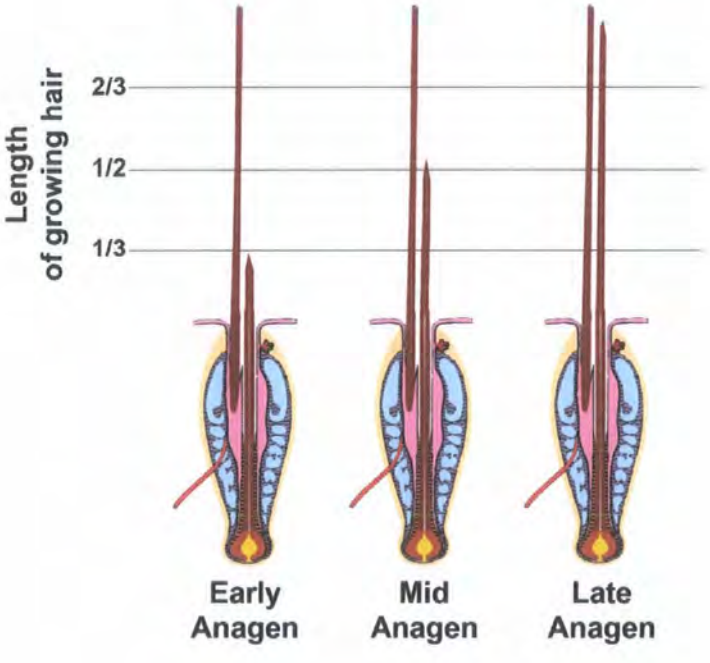

Figure 2.3. Vibrissa follicle staging
Diagram showing the relative length of the growing hair and club fibre. In early anagen (EA) the growing hair is less than 1/3 of the club fibre length, mid anagen (MA) where the growing hair is 1/2 of the club fibre length and late anagen (LA) where growing hair is more than 2/3 the club fibre length.

2.2 Immunohistochemistry

2.2.1 Cryostat Sectioning

All samples were cut on a Leica 3050S cryostat. Sections were cut at 6μm thickness at a temperature of -20°C. Before sectioning, samples were trimmed using a razor blade then orientated and mounted on the 'chuck' using TissueTek O.C.T. Serial sections were put alternatively onto fresh poly-l-lysine coated slides with each slide holding a maximum of 10 sections. The slides were left to adhere to the surface for up to 30mins before being fixed.

2.2.2 Fixing of Samples

All sections were fixed in ice cold 5% acetone in methanol to dehydrate and permeabilise the cells allowing unhindered access of the antibodies to all cell compartments. This fixation was chosen to ensure damage to cell architecture and morphology was minimal.

Methanol-Acetone Fixing

Slides were rinsed in filtered PBS for 5 minutes to remove the TissueTek O.C.T compound then fixed with methanol-acetone at -20°C for 20 minutes. The slides were removed and left to air dry for 15 minutes. They were then either stored at -80°C until needed or rehydrated in filtered PBS for 2 x 5 minutes in preparation for blocking.

2.2.3 Blocking

Blocking was performed to reduce non-specific antibody binding and reduce any background. Slides were incubated for 30 minutes in fresh FSG (Sigma, UK) (0.2% in PBS). After incubation, each slide was removed and areas between samples dried using tissue to enable neat spots of primary antibody to be applied. Care was taken to ensure the sections did not dry out. Blocking was continuous as both primary and secondary antibodies were diluted in blocking solution.

Blocking was initially performed using normal serum raised in the same species of host as the fluorochrome conjugated secondary antibody, but was subsequently replaced with FSG because it performed as well if not better than the host serum against a panel of antibodies.

2.2.4 Controls

The following controls were used for each experiment: no primary antibody, and no secondary antibody.

2.2.5 Primary Antibody

The primary antibody (Table 2.1) was diluted in blocking solution (0.2% FSG in PBS) and applied ensuring a neat spot over each sample. The slides were incubated in a humidity chamber either for 1 hour at room temperature or overnight at 4°C. All controls had the primary antibody omitted and were incubated in blocking solution instead.

2.2.6 Secondary Antibody

The primary antibody was removed with 3 x 5 minute washes in PBS and dried around the samples as previously. The secondary antibody (Table 2.2), conjugated to FITC or TRITC fluorochromes, was diluted in blocking solution and applied over the samples. Slides were incubated in a humidity chamber in the dark for 1 hour at room temperature.

2.2.7 Double-labelling Immunofluorescence

Some sections were labelled with two primary antibodies, raised in different species. At the addition of the primary antibody both antibodies were diluted together to the correct working titre in blocking solution and added to the slides. The slides were incubated as described in 2.2.5.

Secondary antibodies conjugated to FITC and TRITC fluorochromes were also diluted in blocking solution and applied to the slides. The slides were incubated in the dark as described in 2.2.6. Immunocytochemistry was performed on at least 3 and up to 5 different specimens for each sample, ensuring the results were of high quality and consistent.

2.2.8 Hematoxylin and Eosin Staining (H&E)

Slides used to examine the general histology of the samples were stained using Mayer's hematoxylin and eosin. The samples were fixed methanol:acetone for 20 minutes at -20°C (see 2.2.2), then rehydrated through 95% and 70% ethanol to distilled water for 1 minute each. Following this, the samples were incubated in Mayer's hematoxylin for 5-10 minutes (adjusted for each sample), dipped in alkaline water to blue the nuclei and rinsed in distilled water several times. The

samples were then dehydrated through 70% and 95% ethanol for 1 minute each then incubated in eosin for 10-30 seconds (adjusted for each sample), then dipped into 95% and absolute ethanol. The slides were cleaned by incubating in Histoclear for 1 minute, then repeating with fresh Histoclear. In preparation for viewing, the slides were dried at the edges and a glass cover slip mounted using DPX. Slides were viewed as described below in 2.2.9 with the microscope being used as just a light microscope.

The slides were viewed as described below in 2.2.9 with the microscope being used as just a light microscope.

2.2.9 Mounting and Viewing

After incubation of the secondary antibody, the slides were washed 3 x 5mins in PBS. Mowiol:Dabco (see Appendix 5.1.2) was used as the mounting agent with 80µl added uniformly to the slide and a coverslip placed on top using tweezers to ensure no bubbles were present. The slides were left to dry and harden for 1-2 hours before viewing. Mowiol:Dabco is effective in retarding photobleaching.

The slides were examined using an inverted epi-fluorescence microscope (Zeiss Axiovert 135) using x5, x10, x20 and x40 objectives. All images were taken with a mounted digital camera (Spot RT) and processed using Adobe Photoshop CS graphics software. For slides which were double-labelled with FITC and TRITC, separate green and red fluorescent images were taken of the same section and combined to give a double-labelled image.

Table 2.1 Details of antibodies used for immunohistochemistry

Host	Antibody Specificity	Isotype	Epitope	Working Concentration (µg/ml)	Source
Rabbit	Id2	IgG	C-20	1:20	Santa Cruz Biotechnology
Rabbit	Id3	IgG	C-20	1:20	Santa Cruz Biotechnology
Mouse	β-catenin	IgG1	Clone 14	1:100	Transduction Labs
Mouse	Cytokeratin-20	IgG1	IT-K_s 20.10	1:10	Progen
Mouse	Synaptophysin	IgG1	Clone SVP-38	1:100	Sigma
Mouse	Lamin-A	IgG1	Jol4	1:5	Prof. Chris Hutchinson, Uni. of Durham

Table 2.2 Details of secondary antibodies used for immunohistochemistry

Host	Specificity	Isotype	Fluorophore	Working Concentration (µg/ml)	Source
Donkey	Anti-Rabbit	IgG (H+L)	FITC	1:100	Jackson
Donkey	Anti-Mouse	IgG (H+L)	TRITC	1:100	Jackson

2.3 RNA Isolation

All techniques were carried out under RNase free conditions using filtered pipette tips (Starlabs). The workbench and pipettes were sprayed with 70% ethanol and RNA-Zap (Ambion) before commencing.

Adult vibrissa follicles were isolated and staged from six rats (see 2.1.1). Once staged the follicles were cut transversely at the neck to remove the hair fibre/s and subsequently split into two groups (stored in culture dishes containing MEM) i) Mid-Anagen ii) other stages. The other stages were mounted and snap frozen for immunohistochemistry (see 2.2.1) so material was not wasted, as only RNA from the Mid-Anagen stage was required. Each follicle from the Mid-Anagen group was dissected into Upper Follicle (MA-UF), Mid Follicle (MA-MF) and End Bulb (MA-EB), with incisions made at the level of the ringwulst and just above the end bulb. To isolate the RNA, the kit ToTALLY™ RNA (Ambion) was used. Dissected follicle sections were put into the appropriate test tubes containing 750µl Denaturising Solution.

All samples were manually processed to homogenisation. Following homogenisation the samples were centrifuged for 2-3 minutes at top speed to remove any debris present in the lysate. After lysate preparation, each sample was ready to continue with the RNA isolation.

2.3.1 Phenol:Chloroform:IAA Extraction

The volume of the lysate at this point is now the *Starting Volume*. After centrifugation the lysate was transferred to another 1.5ml tube where 1 *Starting Volume* of Phenol:Chloroform:IAA was added to the lysate. Care was taken to ensure the organic phase of the solution was taken and not the interphase or below layers. The tube was then vortexed for 1 minute, incubated on ice for 5 minutes then centrifuged at 11,000 x g for 5 minutes. After centrifugation, the upper aqueous layer was carefully transferred to a new vessel and measured again.

2.3.2 Acid Phenol Extraction

1/10 of Aqueous Phase volume of Sodium Acetate solution was added to the phenol extracted lysate and mixed by shaking for approximately 10 seconds. 1 *Starting Volume* of Phenol:Chloroform:IAA was added to this mixture and then vortexed for 1 minute. The lysate and phenol were then stored on ice again for 5 minutes and centrifuged at 11,000 x g for 5 minutes. After centrifugation, the upper aqueous layer was carefully transferred to a new RNase-free vessel and measured again.

2.3.3 Isopropanol Precipitation of RNA

Using the new measured volume, an equal volume of isopropanol was added to the RNA prep and mixed well. The tube was stored at -20°C overnight to allow a white precipitate to form, indicating the presence of RNA.

The precipitation mixture was centrifuged at 11,000 x g for 15 minutes and the supernatant carefully removed and discarded using a fine-tipped pipette. The tube was re-spun briefly and any residual fluid was removed.

To remove any residual salts the pellet was washed in 70% ethanol. 300µl ethanol was added to the tube and gently vortexed for 2-3 minutes. The RNA was recovered by centrifugation at 3,000 x g for 10 minutes and the supernatant was carefully removed. The pellet was resuspended in 100µl of DEPC treated distilled water yielding a reasonable RNA concentration.

2.3.4 Quality of RNA

A small aliquot of the total RNA isolation was mixed with 5µl of 10X RNA loading buffer and loaded onto a 2% agarose gel (see Appendix 5.1.7). The gel was electrophoresed at 90 volts until the loading dye had moved 4-5 cm and a Polaroid taken using a Gel Doc 2000 transilluminator (Bio-Rad, UK) running Quantity One software. This was performed to check the quality of RNA and to check for DNA contamination.

2.3.5 DNase Treatment

To remove genomic contamination from the total RNA preparation Ambion's DNA-free kit was used by the following method. 10µl of 10X DNase I buffer and 1µl of rDNase I (2U) was added to 100µl of RNA and incubated for 30 minutes at 37°C. 10µl of resuspended DNase Inactivation Reagent was then added and incubated for 2 minutes at room temperature, mixing occasionally. The mixture was then centrifuged at 10,000 x g for 1 minute to pellet the DNase Inactivation Reagent. The supernatant containing the DNA-free RNA was transferred to a clean tube. The extracted RNA was stored at -80°C for long-term storage.

2.3.6 Quantification of RNA by Spectophotometry

To check the purity and concentration of the DNase treated RNA a small sample was analysed in a spectrophotometer. The RNA was diluted 1:100 using DEPC treated distilled water and transferred to a clean glass cuvette. Absorbance readings were taken at 260 and 280nm against a DEPC water blank. The concentration of RNA was estimated by calculating the ratio of the OD readings. Readings above 1.7 were considered to indicate good quality RNA, according to the kit instructions.

2.4 Reverse Transcription Polymerase chain reaction

2.4.1 Reverse transcriptase (RT)

Total RNA samples were reverse transcribed using the T7 oligo-dT primer (Invitrogen). 1µl of the primer and 1µl of dNTPs (Invitrogen) was added to the correct amount of RNA sample (1000ng/µl) then made up to 12µl with DEPC treated distilled water. The resulting mixture was heated at 65°C for 10 minutes to disrupt the RNA secondary structure then immediately ice cooled for a further 5 minutes. 2µl of 0.1M DTT (Invitrogen) and 4µl of 5X first strand buffer (Invitrogen) were added to each reaction, mixed gently by pipetting and heated at 42°C for 2 minutes. 1µl of Superscript II RT (Invitrogen) was added then made up to a final 20µl volume by adding 1µl of DEPC treated distilled water. The resulting mixture was mixed by pipetting and incubated at 42°C for 50 minutes then at 70°C for 15 minutes to inactivate the enzyme. The cDNA samples were then stored at -20°C until required for PCR on the genes of interest.

The cDNA samples (MA-UF, MA-MF, MA-EB) together with -RT controls for each sample (the -RT is a mock reverse transcription containing all the RT-PCR reagents, except the reverse transcriptase) were used in a PCR (see 2.5.3) for the housekeeping gene glyceraldehyde-3-phosphate dehydrogenase (GAPDH). Absence of product in the -RT wells was taken to indicate no detectable genomic contamination.

2.4.2 Primer Design

Specific primers (Table 2.3) were designed from the cDNA sequence of the gene of interest using data available from www.ncbi.nlm.nih.gov. Primers were designed complimentary to both rat and mouse cDNA sequences where possible. This was achieved by aligning both sequences (noting the accession number) for the same gene of interest using BLAST (bl2seq). Sequences towards the 3' end were chosen using the following criteria: between 20-30 base pairs (bp) long; having a GC content between 50-60%; giving a product between 300-600bp; having a basic melting temperature (T_m) of around 60°C. An oligonucleotide properties calculator was used to assist in primer design (www.basic.nwu.edu/biotools/oligocalc.html). The resulting sequences were checked for specificity using a nucleotide-nucleotide blast search (blastn) before being sent to Sigma for production. The stock primers received from Sigma were diluted to give a concentration of 500pmol/µl, with working stocks made up using a 1:100 dilution giving a 5pmol/µl working concentration. All primers were kept at -20°C.

2.4.3 Polymerase chain reaction (PCR)

For the polymerase chain reaction the following reagents (Invitrogen) were added to each reaction tube with the cDNA added last (Note a master mix was made depending on the number of simultaneous reactions to reduce error between reactions):

ddH_20	19.75µl
10X Buffer	2.5µl
cDNA sample	1.0µl
50µM $MgCl_2$	0.75µl
5' Primer	0.75µl
3' Primer	0.75µl
10mM dNTP	0.50µl
Taq Polymerase	0.25µl

On addition of the cDNA, the reaction tubes were spun at 3000 x g for 20 seconds. The PCR reactions were carried out on a Perkin Elmer thermal cycler using the following programme:

94°C	3 minutes	1 cycle
94°C	1 minute	25-35 cycles
'Primer Annealing Temperature' (Table 2.3)	1 minute	25-35 cycles
72°C	2 minutes	25-35 cycles
72°C	10 minutes	1 cycle

The PCR products were run down a 2% agarose gel (see Appendix 5.1.7) with 5µl of Molecular Marker (Invitrogen). The resulting images of the DNA bands were visualised using a Gel Doc 2000 transilluminator (Bio-Rad, UK) and a Polaroid taken for records.

To check that the concentration of cDNA in each sample (MA-UF, MA-MF, MA-EB) was equal, a PCR was setup for GAPDH comparing the products for 0.5µl and 1µl cDNA at 25 cycles. If loading is equal all the 0.5µl cDNA samples will have identical bands, as will the 1µl samples. The 0.5µl reactions were included

for comparison incase the 1µl reactions had passed through the exponential phase of the reaction and reached a plateau. All PCR reactions were repeated at least twice for consistency.

Table 2.3 Primers designed and used for RT-PCR analysis

Gene	Primer Sequence	Product Size (bp)	Accession Number	Annealing Temperature (°C)
MRP1	(F) CTGTGGATCATCTGCTGGGCAGA	448 (R)	NM_022281.2 (R)	62
	(R) GCACCATCATCCCTGTAATCCACC	448 (M)	NM_008576.1 (M)	
BCRP	(F) AGGCGGAGGCAAGTCTTCGTTG	391 (R)	NM_181381.2 (R)	61
	(R) GGGCTCATCCAGGAAGAGGATG	391 (M)	NM_011920.1 (M)	
Id2	(F) CACGGACATCAGCATCCTGTCCTT	559 (R)	BC086391.1 (R)	61
	(R) CAGTAGGCTCGTGTCAAAAAGGCC	532 (M)	NM_010496.2 (M)	
Id3	(F) CTGAGCTCACTCCGGAACTTGTGA	430 (R)	BC064658.1 (R)	62
	(R) CAGCTCTTATGCTGCCTTGGCAG	426 (M)	NM_008321.1 (M)	
GAPDH	(F) ATGGCCTACATGGCCTCCAAGG	184 (R)	BC_087743 (R)	58
	(R) AGGCCCCTCCTGTTGTTATGGG	184 (M)	BC_083149 (M)	

2.5 Cell Culture

2.5.1 Glandular Morphogenesis Experiment

2 female Wistar rats (LSSU, Durham University) bred to obtain embryos of a known age provided the tissue for organ culture. Their age was calculated by regarding the appearance of a vaginal plug as the beginning of day 0. Skin was dissected from the developing mystacial pad of embryos aged 13.5 and 14 days (see 2.1.4). Because of variation in development of supposed same stage embryos, whisker pads from the same embryo were noted for analysis of results later.

The retinoid used for culturing was all-*trans* retinoic acid (tRA; Sigma). RA was completely dissolved in absolute ethanol to give a stock concentration of 500μg/ml. The stock was aliquoted into sterile 1.5ml tubes and kept at -20°C. Because of the instability of RA, this compound and mixtures containing it were handled in dim light, protected with aluminium foil and stored at either -20°C or 4°C. 10ml of fresh culture medium containing 20% FCS was prepared in a universal tube (see Appendix 5.1.5) with 0.1ml of tRA stock added to give a final working concentration of 5μg/ml. Control medium was prepared in the same way except RA was replaced by absolute ethanol. Cultures were incubated at 37°C in an atmosphere of 5% CO_2, 95% air.

2.5.2 Embryo Mystacial Pad Culture

The embryo mystacial pads were cultured in 24-well plates (Nunc) containing membrane inserts (Millipore) and 550μl of prepared culture medium (see Appendix 5.1.5). For each embryo, 13.5 and 14 day (E13.5 and E14), one pad

was set up in RA containing medium (+RA) and the complimentary pad set up in control medium (-RA).

The 13.5 day embryo mystacial pads were set up according to Figure 2.4, with a total of 4 RA and 4 control cultures. The 14d embryo mystacial pads were set up similarly with a total of 6 RA and 4 control cultures. All mystacial pads were placed dermis-side down and ensured they had enough medium but were never submerged or lacking in medium. The number of mystacial pads cultured was not equal due to differences in the number of embryos being carried by the female rats.

Cultures were removed after 2.5, 4 and 5 days (no 2.5 day cultures were removed in the E13.5 mystacial pads because of less mystacial pads to culture and it was preferred to have results from pads that had been cultured longer). The cultures were removed and either mounted and snap frozen in liquid nitrogen (see 2.1.1) for immunohistochemistry (see 2.5.3) or fixed in 4% formal saline for paraffin wax embedding (Table 2.4 and 2.5) (see 2.5.4).

2.5.3 Immunohistochemistry

Frozen mystacial pad cultures were used for immunohistochemistry following the procedure described in 2.3. Double-immunolabelling was performed using the antibodies Id2 and CK-20, Id2 and Synaptophysin and Id3 and β-catenin (Table 2.1). An H&E stain was also performed on the serial sections (see 2.2.8).

2.5.4 Paraffin Wax Embedding

Cultures fixed in 4% formal saline were prepared for wax embedding. The samples were dehydrated through 70%, 90% and absolute alcohol for 30 minutes with 3 repetitions each. Following this the samples were incubated in Histoclear for 30 minutes, again with 3 repetitions. Molten wax was added to the samples and left in the oven for 1hour at 60°C, repeated 3 times whilst discarding as much of the old wax as possible each time. The samples were then transferred to fresh wax in a hot glass mounting block, orientated whilst it was setting then left for a further hour in the fridge to set properly.

2.5.5 Microtome Sectioning

The wax embedded cultures were removed from their glass moulds, trimmed using a razor blade and mounted onto a wooden block. The sample was secured by melting wax chippings on the block and positioning the sample on the wax. The samples were sectioned using a Leica Microtome set to a thickness of 10μm. Ribbons of sections were transferred to clean glass slides by floating them on water. The water had been boiled and allowed to cool to reduce air bubbles when sticking the sections to the slides. The slides were then left on a slide heater to evaporate the water and melt the wax sections enabling them to adhere to the slides.

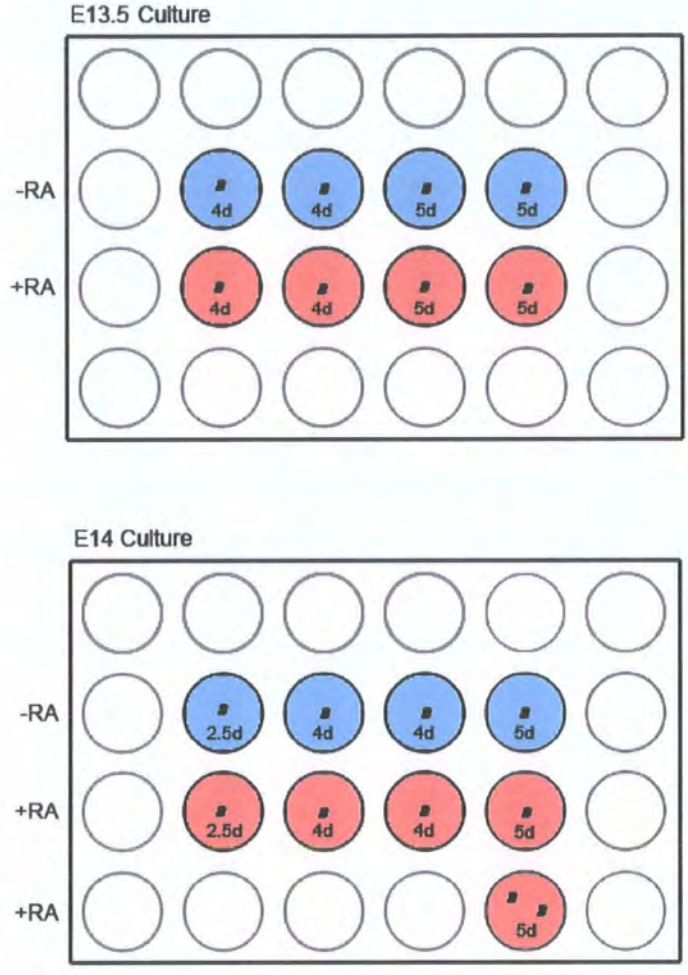

Figure 2.4. Embryo mystacial pad cultures
Diagram showing the set up of E13.5 and E14 mystacial pad cultures in a 24-well plate. The -RA controls (blue) and the +RA cultures (blue) were stopped after 2.5, 4 and 5 days as shown. E13.5 samples were stopped after 4 and 5 days only. The cultures were either snap frozen or fixed in 4% Formal Saline for analysis. Note: one well in E14 cultures had 2 mystacial pads being cultured.

Table 2.4 Summary of E13.5 mystacial pad cultures detailing the duration of culture and method of preservation for analysis.

Culture Length	+RA		-RA	
	Frozen	Fixed	Frozen	Fixed
2.5d	n/a	n/a	n/a	n/a
4d	1	1	1	1
5d	1	1	1	1

Table 2.5 Summary of E14 mystacial pad cultures detailing the duration of culture and method of preservation for analysis.

Culture Length	+RA		-RA	
	Frozen	Fixed	Frozen	Fixed
2.5d	1	0	1	0
4d	1	1	1	1
5d	2	1	0	1

3.0 Results

Throughout the results and discussion, vibrissa follicle development is described in stages. Please refer to Figure 3.1 for a description.

3.1 Id2

Id2 expression was investigated in the mystacial pad of rats, covering early follicle development through to newborn and adult follicles. In early development (stage 1-2) Id2 immunolabelling was significantly higher in the epithelial placode compared to the surrounding epidermis and dermis (Figure 3.2A,B; arrows). At stage 2-3 follicles, Id2 staining was strong at the base of the hair peg (Figure 3.2C; arrows), although this expression was not consistent throughout every follicle. Interestingly, a few individual cells around the neck of developing follicles displayed very high expression of Id2 (Figure 3.2C-E; arrowheads). These cells were first apparent in embryonic day 16 (E16) sections (stage 1-4 follicles).

Id2 expression was not limited to follicle development and the epidermis, but was also found significantly in the developing eye and palate of E16 head sections. Nerve-like staining was seen with Id2 expression in the developing eye (Figure 3.3A,B) whilst highly specific and polarised staining of the epithelial palate was demonstrated with Id2 targeted to the membrane of cells at the epithelial-mesenchymal border (Figure 3.3C,D; arrows). Occasionally a few distinct cells in the basal layer of the palate also stained significantly for Id2 (Figure 3.2D; arrowhead).

Immunostaining of embryonic day 18 (E18) sections revealed a population of Id2 expressing cells in the outer root sheath (ORS) of stage 6+ follicles located around the bulge region (Figure 3.4B; arrows). Serial sections through the follicles revealed these cells to densely populate the ORS at the bulge level, surrounding the inner root sheath (IRS) and hair shaft. Similarly stained cells were also present in large numbers around the neck of the follicle, the rete ridge collar, with very few of these cells appearing to be between these distinct regions (Figure 3.4C). The basal layer of the epidermis was also found to contain many Id2-positive cells throughout the mystacial pad (Figure 3.4E; arrows). On the opposite side to deep vibrissal nerve entry (DVN), Id2 staining was seen in cells lining the outside of the mesenchymal capsule, spanning the suprabulbar and isthmus regions (Figure 3.4A,G; arrowheads). These cells were not present on pelage follicles or developing vibrissae before stage 6. In developing pelage follicles, high Id2 expression was seen in cells at the base of the epithelial peg (Figure 3.4D; arrows). Distinctive Id2 staining was also seen in basal cells of the interfollicular epidermis (Figure 3.4D; arrowhead).

At this stage of development, a developing structure located in a region of the rat forebrain also showed distinct Id2 immunolabelling (Figure 3.4F). It should be noted that due to the fibrous and keratinizing nature of the hair shaft and cells above the matrix respectively, ambiguous staining was seen (Figure 3.4A,B,D,E,G; asterisk). Unfortunately this was quite common when staining vibrissa follicles with polyclonal antibodies. These results indicated that Id2 may be staining specialised nerve cells in the mystacial pad, but it was not labelling the main DVN or the large nerves of the hypodermis. To investigate nerve activity in vibrissae and the mystacial pad, double immunolabelling was performed with Id2 and synaptophysin (Syp).

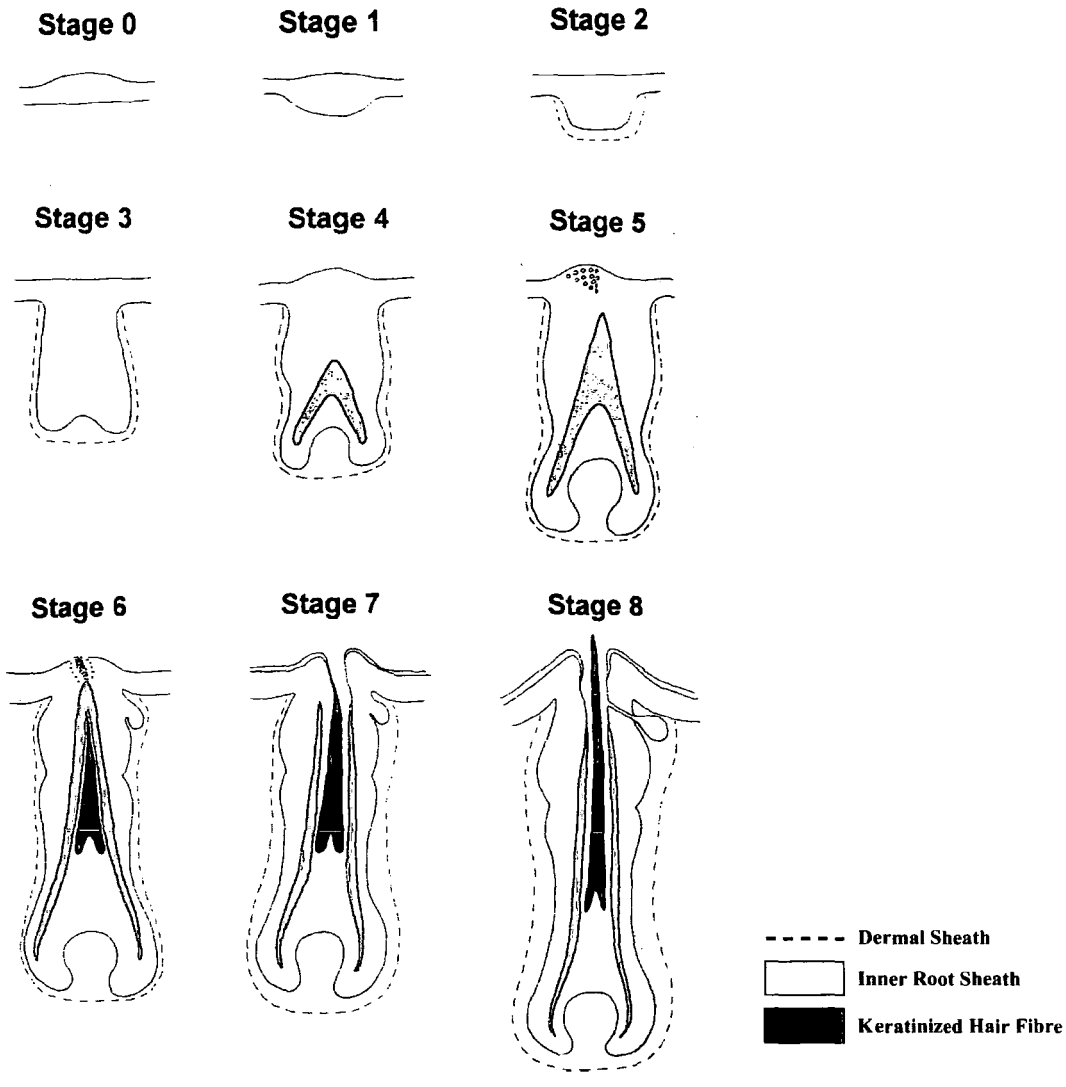

Figure 3.1. Stages of vibrissa morphogenesis

Diagram showing the developmental stages of vibrissa follicle morphogenesis. Stage 0, thickening of the epidermis results in the epidermal placode forming; Stage 1, epidermis begins to invade the underlying dermis; Stage 2, the epidermal plug is now surrounded by the densely packed dermal cells which will become the dermal papilla and sheath; Stage 3, the presumptive dermal papilla is now surrounded by the invaginating epidermal downgrowth; Stage 4, the characteristic bulbous shape of the follicle starts to appear as does the keratinized inner root sheath; Stage 5, cells at the surface of the epidermis begin to differentiate in preparation for formation of the hair canal; Stage 6, apoptosis occurs at the presumptive hair canal, the developing sebaceous gland is visible and keratinized hair fibre is present; Stage 7, the hair canal opens; Stage 8, keratinized hair fibre emerges from the follicle (adapted from Davidson & Hardy, 1952).

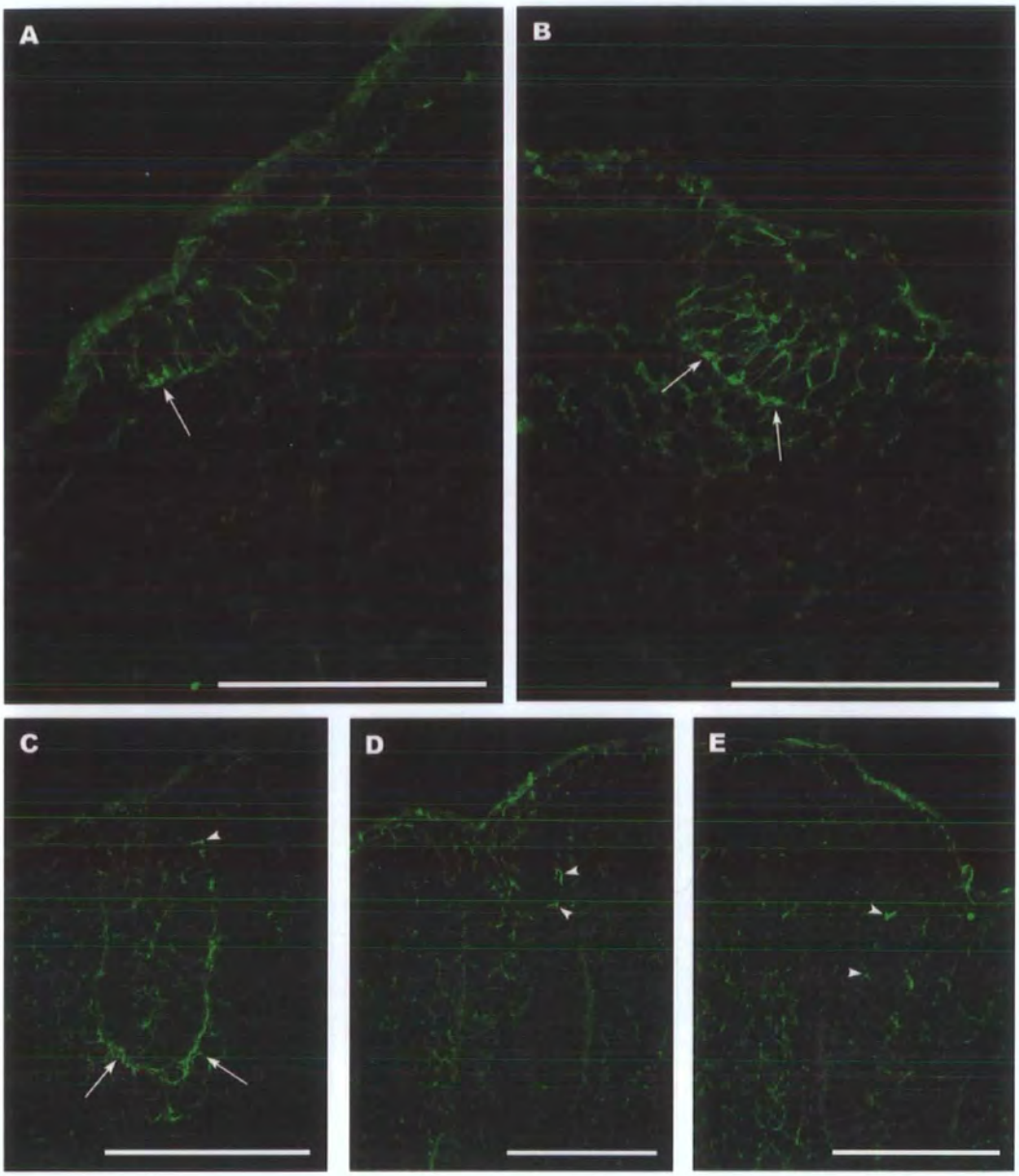

Figure 3.2. Immunocytochemical staining of E16 mystacial pads.
Staining with Id2 in stage 1-2 developing follicles shows higher levels of Id2 in the epithelial placode and hair peg compared to the surrounding mesenchyme (A-C; arrows). High levels of Id2 expression is seen in some cells in the basal epithelium at the neck of the follicle (C-E; arrowheads). Scale bar, 100μm (A-E).

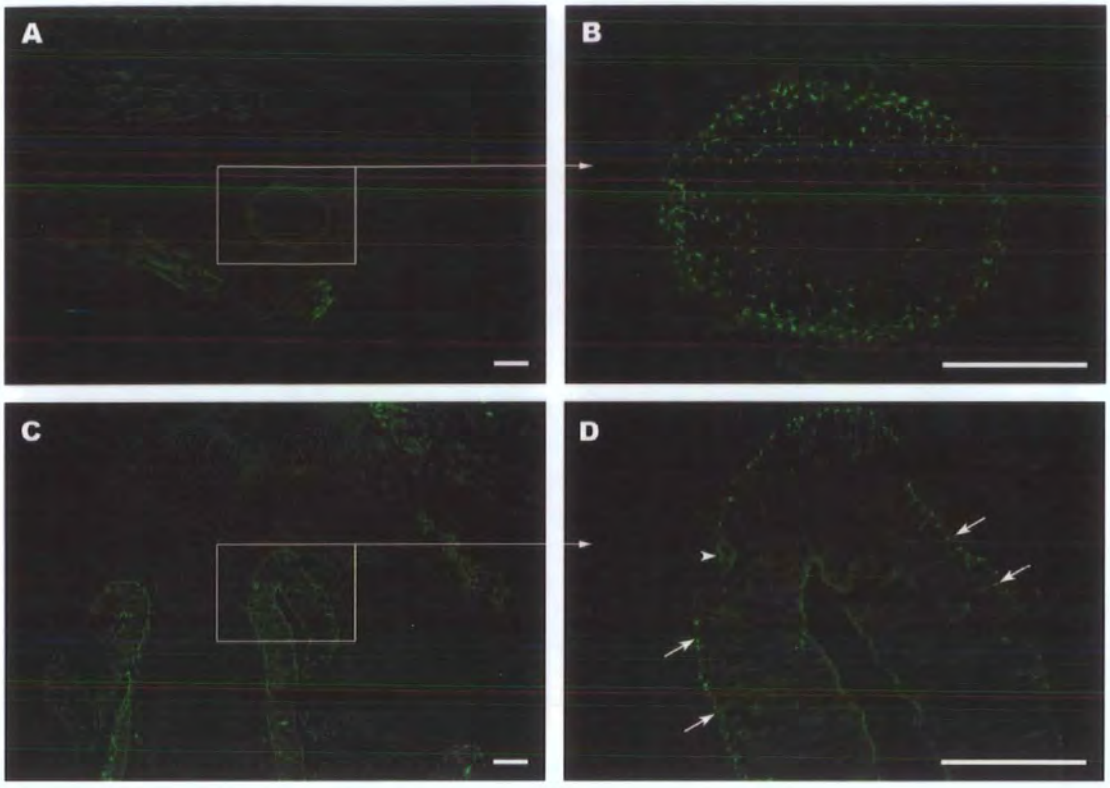

Figure 3.3. Other structures expressing Id2 in E16 head.

Id2 expression was seen in the developing eye and main nerves around the eye (A,B). High expression was also seen in cells in the basal layer of the epithelial palate (C,D). All expression appears to be cytoplasmic and basally polarised. Scale bar, 100μm (A-H).

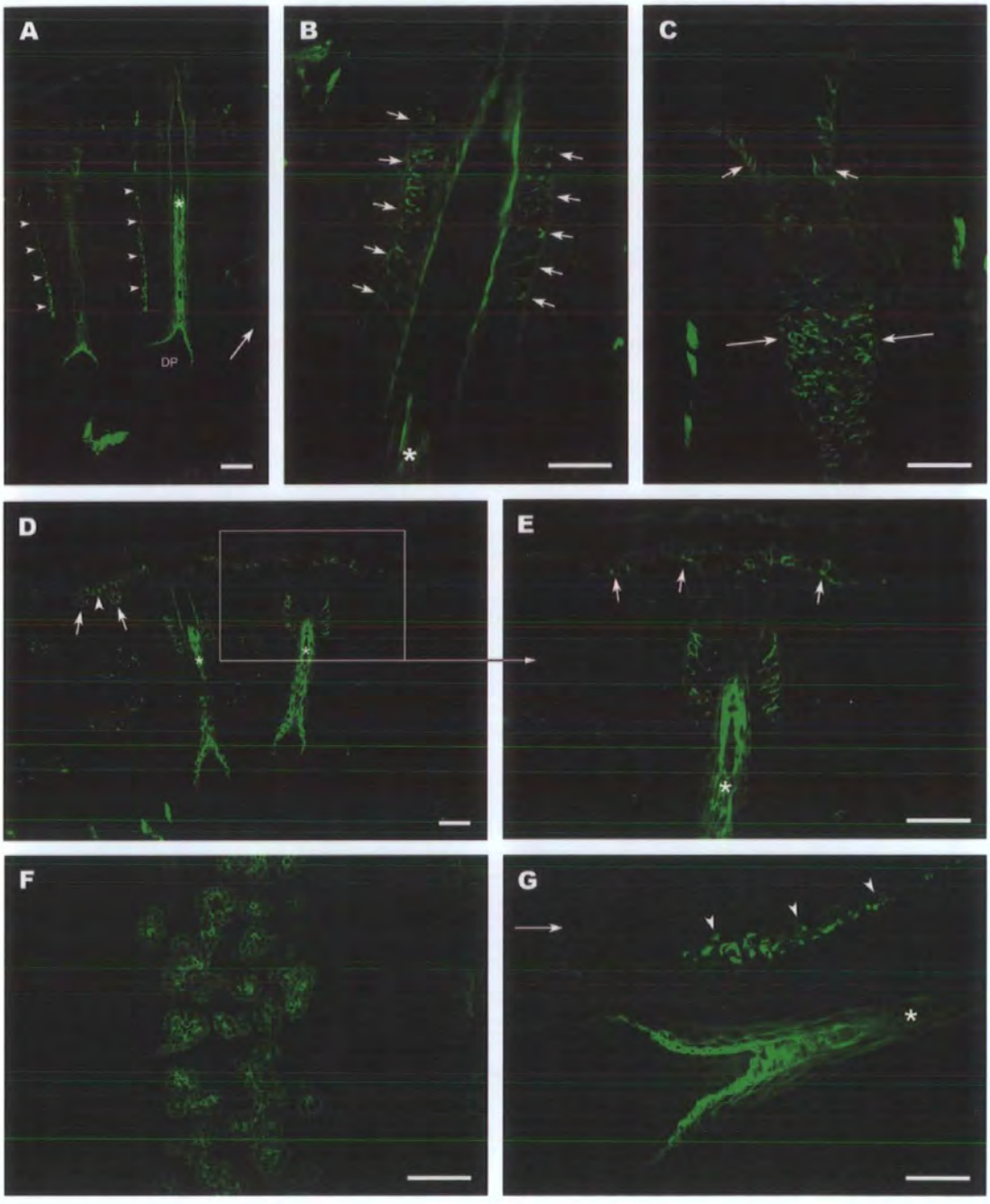

Figure 3.4. Id2 expression patterns in E18 head.

Cells very immunoreactive for Id2 were seen in the ORS of vibrissae at the bulge region, the rete ridge collar and spread throughout the basal epidermis of the skin (A-E). Id2 staining also seen on the outside of the mesenchymal capsule (A,G; arrowheads), on the opposite side to deep vibrissal nerve (DVN) entry (A,G; arrows). In the developing rat forebrain, positive staining was also seen (F). Note ambiguous staining of the hair shaft and cells in the keratinising zone of the matrix (A,B,D,E,G; asterisk). Scale bar, 100μm (A-G).

3.2 Id2 and Synaptophysin

Double immunolabelling was performed with Id2 and synaptophysin (Syp), a marker of synaptic vesicles, covering early follicle development through to adult follicles. In E16 sections, at stages 1-2 no Syp was present in the epithelial placode or in the mesenchymal cells directly beneath it, however small amounts were detected deeper in the dermis below the developing placode (Figure 3.5A). By stage 3, the developing follicle had elongated into the dermis and the dermal condensation had started to aggregate to form the presumptive papilla. It was at this stage Syp labelling was intense around the dermal condensation, with small traces extending up the side of the epithelial hair peg. Syp expression was also much higher in the dermis between developing follicles. Interestingly, the Id2-positive cells in the basal epithelium of the developing follicle showed no Syp immunoreactivity (Figure 3.5E,F,H; long arrows). At stage 4-5 of development, the DVN had clearly innervated the mid-follicle with high Syp expression in the mesenchymal cells directly either side of the hair peg. Serial sections showing different stages of follicle development illustrated how the DVN branched to innervate the mid-follicle (Figure 3.5F,G; arrowheads).

Immunostaining of well developed follicles in embryonic day 20 (E20) mystacial pad gave some very interesting results with Id2 and Syp antibodies. Id2 as expected was expressed in the cells at the bulge region in the ORS and down the side of the follicle on the opposite side to DVN entry. Upon staining with Syp, it was apparent that synaptophysin was co-localised in the Id2 expressing cells of the ORS and also strongly expressed in the cells in direct contact in this region, namely the mesenchymal connective tissue (Figure 3.6E,F; arrows). Syp expression continued

lower down the follicle (Figure 3.6E; arrowheads) where Id2 expression was absent. The Id2-positive cells lining the mesenchymal capsule also showed Syp expression in cells in direct contact with the Id2 expressing cells and appeared not to be co-expressed (Figure 3.6G-I; arrows).

In the basal epithelium, the cells immunoreactive for Id2 also strongly expressed Syp (Figure 3.7A,B,C; short arrows). Double immunolabelling illustrated this particularly well in a developing follicle (Figure 3.7C). Although some Id2-positive cells appear not to express Syp, this could be because Syp expression may not be uniform throughout the cell so would depend on the section. Synaptophysin staining revealed not just co-localisation to Id2-positive cells but elaborate networks of synaptic transmission running throughout the dermis and epidermis (Figure 3.7D; arrowheads).

High power microscopy of the basal epithelium containing these cells immunoreactive for Id2 showed their detailed ultrastructure(Figure 3.7D; arrow). As observed in E18 sections, these specialised cells were still present in large numbers at the bulge region and the rete ridge collar of the follicle, but showed little or no presence between these distinct areas (Figure 3.4C,E; 3.6F; arrowheads).

Later on in development, Id2 and Syp expression was examined in the neonatal mystacial pad, with ages ranging from newborn (P0) to 4 day old (P4). Compared to E20, the vibrissa follicles were much bigger with more defined inner root sheath (IRS) layers and a relatively thinner ORS (Figure 3.8D).

Double immunolabelling with both antibodies at P1 revealed the cells in the ORS at the bulge region were still co-localised for both Id2 and Syp. Expression of synaptophysin was still strong in these cells but it appeared that Id2 immunoreactivity had decreased compared to previous staining (Figure 3.8D,E,F; arrows). Interestingly the cells lining the mesenchymal capsule seen in E18 and E20 sections which expressed Id2 highly appeared to be present on both sides of the follicle now. These cells showed characteristics of being muscle cells and were still interspersed with Syp expressing cells (Fig 3.7A,C; arrowheads).

Immunolabelling of Id2 was still seen in cells in the basal epithelium and at the follicle neck of vibrissa follicles but no distinctive Id2 cellular staining was seen in pelage follicles. Consistent with earlier staining, Id2-positive cells within the basal epidermis were still found scattered throughout the skin but it was more apparent in neonatal skin that they were found at or near sites of follicle development. Although the numbers of these cells in the basal epithelium seem to have diminished at this stage, it is likely they have remained unchanged whilst the surrounding skin has grown considerably spreading them out.

Expression of both antibodies in P4 mystacial pads produced results consistent with those seen previously (Figure 3.9). Serial sections through these large follicles stained for Id2 and Syp illustrated the morphology and density of these specialised cells (Figure 3.9C,D; arrows) and also their innervation revealed by synaptophysin staining nearby.

To complete the profile for the Id2 expression, adult follicles in various stages of the cycle were double labelled for Id2 and Syp. In a mid-anagen follicle, Id2 staining revealed cells in the ORS expressing Id2. Due to the increased background staining seen in adult follicles and the relatively thinner ORS layer, locating these cells was difficult. Closer inspection revealed they were still present in large numbers and still expressing Id2 (Figure 3.10A; long arrows). Comparing with synaptophysin labelling confirmed the co-localisation in these cells and also highlighted regions of the collagen capsule and layers immediately outside the ORS expressing high levels of Syp (Figure 3.10B,C; long arrows). In the IRS layers surrounding the hair shaft, a few cells expressed high levels of Id2, many of these also showed increased background levels with Syp staining. These are artefacts of staining due to the level of keratinisation here (Figure 3.10A,B; short arrows).

Immunostaining of catagen follicles gave results consistent with those seen in the mid-anagen stage of the vibrissa cycle. The Id2-positive cells in the ORS clearly showed high expression above background levels and also co-localisation for Syp (Figure 3.10D,E; arrows). Synaptophysin was also abundant in the collagen capsule in this region (Figure 3.10E; arrowheads). Under high magnification in a different catagen, these cells were easier to locate, expressing high levels of both antibodies (Figure 3.10G,H,I; long arrows).

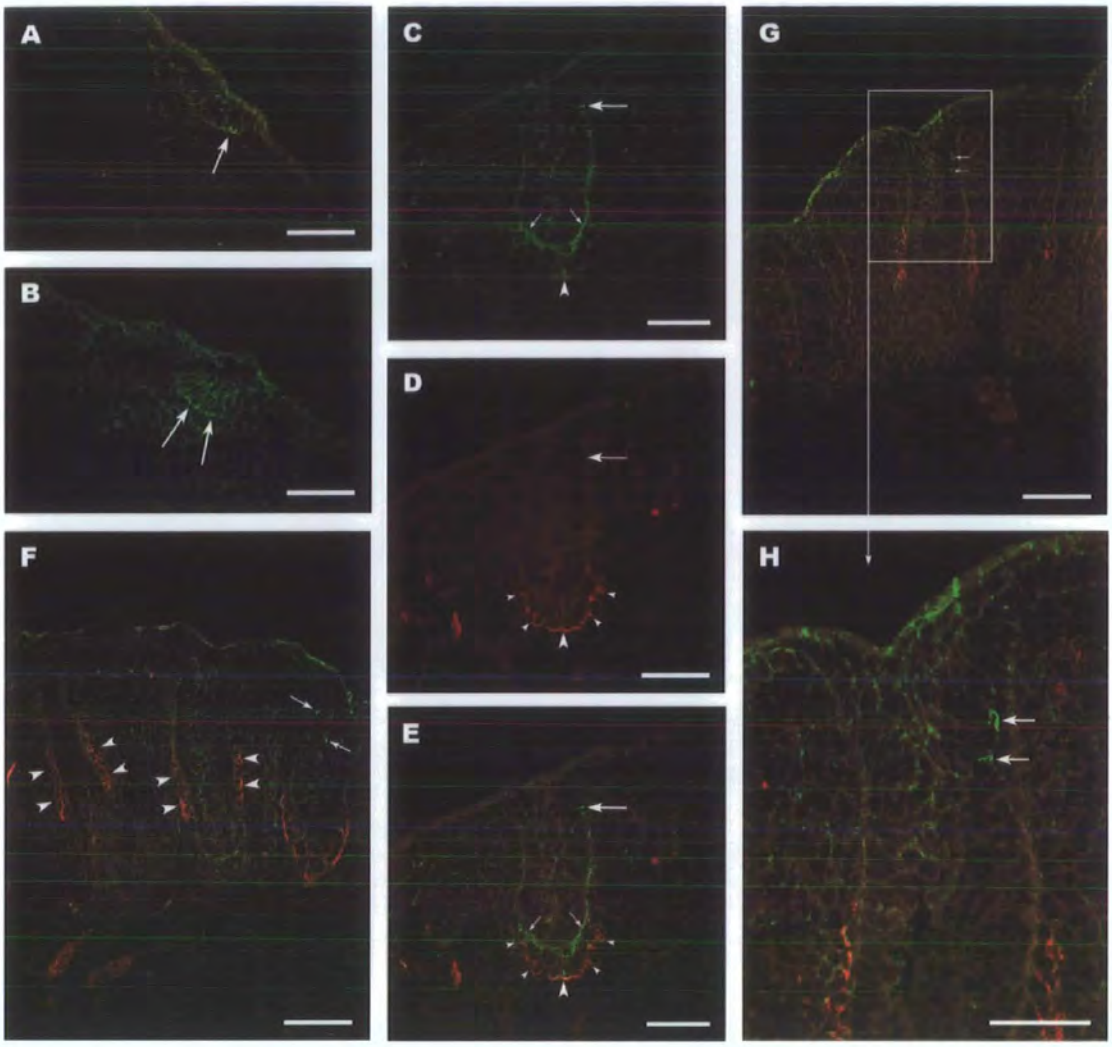

Figure 3.5. Double immunolabelling with Id2 and Synaptophysin in E16 mystacial pads.

Staining with Id2 in stage 1-2 developing follicles shows higher levels of Id2 (green) in the epithelial placode compared to the surrounding mesenchyme (A,B). Double immunolabelling with Id2 (green) and synaptophysin (red) shows the level of innervation in the developing follicles, around the presumptive papilla in stage 3 (D,E) then extending towards the mid-follicle level by stage 4-5 (F,G). Strong Id2 (green) expression is seen in some cells in the basal epithelium at the neck of the follicle (C,F,H; arrows). Scale bar, 100μm (A-H).

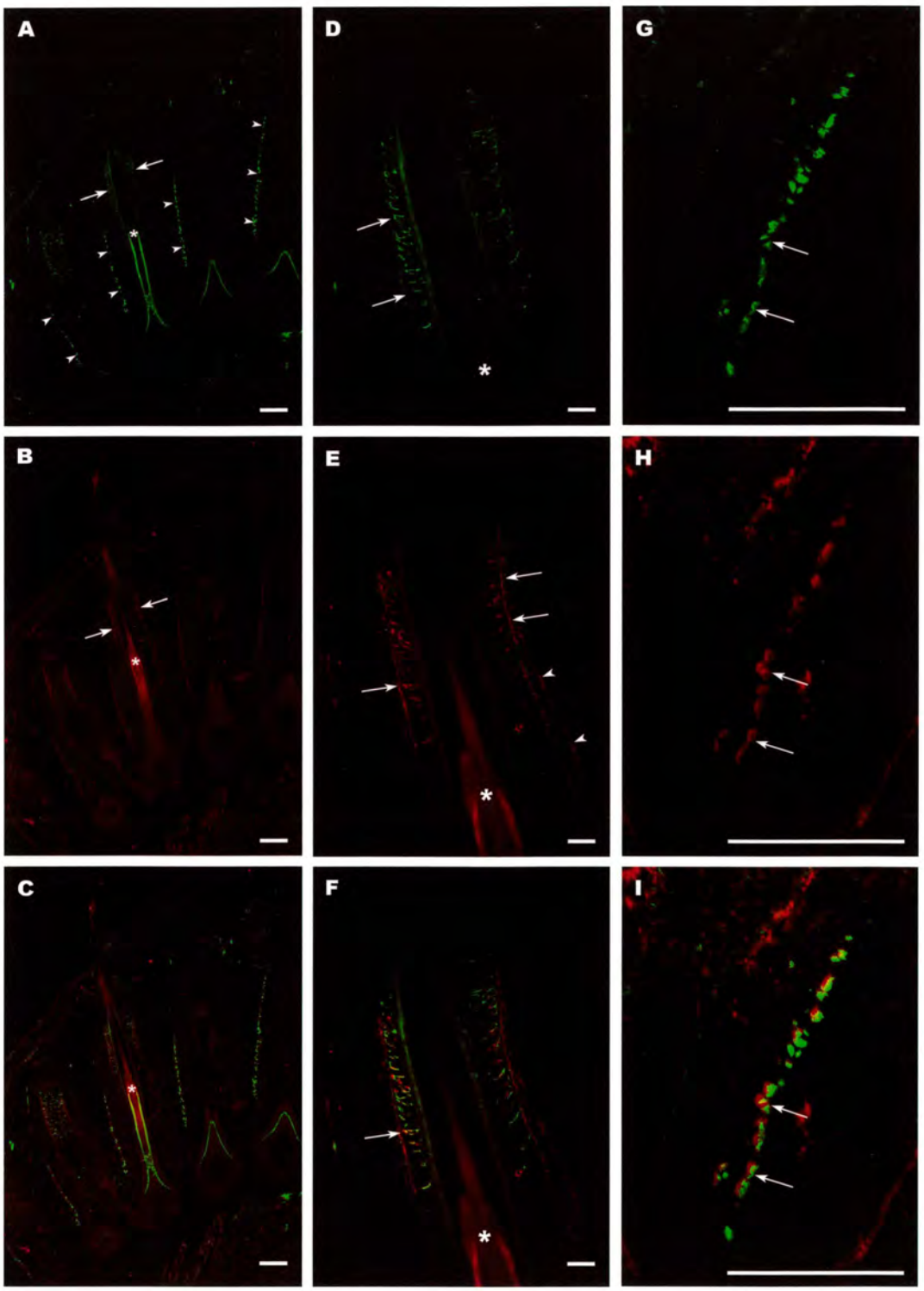

Figure 3.6. Id2 and Synaptophysin co-localisation in E20 mystacial pad.

Id2 (green) expressing cells in the ORS show co-localisation with synaptophysin (red) (C,F; arrows). Synaptophysin was expressed not just in the same cells expressing Id2, but on the membrane outside the ORS and was seen to extend further down the follicle (E,F; arrowheads). Synaptophysin (red) expressing cells were located next to cells expressing Id2 (green) (G-I; arrows) down the side of the mesenchymal capsule. Note the ambiguous staining of the hair shaft (A-F; asterisk). Scale bar, 100μm (A-C, G-I), 50μm (D-F).

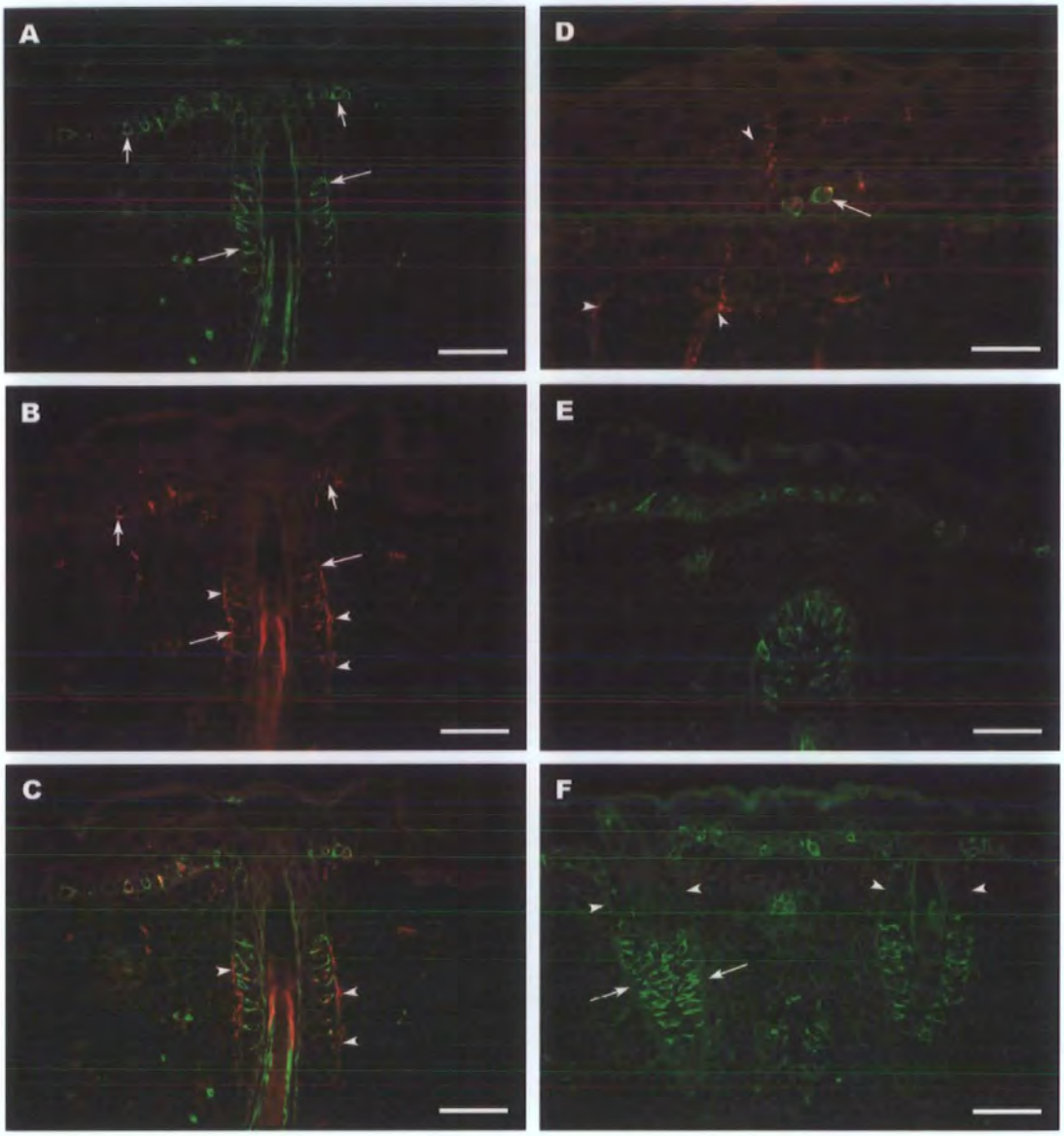

Figure 3.7. Id2 and Synaptophysin co-localisation is not limited to the follicular ORS in E20 mystacial pad.

Double immunolabelling with Id2 (green) and synaptophysin (red) shows co-localisation in the ORS cells of the follicle at the bulge region and also in the basal epidermis of the skin (A-C; arrows). Co-expression is shown in yellow (C,D; arrow). Closer examination of synaptophysin staining revealed networks running throughout the dermis and epidermis (D; arrowheads). Id2-positive cells in the ORS of the follicles are densely packed in the bulge region (F; arrows) but are present in much reduced numbers just above this region (F; arrowheads). Scale bar, 50μm (A-F).

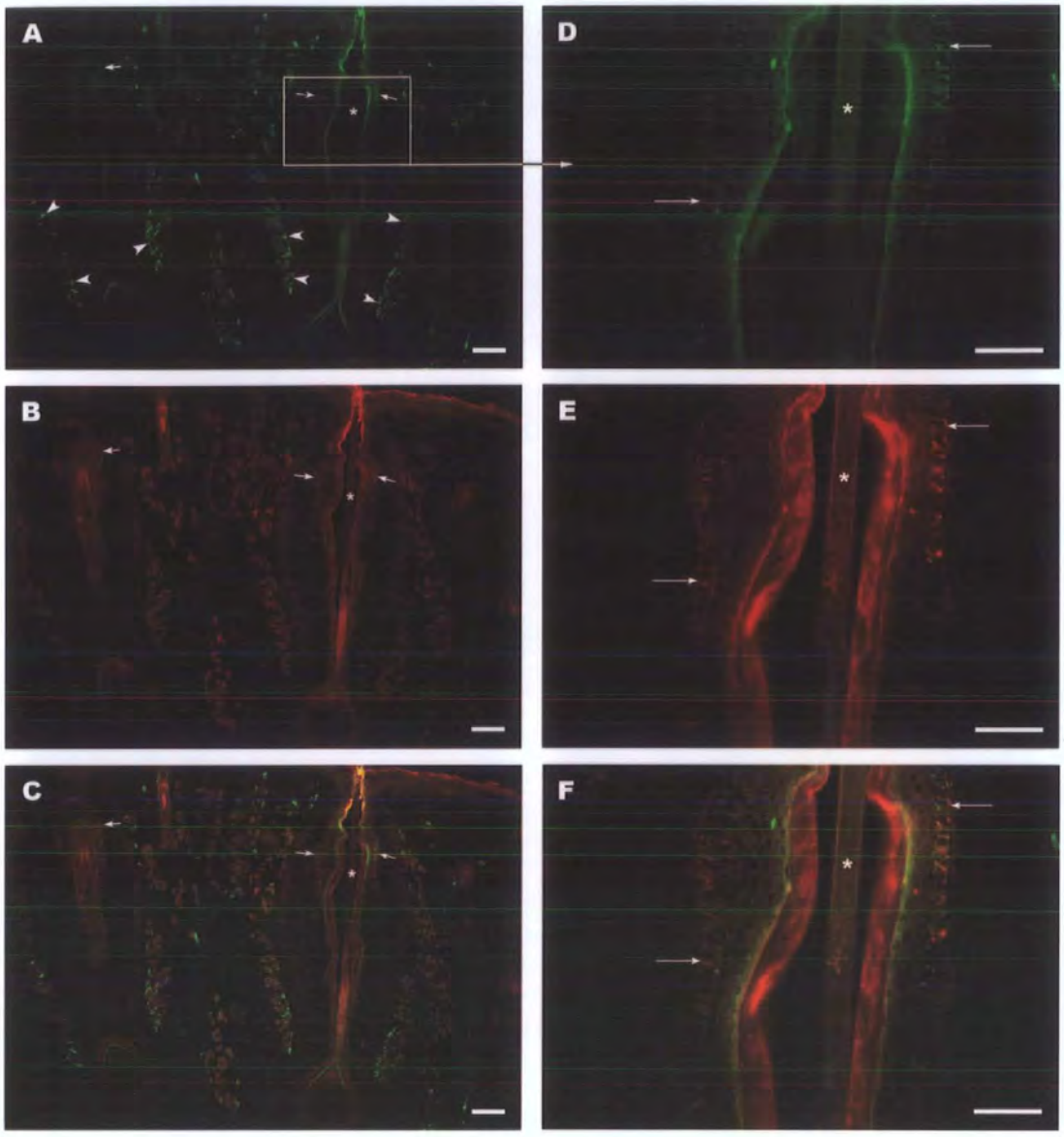

Figure 3.8. Id2 and Synaptophysin co-localisation in neonatal (P1) mystacial pad.

Cells in the bulge region of the ORS were still expressing Id2 (green) but at lower levels than seen in embryonic skin (D; arrows). The Id2-positive cells lining the mesenchymal capsule are absent but new staining is seen in the muscle cells either side of the vibrissae (A; arrowheads). Double labelling with synaptophysin (red) confirms co-localisation still in the ORS cells but not in the muscle cells (E,F; arrows). Note ambiguous staining of the IRS layers and hair shaft for both antibodies (A-F). Scale bar, 100μm (A-C), 50μm (D-F).

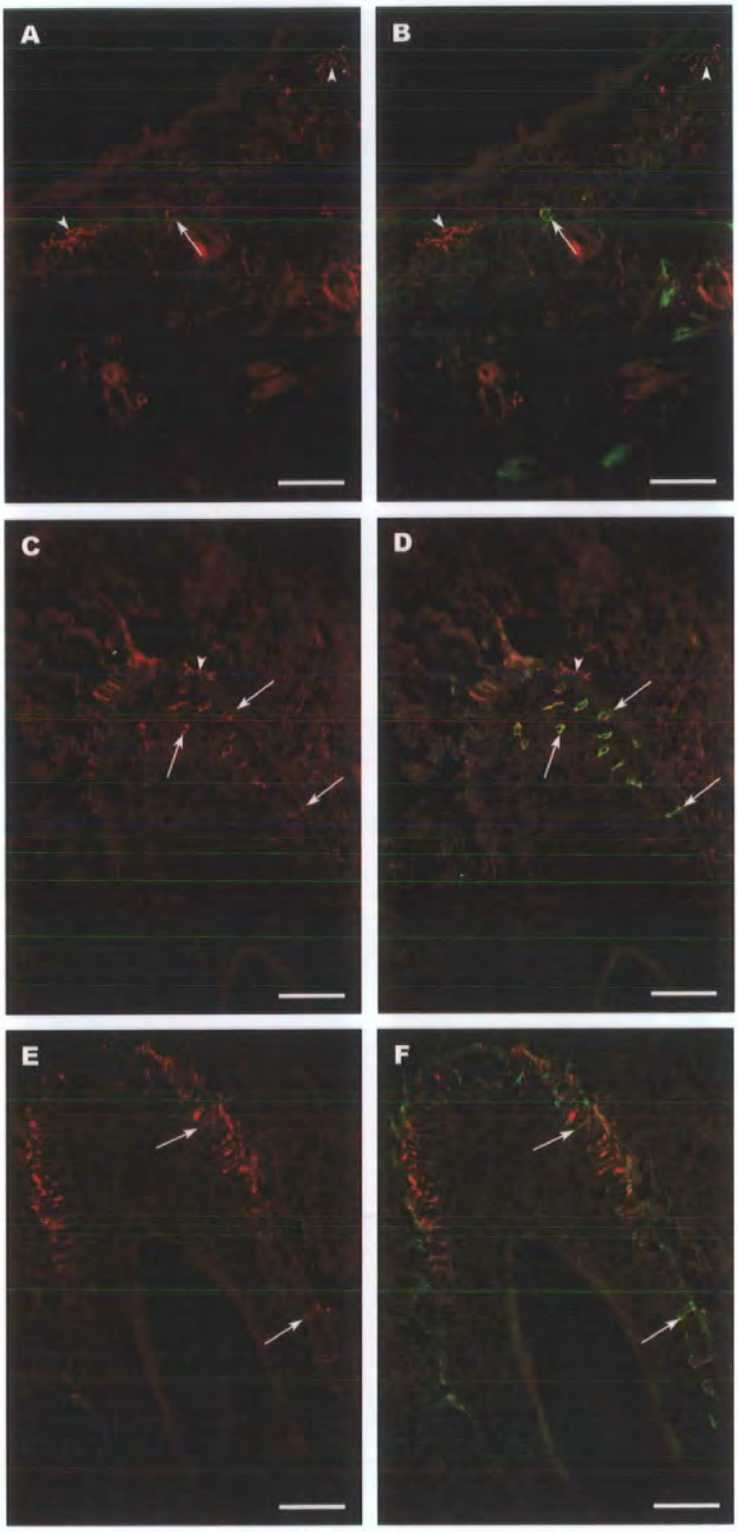

Figure 3.9. Id2 and Synaptophysin expression patterns in neonatal (P4) mystacial pad.

Synaptophysin expression (red) (A-C) was seen in the dermis and epidermis highlighting nerve rich areas of the skin (A; arrowheads), but also more specifically in a single cell in the basal epidermis (A; arrow). Double labelling with Id2 (green) shows co-expression only to this cell (B; arrow). Neonatal vibrissae continued to express Id2 and Syp (C,D and E,F) in ORS cells at the bulge region. Scale bar, 50μm (A-F).

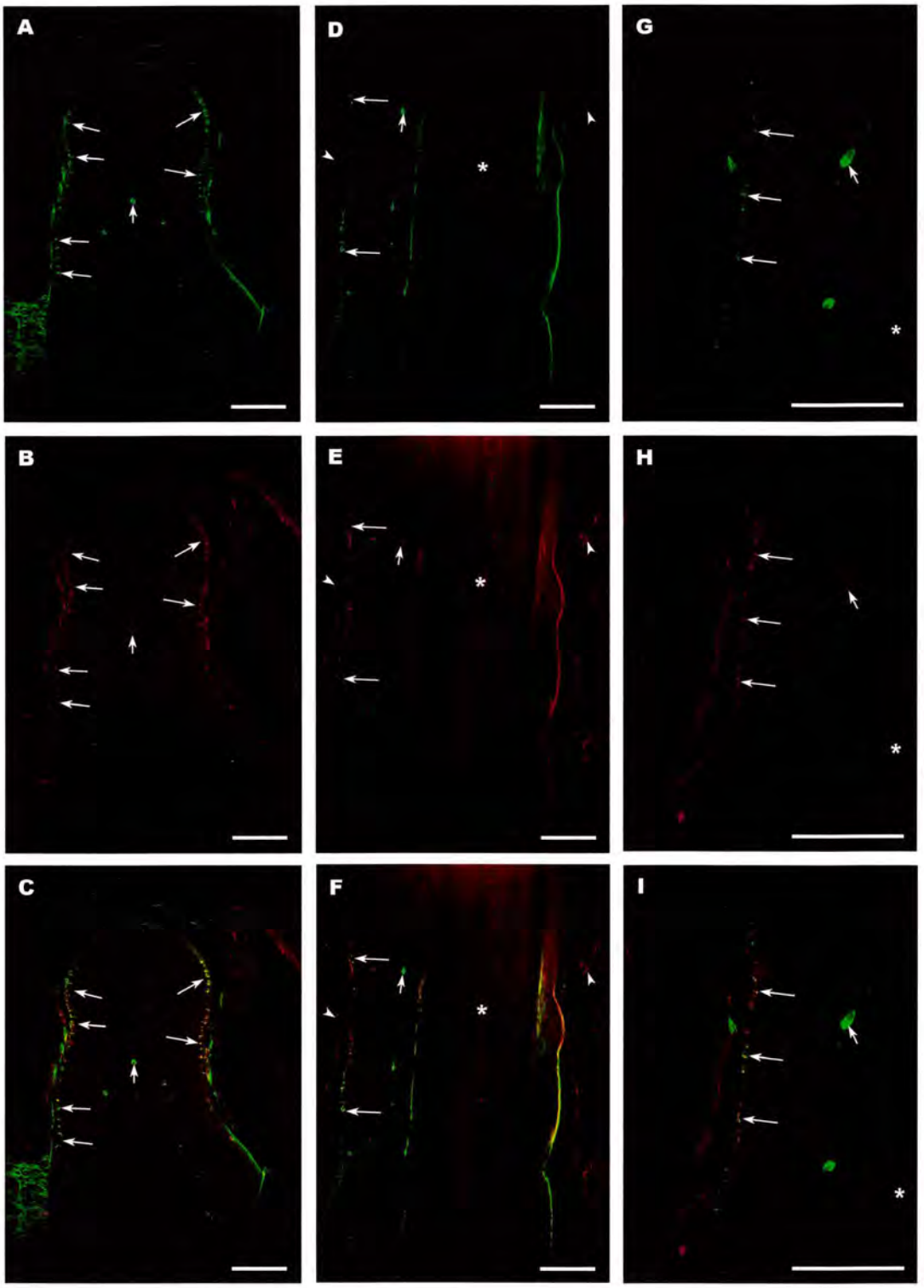

Figure 3.10. Adult vibrissa follicles double immunolabelled for Id2 and Synaptophysin.

A mid-anagen follicle (A-C) stained for Id2 (green) (A) and synaptophysin (red) (B) shows co-expression in the cells in the ORS of the adult follicle (C; long arrows). Synaptophysin is also expressed outside the ORS in the collagen capsule, but in close contact with the Id2 expressing cells (B,C). The same was found in catagen follicles (D-F and G-I). Note the small arrows (A-I) highlight ambiguous staining. Scale bar, 100μm, (A-I).

3.3 Id2 and Cytokeratin-20

From the observations made with Id2 and double labelling with Syp, it was clear these specialised cells in the ORS had the capacity for synaptic transmission. It was suspected these cells could be Merkel cells due to their location in the ORS and basal epithelium and also contained synaptic vesicles, all traits of Merkel cells.

Double immunolabelling was performed with Id2 and cytokeratin-20 (CK-20), a Merkel Cell (MC) marker, covering early follicle development through to adult follicles. In E16 mystacial pads, cells expressing high levels of Id2 were found in the basal epithelium and developing follicles, although generally these cells were not found in great numbers at this stage. When examined for cytokeratin-20 these cells were also found to contain high levels of CK-20. This co-expression was confirmed in a single cell in the basal layer of the epidermis, stained for both antibodies (Figure 3.11A-C). When the images were combined they showed co-expression confirming the identity as a MC. Other evidence for MCs at this age was found in stage 2 follicles with cells at the top of the epithelial downgrowth co-expressing both antibodies (Figure 3.11D-F; arrows). Interestingly a few of the Id2 expressing cells appeared negative for CK-20 (Figure 3.11D-F, arrowhead). Again this could be because cytokeratin-20 may not be uniform throughout the cell and may depend on the section taken. It is likely this cell is also a MC.

Immunostaining of E20 sections showing stage 6+ follicles reveal the extent of MC innervation in the developing follicles and embryonic skin. In the bulge region of the ORS of vibrissae, the cells expressing high levels of Id2 were also very immunoreactive for CK-20, shown by the yellow-orange colour (Figure 3.12A,B,E).

No evidence of co-expression was found in any pelage follicles. The presence of MCs was also confirmed in the basal epithelium and at the rete ridge collar, previously double stained by Id2 and Syp. The cells lining the mesenchymal capsule of vibrissae were negative for CK-20, as expected, but as reported previously expressed high levels of Id2 (Figure 3.12A; arrowheads).

Upon closer examination of the staining at the follicular bulge region, some cells appeared to be immunoreactive for Id2 and not CK-20, apparent when the images were combined (Figure 3.12E; short arrow). When the antibody staining was considered individually it was clear that all the cells were co-expressing Id2 and CK-20, but at different levels (Figure 3.12C,D; short arrow). This was also apparent in other follicle sections towards the neck of the follicle, but co-expression was confirmed by comparing the Id2 and CK-20 images with the combined image (Figure 3.13C-E; long arrow).

In neonatal mystacial pads (P1 and P4), Id2 was co-expressed with CK-20 in the basal epithelium and ORS of follicles as expected. The MCs were highly immunoreactive for CK-20 highlighting their density and numbers in various parts of the skin. Once again, dense groups of MCs were found at the rete ridge collar of vibrissae (Figure 3.14A-C; short arrows) and in the ORS at the bulge region (Figure 3.14A-F; long arrows). Between these two distinct regions, very few MCs were found (Figure 3.14A,B; arrowheads). Double immunolabelling of a P4 mystacial pad with Id2 and CK-20 revealed the same staining as seen previously (Figure 3.15).

Adult follicles were also investigated to see if MCs were still present in the mature cycle. Double immunolabelling was performed on a range of adult follicles at different stages of the cycle. In mid-anagen follicles, the Id2 expressing MCs were just visible above the background in the ORS surrounding the club hair (Figure 3.16A,D; arrows). Staining of the same section with Cytokeratin-20 revealed the extent of MCs in this part of the adult follicle, with very high immunoreactivity for CK-20 (Figure 3.16B,E; arrows). Merging of the two images confirmed the co-expression in this region (Figure 3.16C,F; arrows). In other follicles staged as early anagen, Id2 was still expressed in these strongly CK-20 positive MCs and appeared to be present in similar numbers (Figure 3.16G,H,I; arrows).

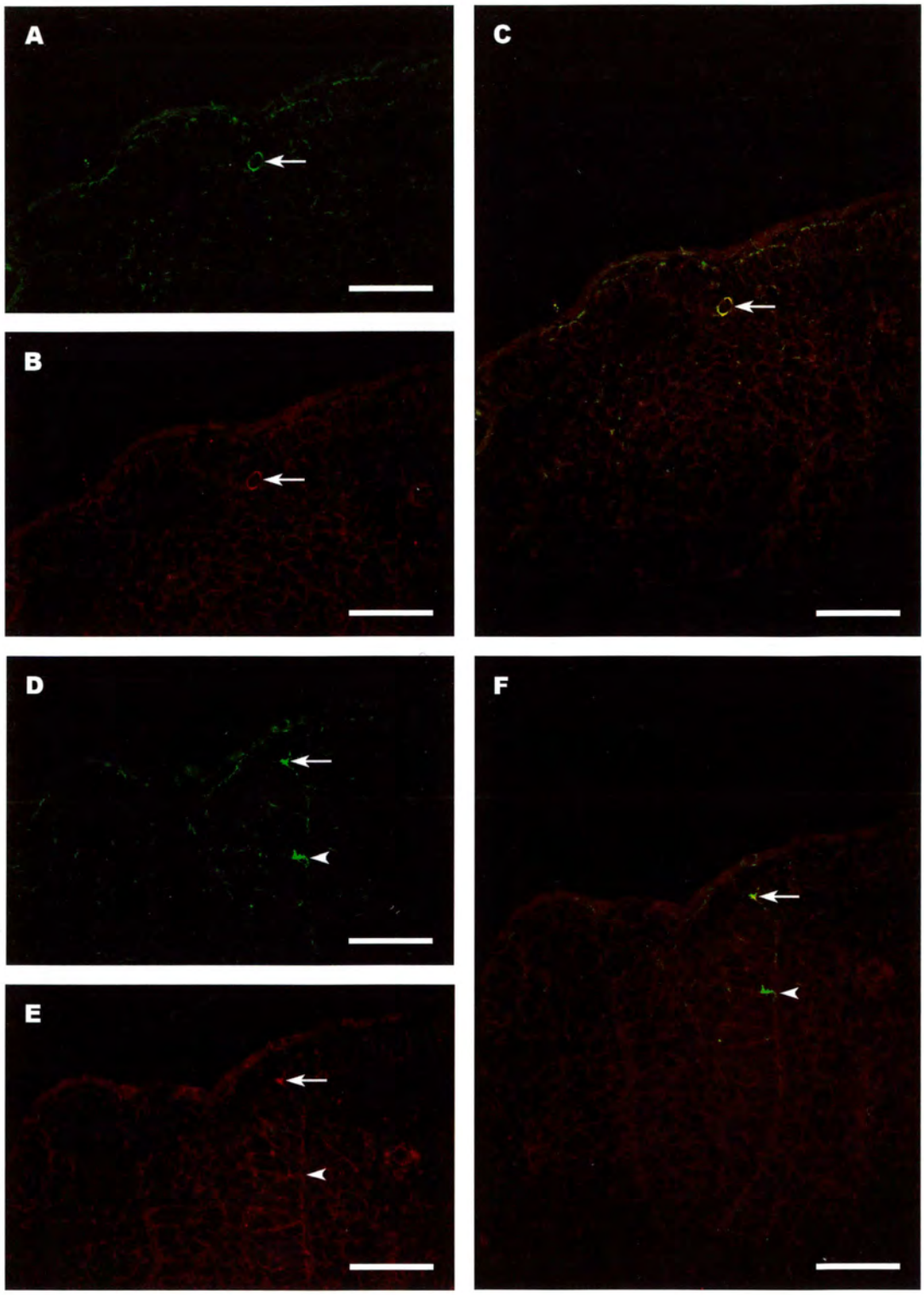

Figure 3.11. Merkel Cells detected in E16 mystacial pad.

Staining for Id2 (green) and cytokeratin-20 (red) reveal co-expression in a very small number of cells in the basal epithelium and the developing hair peg of stage 2 follicles. Co-expression is demonstrated by the yellow colour (C,F). Scale bar, 50μm, (A-F).

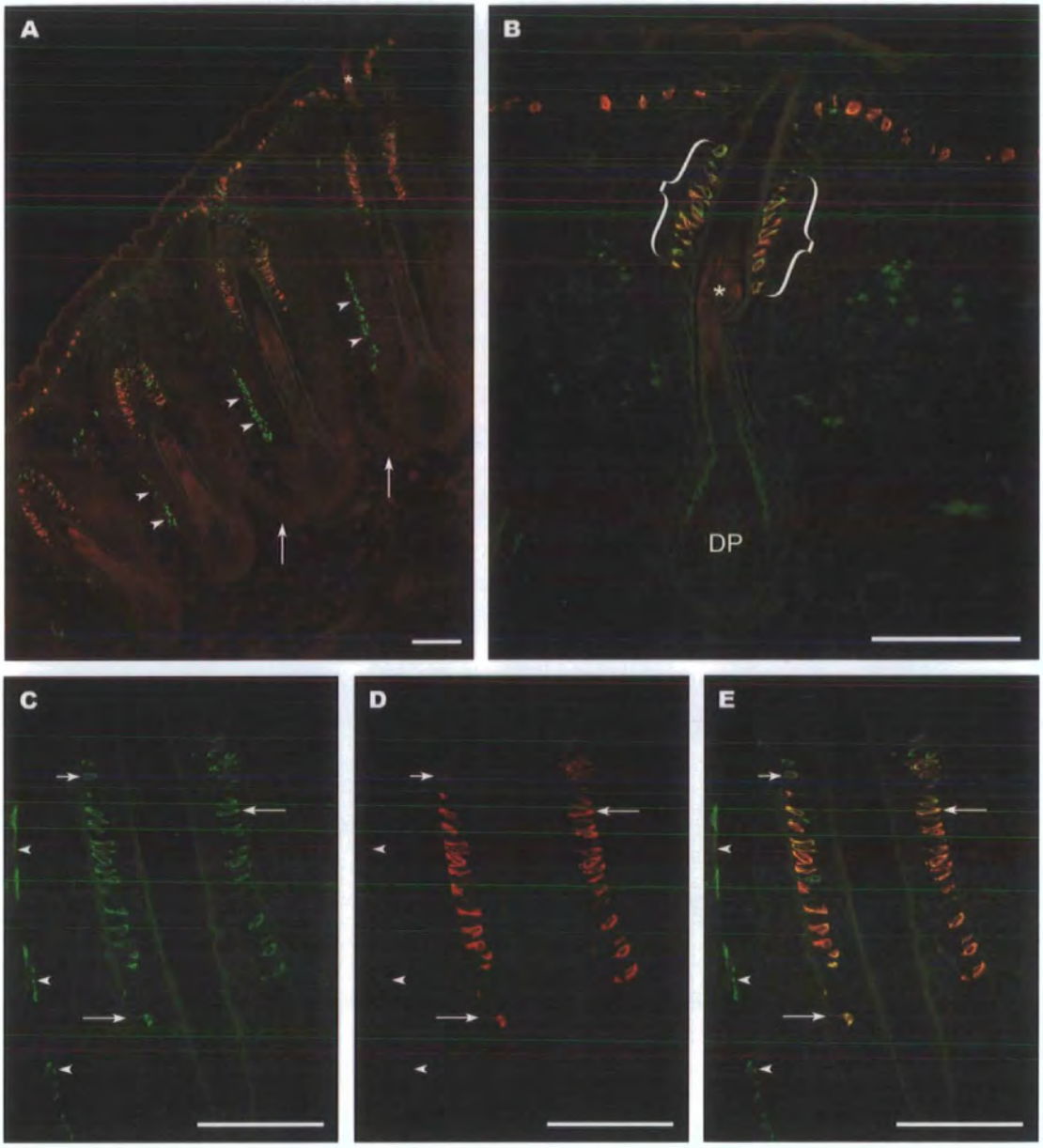

Figure 3.12. Id2 and Cytokeratin-20 expression in E20 mystacial pads.
Merkel cells were detected by double immunolabelling (Id2, green) (CK-20, red) in stage 6+ follicles, both in the ORS in the bulge region, the rete-ridge collar of follicles and throughout the basal epidermis. Note the cells positive for Id2 only (arrowheads) on the opposite side to deep vibrissal nerve entry (A; arrows). Scale bar, 100μm, (A-E).

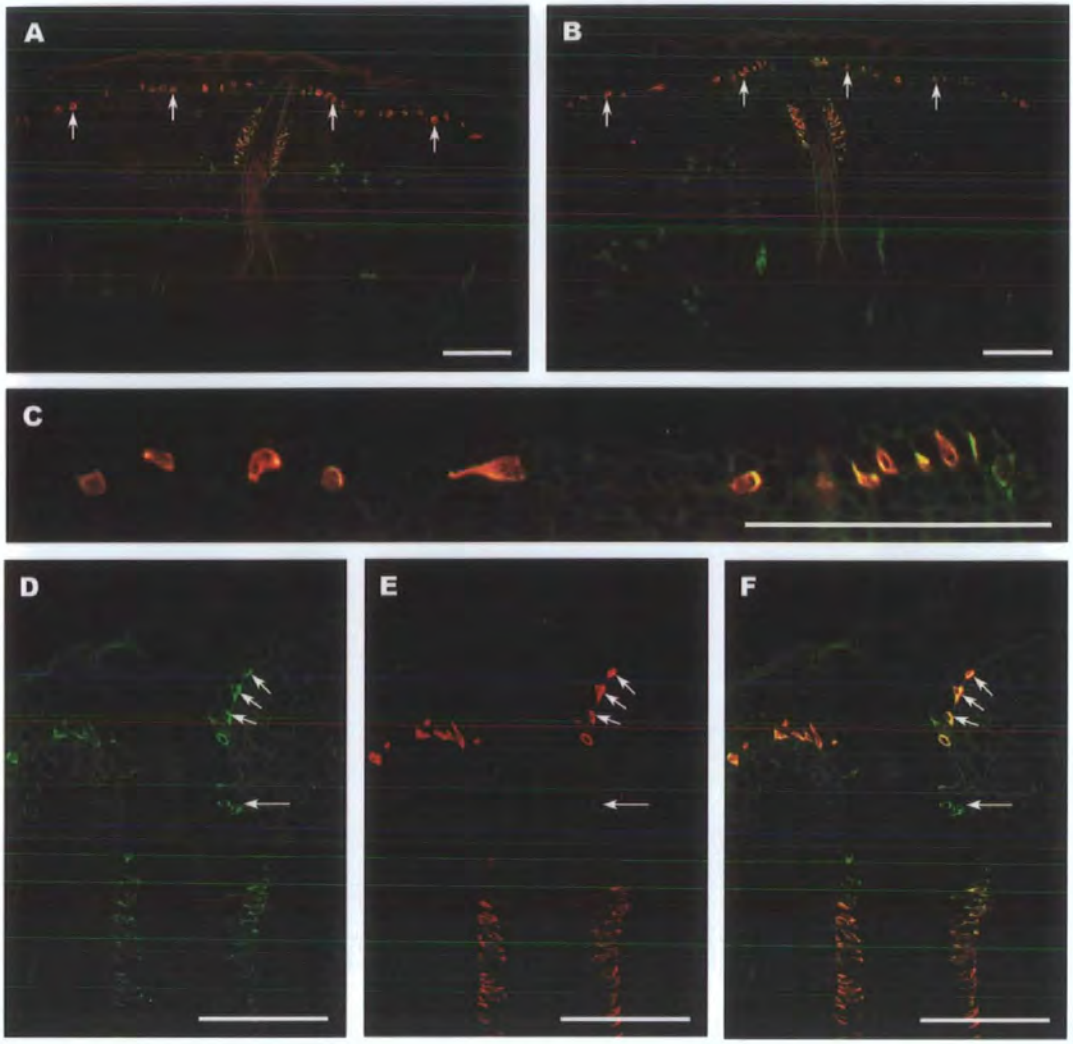

Figure 3.13. Merkel Cells are densely populated in specific regions.
Double immunolabelling was performed with Id2 (green) and cytokeratin-20 (red). The specialised Merkel cells were found densely packed in specific regions of the developing vibrissae, notably the ORS at the bulge region and the rete-ridge collar of follicles (D-F; short arrows) in E20 mystacial pads. Merkel cells are low in numbers between these two regions (D-F; long arrows). (A,B) shows developmentally younger vibrissae with an abundance of Merkel cells in the surrounding basal epidermis and ORS of the follicles themselves. (C) Merkel cells in basal epidermis. Scale bar, 100μm (A-F).

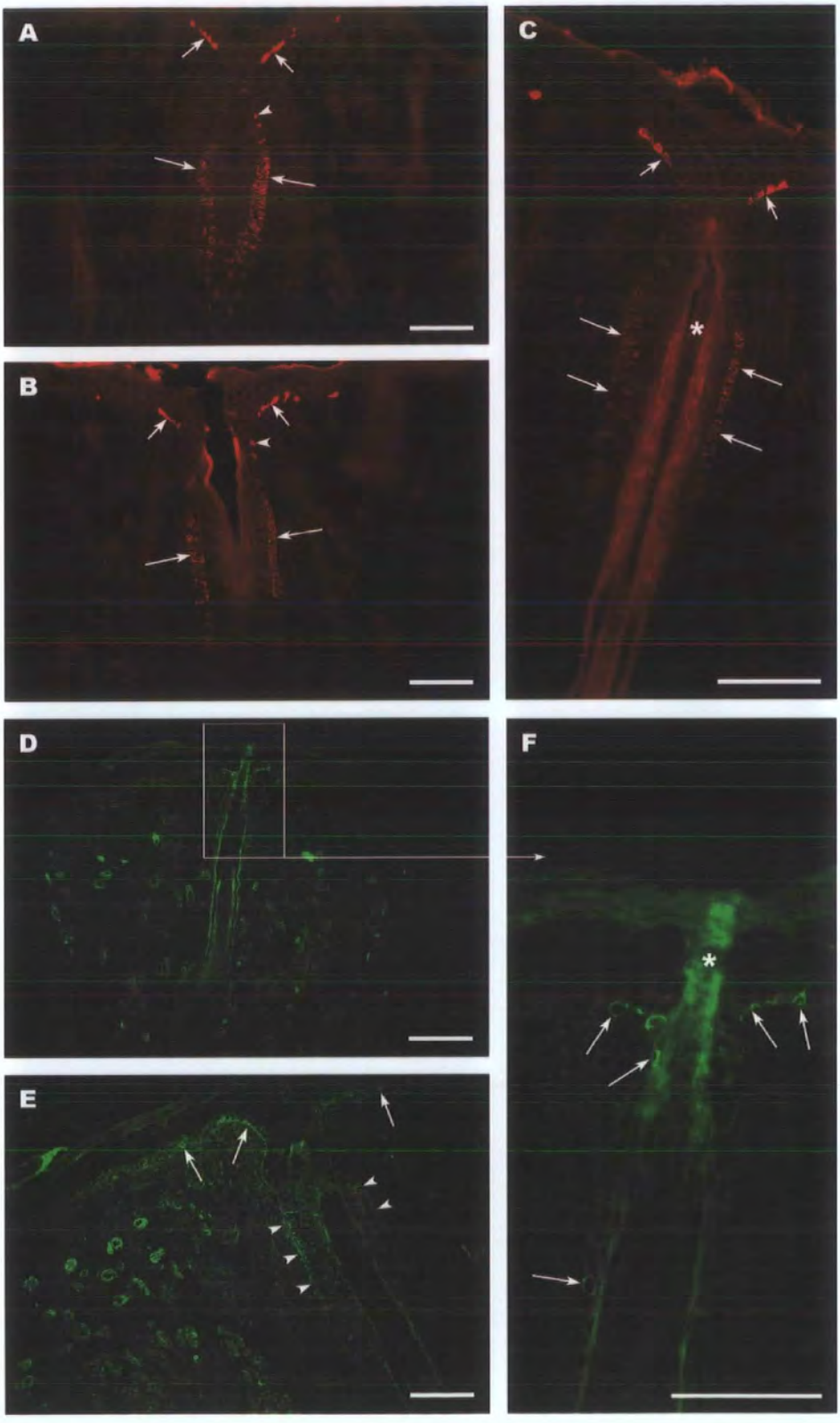

Figure 3.14. Id2 and Cytokeratin-20 expression in neonatal (P1) mystacial pad.

In neonatal skin Merkel cells were found in the same specific regions as seen previously and in similar numbers (A-C). P1 sections stained with Id2 (green) reveal cells expressing high levels in vibrissa follicles at the rete-ridge collar and ORS (D-F). Double labelling with cytokeratin-20 was not performed on these sections but they are unequivocally Merkel cells. Scale bar, 100μm, (A-E), 50μm, (F)

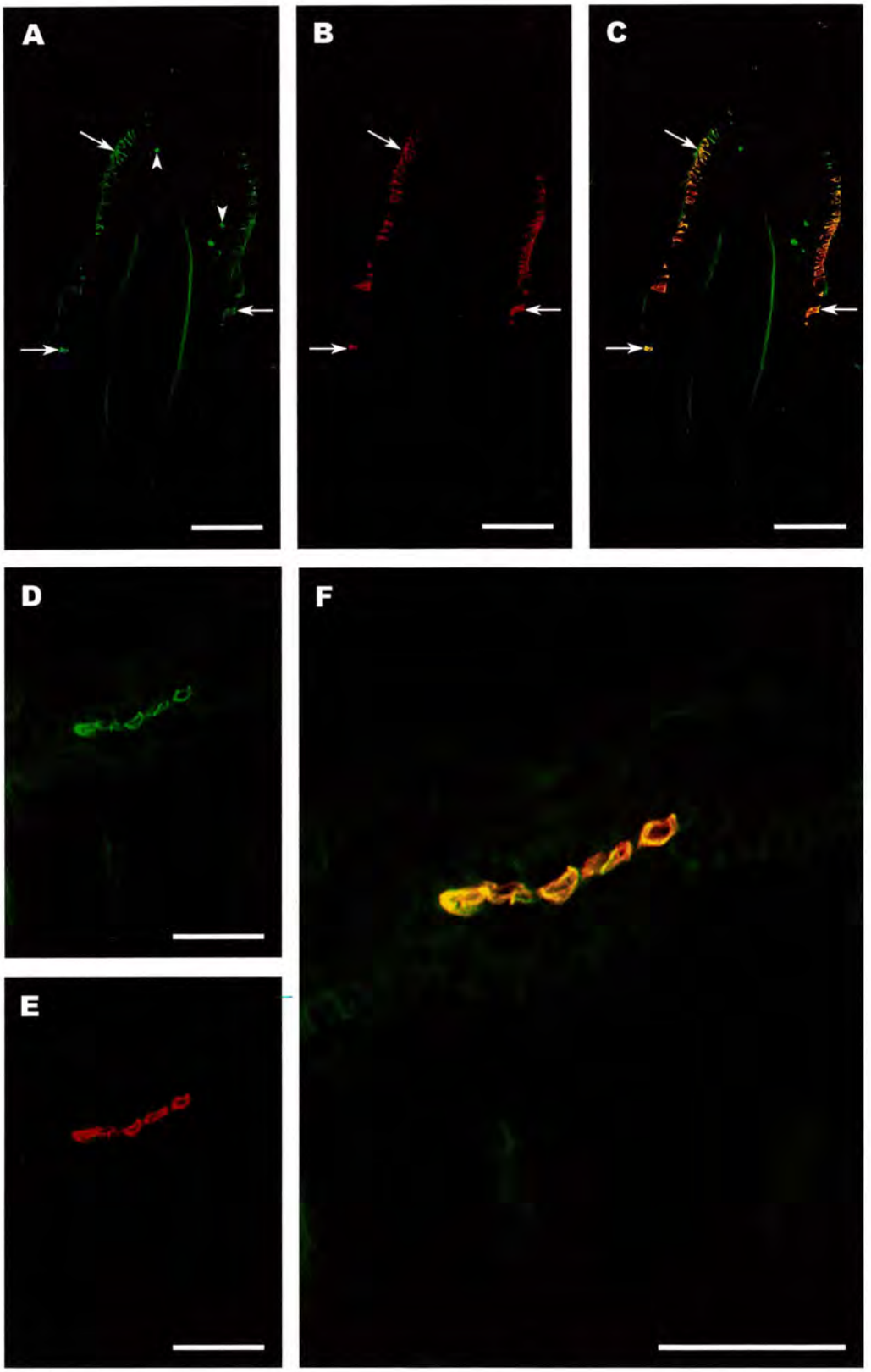

Figure 3.15. Merkel Cells in neonatal (P4) mystacial pad.

Double immunolabelling with Id2 (green) and Cytokeratin-20 (red) reveal Id2 is still being expressed by the Merkel cells both in vibrissae (A-C) and in the basal epidermis of surrounding skin. (D-F) show a group of Merkel cells in a section cut off-centre at the site of a pelage follicle. Note the ambiguous antibody staining (A; arrowheads). Scale bar, 100µm, (A-F).

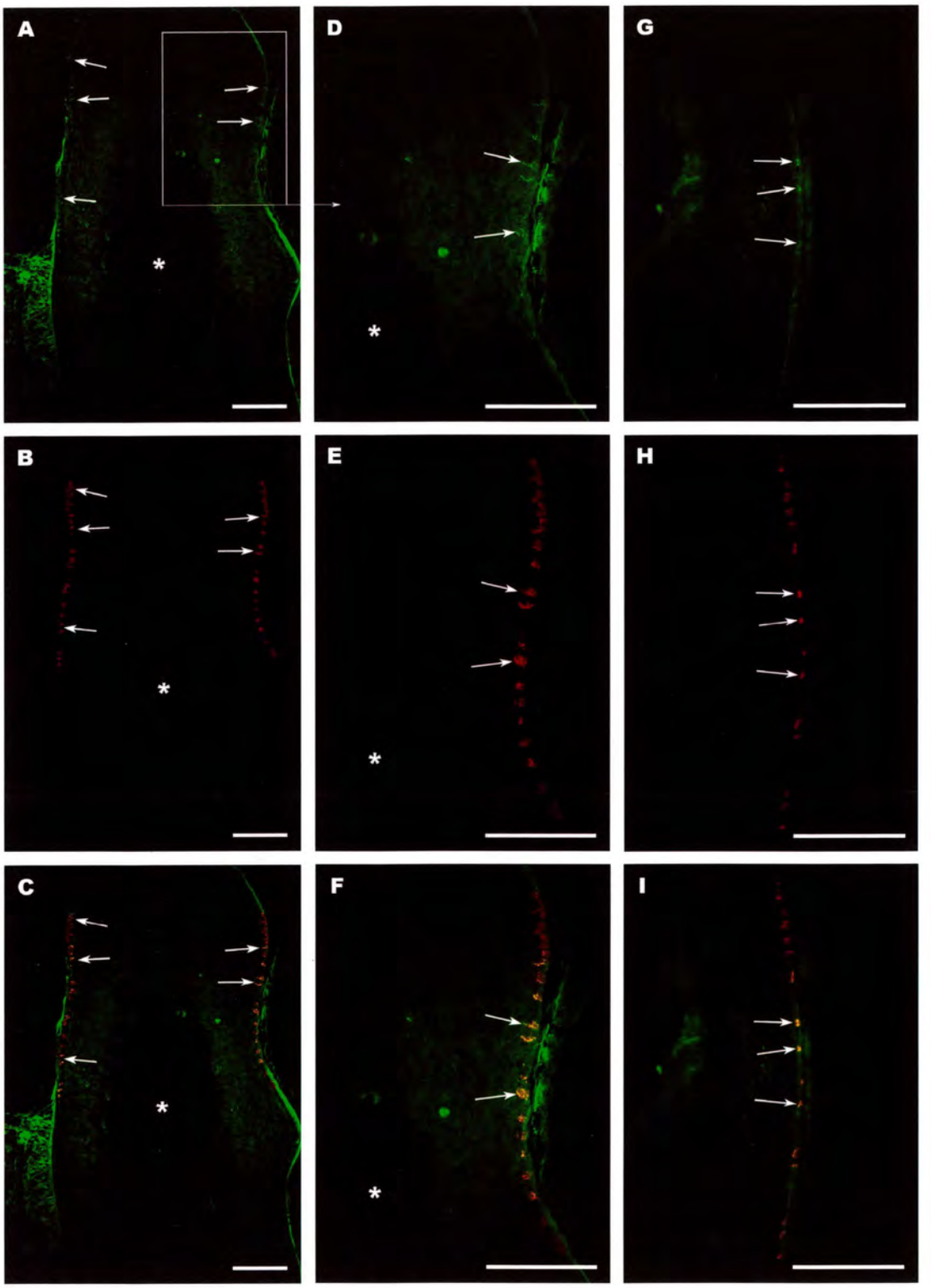

Figure 3.16. Id2 and Cytokeratin-20 expression in adult follicles.

Double immunolabelling of a mid-anagen (A-F) and early anagen (G-I) follicle shows Id2 (green) (A,D,G) is still being expressed in these cells, but are difficult to see due to the high background levels. Staining with cytokeratin-20 (red) confirms these cells are Merkel cells (B,E,H). Scale bar, 100μm, (A-I).

3.4 Id3

Id3 expression was investigated in rat mystacial pads covering early follicle development in the embryo, through to newborn and adult follicles.

In stage 1-2 developing follicles (E16), Id3 was highly expressed in the epidermis and in the basal cells at the edge of the epithelial downgrowth, marking the boundary between the developing follicle and the surrounding mesenchymal cells. Id3 expression appeared to be cytoplasmic, but also basally polarised (Figure 3.17D; arrows). Some of the surrounding dermal cells were also immunoreactive for Id3. Staining was peri-nuclear but at low levels.

At this stage, Id3 was double immunolabelled with β-catenin to mark the cell surfaces and show where in the cell Id3 was being expressed. The double labelling showed Id3 was being expressed in the cytoplasm but mostly located at the cell membranes of cells in direct contact with the surrounding mesenchymal cells (Figure 3.17E; arrows). This polarised staining was also evident in the basal epithelium at sites other than the epithelial downgrowth (Figure 3.17E; arrowhead).

Follicles in developmental stage 3-4 continued to exhibit this staining clearly showing the polarised and asymmetrical nature of Id3 expression, most prominent in the basal epithelial cells around the whole of the developing hair peg (Figure 3.17A,B,C; arrows). At the base of the hair peg, the dermal cells were starting to condense and come together to form the dermal papilla later on. These cells showed very weak peri-nuclear Id3 expression, but demonstrated none of the staining seen in the epithelial cells (Figure 3.17A; arrowheads).

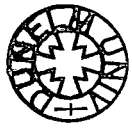

At a slightly later stage of follicle development, Id3 immunolabelling in the basal cells of the epithelial downgrowth was still consistent with earlier stages, but cells forming a very early epithelial column showed peri-nuclear Id3 expression (Figure 3.17B; arrowheads). This was in contrast to the cytoplasmic, polarised expression seen marking the edge of the follicle (Figure 3.17B; long arrows). Once again the presumptive dermal papilla showed no or very low levels of Id3 expression (Figure 3.17B; short arrows).

Immunostaining of E18 sections revealed a dramatic change in Id3 expression. The stage 6+ follicles were now showing peri-nuclear Id3 expression in nearly every cell of the follicle and also throughout the dermis. Strong Id3 expression was present in the dermal papilla, dermal sheath, ORS and mesenchymal capsule of the developing follicle. No evidence of cytoplasmic, polarised Id3 expression was found. High expression of Id3 was demonstrated particularly in the dermal papilla and dermal sheath (Figure 3.18; long arrows) with no expression found in the highly proliferating matrix cells outside the dermal papilla (Figure 3.18; short arrows). Strong Id3 expression was also found in the upper-third of the developing follicles, in the ORS (Figure 3.18A,C; arrowheads). Once again the hair shaft itself and the very upper layer of epidermis appear to be immunoreactive for Id3, but these are artefacts due to the fibrous nature of these structures (Figure 3.18A,B; asterisk, arrowheads respectively).

In E20 mystacial pads, peri-nuclear expression of Id3 was seen throughout the developing vibrissa follicles, but not in the matrix cells around the dermal papilla. Strong Id3 immunoreactivity was seen in the ORS at the bulge region (Figure 3.19A,D; arrowheads), in the dermal papilla and dermal sheath (Figure 3.19A,D; long arrows) and was very noticeable also in developing pelage follicles (Figure 3.19; short arrows). Interestingly, immunostaining for Jol-4 (nuclear lamin type-A, involved in cell cycle regulation) revealed very similar staining to Id3 both in the dermal papilla, dermal sheath and the capsule (Figure 3.19C; arrows).

In neonatal mystacial pads (P0 and P4), Id3 staining of vibrissae was consistent with that seen at previous stages, showing high expression in the dermal papilla, dermal sheath (Figure 3.20C; long arrow) and ORS of the bulge region (Figure 3.20A; arrowheads) with no expression in the matrix cells (Figure 3.20D; short arrows). Pelage follicles at P0 also demonstrated staining of the dermal papilla and dermal sheath, but also showed more intense immunoreactivity in the bulge region of these developing follicles (Figure 3.20B; arrowheads). Staining of P4 mystacial pads with Id3 revealed the same staining as reported for other neonatal stages. Notably, the intense staining of the bulge region seen at P0 in pelage follicles was also seen at P4 (Figure 3.21C,D; arrowheads).

Adult vibrissa follicles at various stages were also stained for Id3. In early anagen, staining was strong in the dermal papilla and dermal sheath (Figure 3.22B). Expression of Id3 was very high in the ORS at the bulge level, especially around the club hair. Cells were also expressing Id3 in the capsule and IRS but to a lesser extent. This staining was consistent throughout the adult cycle.

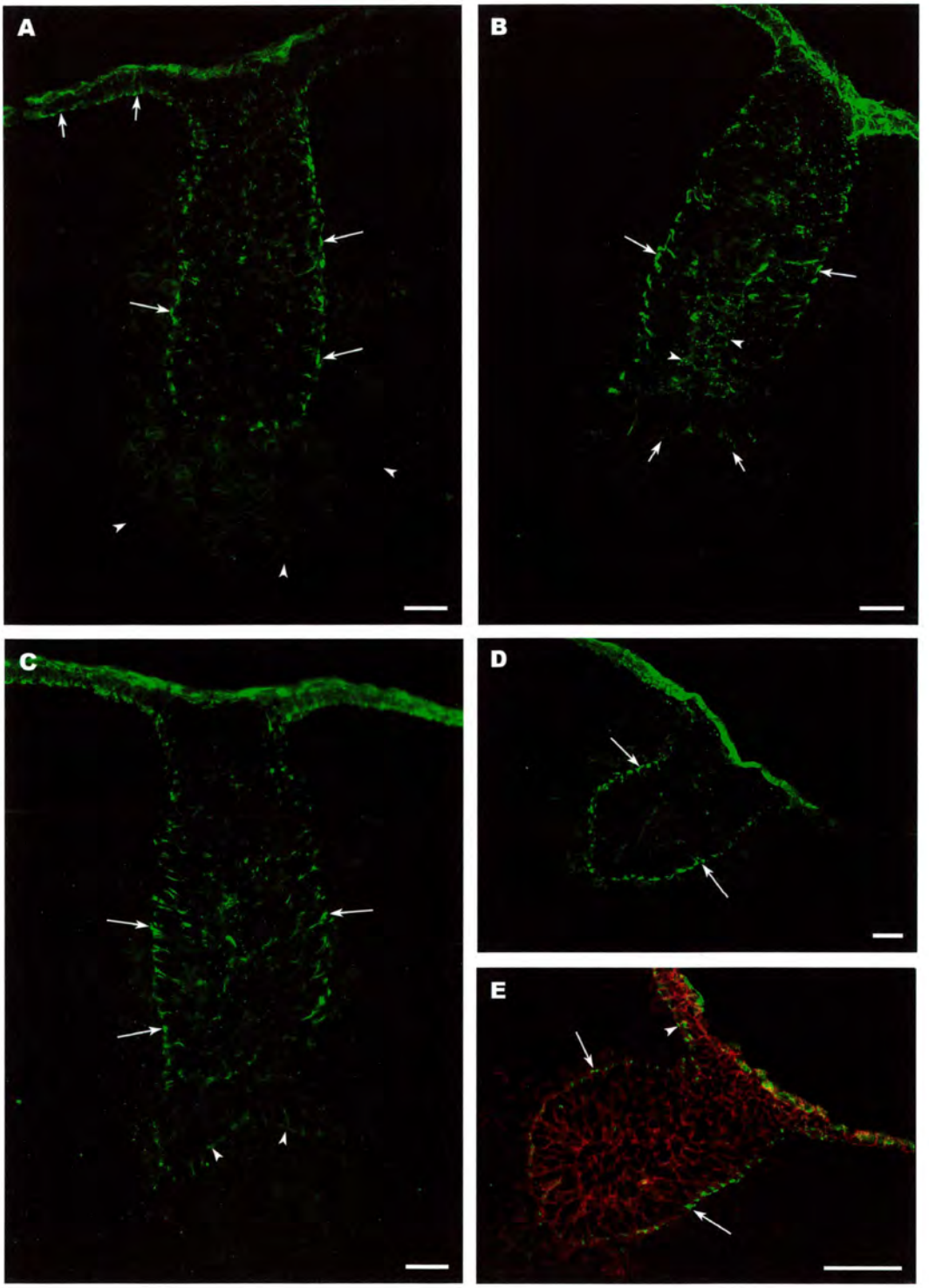

Figure 3.17. Id3 expression in developing follicles of E16 mystacial pad.
Developing vibrissa follicles at stage 2 expressed high levels of Id3 (green) in the basal epithelium and basal layer of the epithelial downgrowth. Expression is cytoplasmic and basally polarised towards the surrounding dermal cells. Double immunolabelling with β-catenin (red) indicates Id3 is being expressed in the cytoplasm next to the cell membrane (E). (A-C) show stage 3-4 follicles expressing both cytoplasmic/polarised (long arrows) and peri-nuclear Id3 (B; arrowheads/short arrows, A; arrowheads). Note staining of the uppermost epidermis is an artefact of the process. Scale bar, 50μm (A-E).

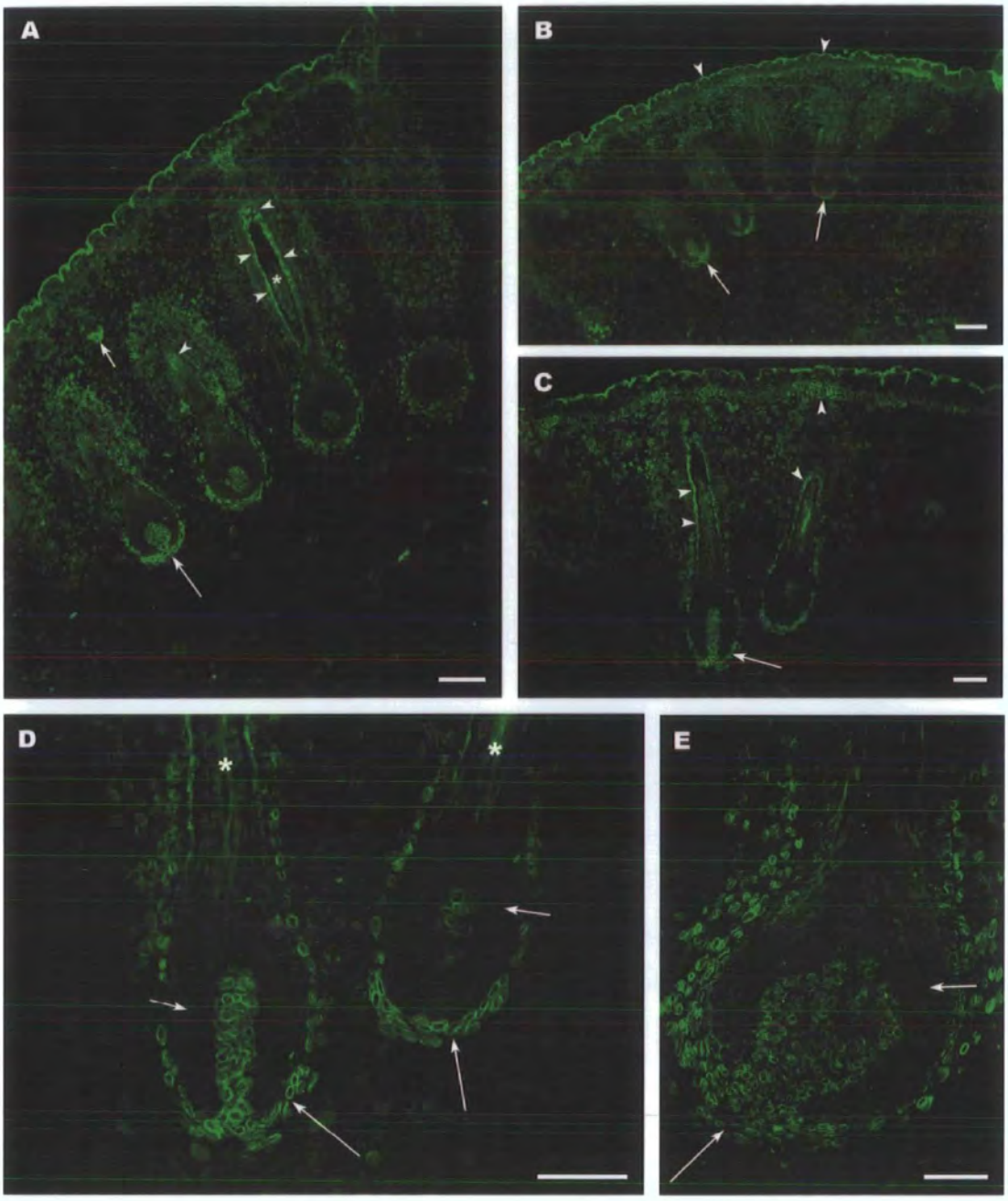

Figure 3.18. Id3 expression patterns in E18 mystacial pad.

Id3 is expressed in many cells of the mystacial pad. All staining is peri-nuclear with high expression in the dermal papilla, dermal sheath, and ORS or both pelage and vibrissa follicles. No expression of Id3 is in the matrix cells of the end bulb (D,E; short arrows). Non specific staining is seen in the hair shaft (A,C; asterisk) and uppermost layer of epidermis (B; arrowheads). Scale bar, 100μm (A,B), 50μm (C-E).

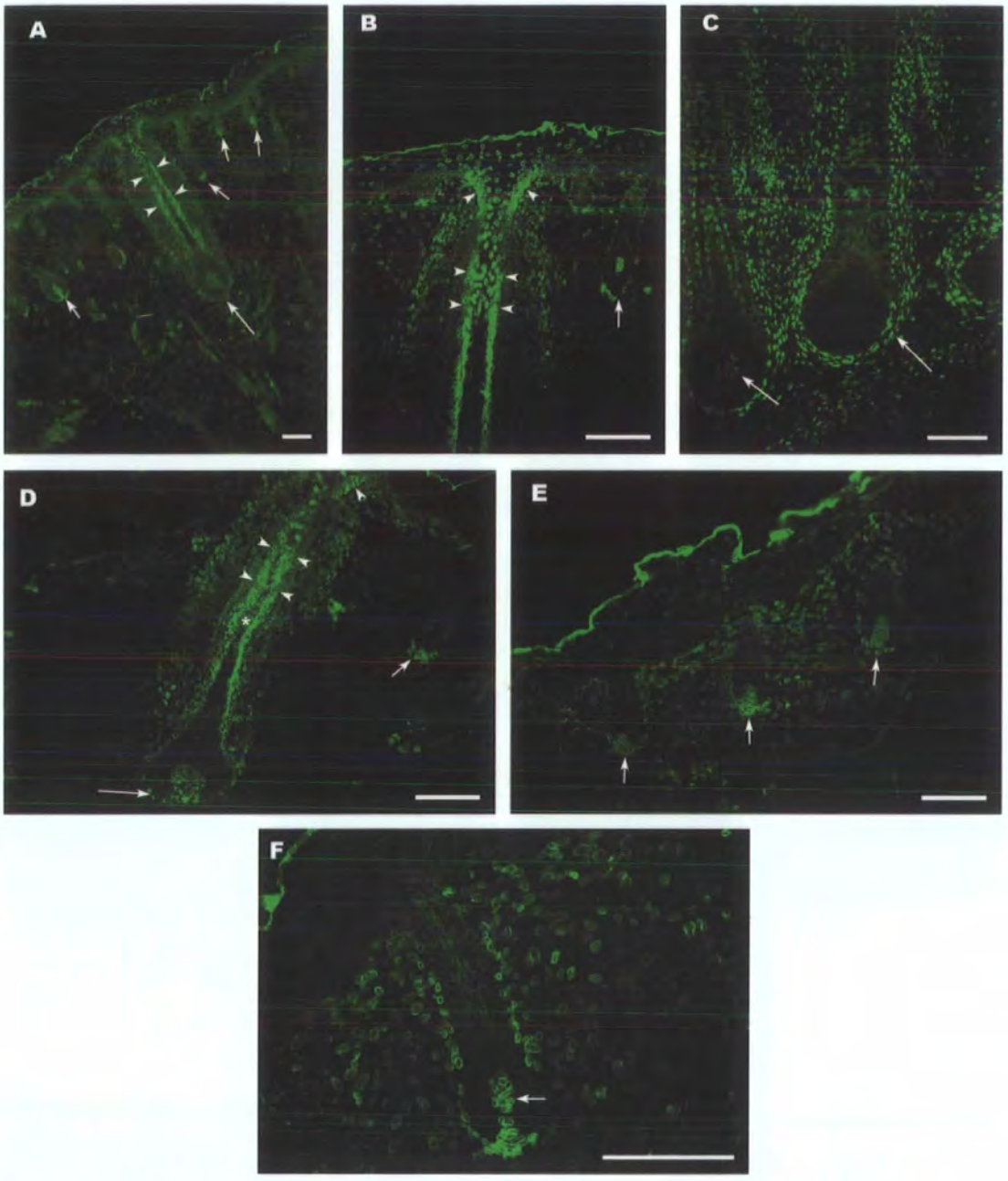

Figure 3.19. Id3 and Jol4 expression patterns in E20 mystacial pad.

Id3 (A,B,D-F) showed the same staining as seen at earlier stages, with the highest expression seen in the dermal papilla, dermal sheath, ORS and interestingly at the rete-ridge collar of vibrissae. Expression of Id3 is also high in pelage follicles in the dermal papilla and dermal sheath (E,F; arrows). A section stained with Jol4 (antibody specific to nuclear lamin-A) shows very similar staining to Id3 (C; arrows). Scale bar, 100μm, (A-F).

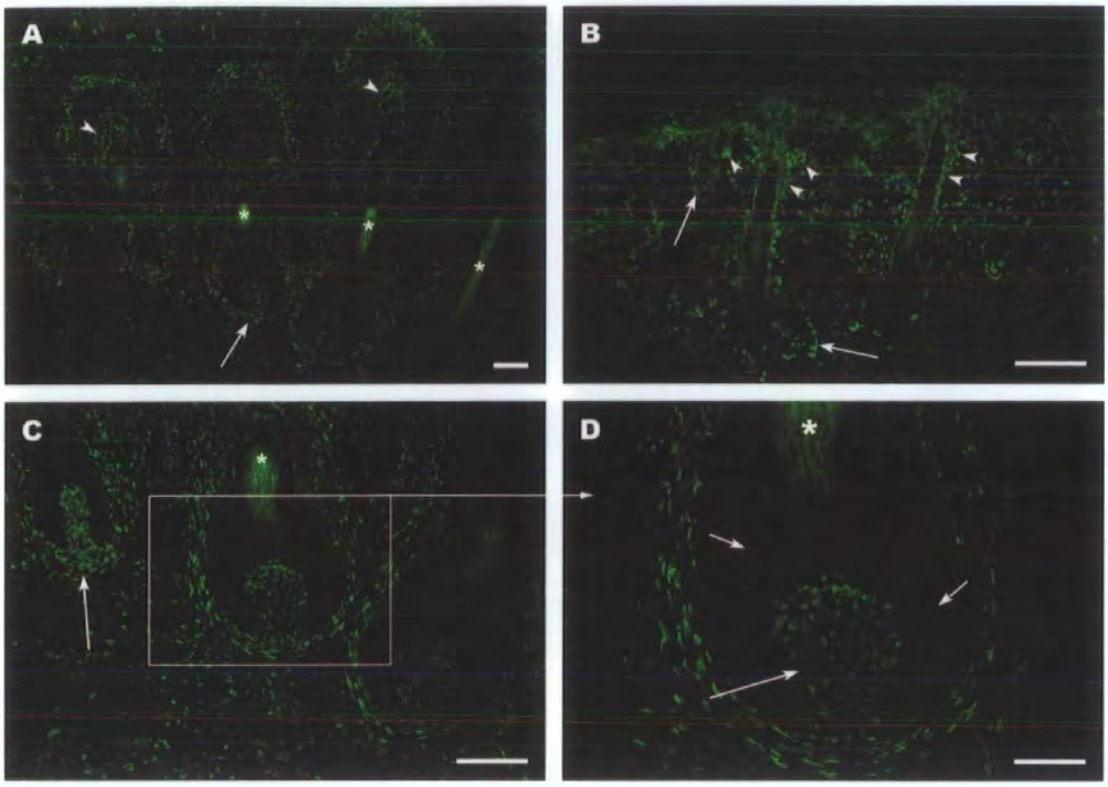

Figure 3.20. Id3 expression patterns in neonatal (P0) mystacial pad.

In neonatal mystacial pads Id3 expression was seen throughout vibrissae but with higher levels in the ORS at the bulge region (A; arrowheads). Pelage follicles also show higher expression in the ORS of the bulge (B; arrowheads). No Id3 immunoreactivity was seen in the matrix cells of the end bulb of the follicles (D; short arrows). Note ambiguous staining of the hair shaft (A,C,D; asterisk). Scale bar, 100μm (A,C), 50μm, (B,D).

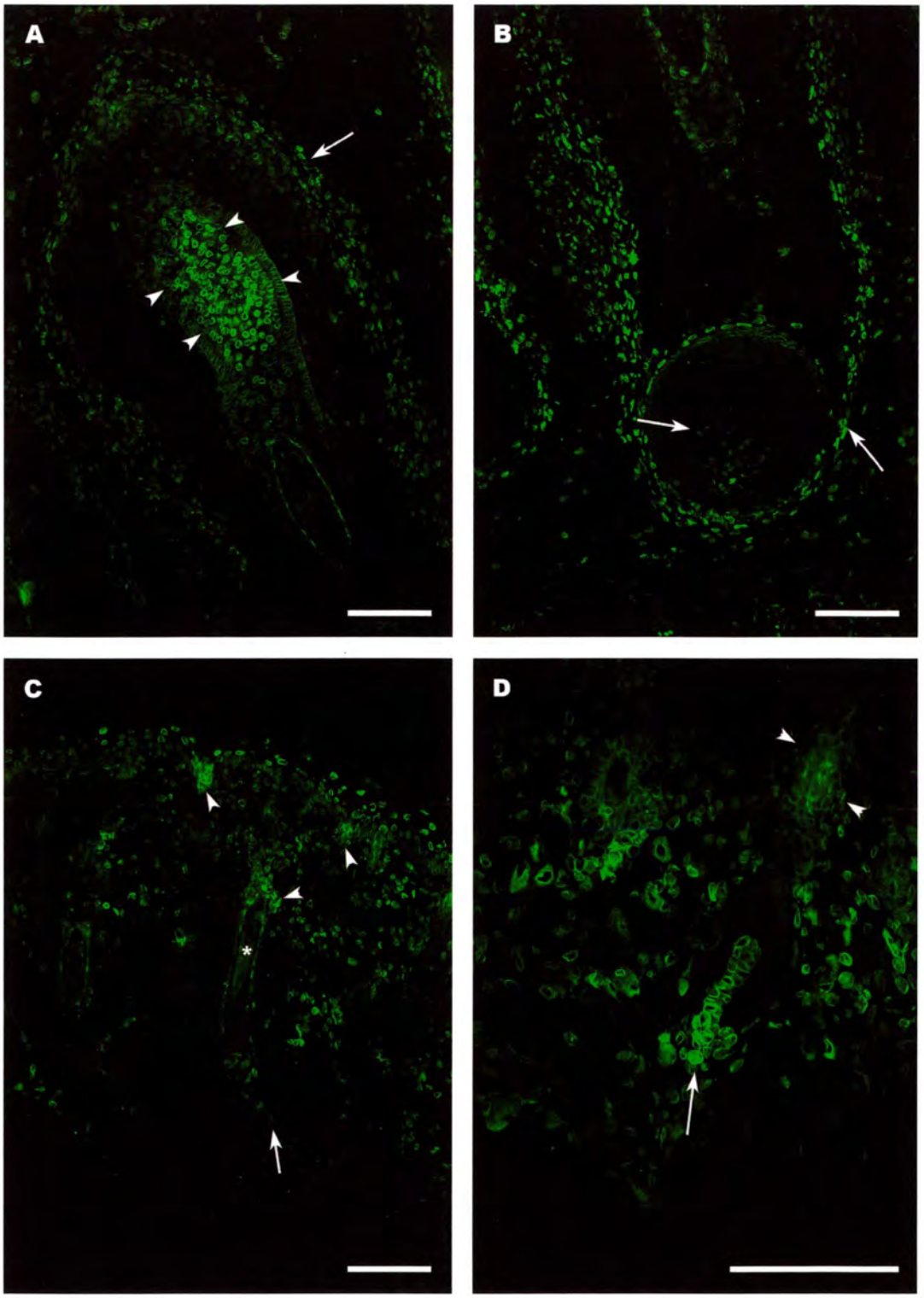

Figure 3.21. Id3 expression patterns in neonatal (P4) mystacial pad.

Id3 staining was the same as at age P0. (A) shows very clearly the high level of expression of Id3 in the ORS. Pelage follicles also showed high expression in the bulge region (D; arrowheads). Scale bar, 100μm, (A-D).

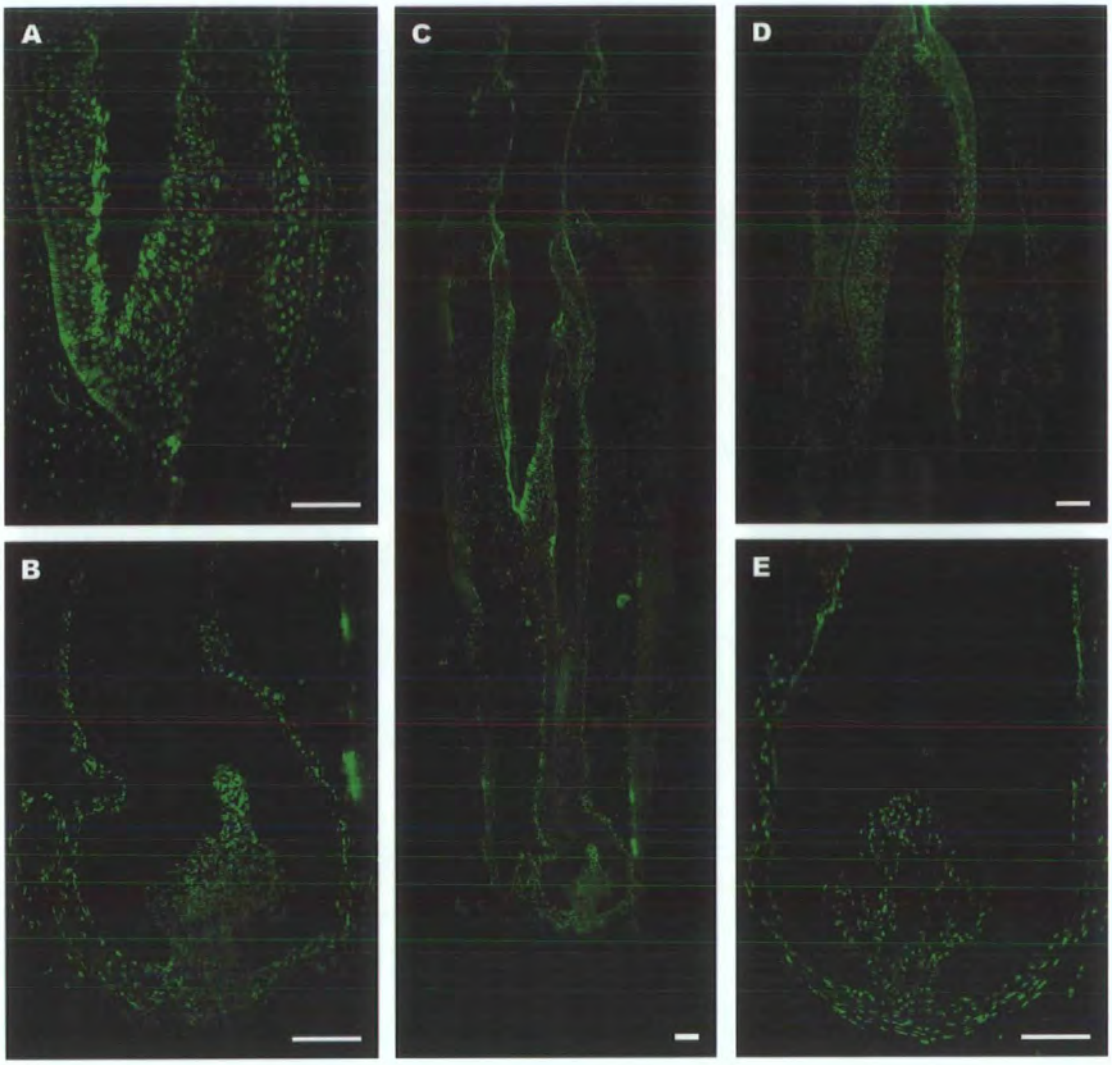

Figure 3.22. Id3 expression in adult follicles.

A follicle staged as early anagen (A-C) displayed high Id3 immunoreactivity in the dermal papilla and dermal sheath (B). Id3 expression was high in the ORS in the bulge region, particularly around the club hair (A). A catagen follicle also showed the same expression pattern (D,E). Scale bar, 100μm, (A-E).

3.5 Retinoic Acid Glandular Morphogenesis

Mystacial pads of E13.5 and E14 embryos were cultured for 2.5, 4 or 5 days. Cultures were prepared with mystacial pads set up in retinoic acid medium (+RA) and complimentary pads set up in control medium (-RA). Once cultured for the specified time the pads were removed and either mounted in TissueTek O.C.T and snap frozen or fixed in 4% formal saline. All the frozen samples were cut on a cryostat (see 2.3.1) with sections either double-labelled with antibodies (see 2.3.7) or stained for Mayer's H&E (see .2.3.8) to analyse the histology. Samples fixed in formal saline and embedded in paraffin wax gave unsatisfactory results and were not used.

3.6.1 H&E staining

Mayer's hematoxylin was used to stain the nuclei blue whilst eosin provided an adequate counterstain colouring the cytoplasm and other structures shades of pink. The results of Mayer's H&E staining are shown in Figure 3.23. Analysis of 2.5day E14 control cultures (Figure 3.23A,B) showed early follicle development at stages 2 and 3 with some evidence of early mesenchymal condensations surrounding the developing peg. The epithelium was relatively thin and primitive. In 2.5day E14 RA cultures the epithelium had thickened considerably (Figure 3.23E; arrowhead) and at similar follicle stages, the mesenchymal condensations were more prominent with a higher number of cells aggregated (Figure 3.23E; arrows). After 4days in control culture medium, the epithelium was multilayered and follicles were more developed showing an apparent large mesenchymal condensation at the base of the hair peg (Figure 3.23C,D; arrowheads). This condensation was distinctive, staining a darker pink than the surrounding tissue. Developing follicles in the control cultures showed

normal development up to stages 2-3 of morphogenesis but no evidence of later stages of follicle development were found. The RA cultures harvested after 4days showed evidence of glands with elaborate branching structures derived from developing hair pegs (Figure 3.23F; arrows). These structures showed no evidence of any mesenchymal condensations or dermal papilla and were rounded in appearance. In 5day RA cultures, rounded, elongated hair pegs were present (Figure 3.23G; long arrow) but no branching structures could be found despite the presence of many developing epithelial pegs. Thickening of the epithelium was very apparent (Figure 3.23G; arrowhead). Although there were numerous developing epithelial pegs (Figure 3.23G; short arrows), none showed normal follicle development.

3.6.2 Id2 and Cytokeratin-20

The E13.5 and E14 mystacial pad cultures were serial sectioned and double-immunolabelled for Id2 and CK-20. The results are shown in Figure 3.24. Analysis of 2.5day E14 control cultures revealed Id2 immunoreactivity in stage 2 developing follicles, displaying cytoplasmic, basally polarised staining at the epithelial-mesenchymal boundary (Figure 3.24A; arrowheads). The upper epithelium stained heavily for Id2 but this was an edge effect consistent throughout skin samples. Staining with CK-20 revealed no cells immunoreactive for the antibody. In 2.5day E14 RA cultures, Id2 staining was much more pronounced in the basal epithelium showing clearly the cytoplasmic, polarised expression (Figure 3.24D,E; arrowheads). Id2 immunoreactivity was also seen inside the developing peg to a lesser extent. Low Id2 expression was also seen throughout the dermis. Interestingly expression of Id2 was seen in the dermis localised below two developing follicles (Figure 3.24D,E; short arrows) but was not seen in mystacial pads cultured over 2.5days. The

developing follicles in RA culture appeared to be at a later stage of development with some displaying a dermal papilla (Figure 3.24D) and the developing pegs were more rounded in appearance. After 4days in control medium, E13.5 mystacial pads displayed intense cytoplasmic, basally polarised expression in the epithelium of both the developing hair peg and the epidermis (Figure 3.24B; arrowheads). Similar expression was also seen inside the developing hair peg and to a lesser extent in the surrounding dermis. Double labelling with CK-20 revealed a few cells co-expressing both CK-20 and Id2 in the basal epithelium indicating the presence of MCs (Figure 3.24B; short arrow). In E14 mystacial pads cultured for the same amount of time (4days) Id2 expression in the basal epithelium was reduced considerably with cytoplasmic, polarised expression largely absent in comparison to E13.5 control cultures (Fig 3.23C). MCs were however still present, strongly labelled both by Id2 and CK-20 giving a yellow appearance on the merged images (Figure 3.24C; short arrows). For the RA cultures, it was interesting to find in E14 4day cultures the cytoplasmic, polarised Id2 staining absent from control cultures of the same duration, was present in the basal epithelium (Fig 3.23F; arrowheads). The expression was however lower than that seen in the E13.5 4day controls (Figure 3.24B) and E14 2.5day RA cultures (Figure 3.24D,E). Elaborate branching structures (Figure 3.24F; long arrows) were seen in E14 4day RA cultures, but interestingly MCs still populated the epithelium, shown by co-expression of Id2 and CK-20 immunolabelled cells (Figure 3.24F; short arrows). After 5days of RA culture, Id2 was still present in the basal epithelium but its expression appeared more uniform along the epithelial-mesenchymal boundary (Figure 3.24G; arrowheads). This was in contrast to that seen previously where Id2 was localised and asymmetric in its expression. Also curiously expression of Id2 appeared to be absent (or expressed at very low levels)

from the epithelial peg. Immunolabelling with CK-20 revealed numerous MCs populating both the developing peg and basal epithelium (Figure 3.24G; short arrows).

3.6.3 Id3 and β-catenin

The E13.5 and E14 mystacial pad cultures were double-immunolabelled for Id3 and β-catenin. The results are shown in Figure 3.25. Analysis of E13.5 4day control cultures revealed prominent Id3 immunoreactivity in the basal epithelium (Figure 3.25A,B; arrowheads). Id3 staining was similar to that seen with Id2 displaying cytoplasmic, basally polarised expression at the epithelial-mesenchymal boundary. This staining was seen in developing epithelial pegs but expression decreased down the length of the epithelial downgrowth (Figure 3.25A; arrowheads). β-catenin staining was high in the developing peg and was also present at lower levels throughout the epidermis. Again high expression seen in the upper layers of the epidermis are artefacts of the staining process (Figure 3.25A-F). In 5day E13.5 RA cultures, Id3 and β-catenin staining was consistent with the E13.5 controls but generally lower expression of Id3 was seen (Figure 3.25D,E; arrowheads). Staining artefacts were much greater in 5day cultures, presumably due to increased numbers of dead cells (Figure 3.25D,E; long arrows). In E14 mystacial pad control cultures there was a dramatic change of Id3 expression. Instead of cytoplasmic, polarised staining seen in E13.5 control cultures, Id3 staining was absent (Figure 3.25C; arrowheads). β-catenin immunolabelling remained unchanged showing high expression in the epithelium. In the complimentary E14 RA culture, Id3 expression was absent from developing epithelial pegs (Figure 3.25F; short arrows) but patchy low expression of Id3 (cytoplasmic, polarised) was seen in the basal epidermis

(Figure 3.25F; arrowheads). Again irregular staining seen in the upper epidermis and the upper developing epidermal pegs appeared to be as a result of artefacts (Figure 3.25F; long arrow). β-catenin expression was still evident throughout the epidermis and developing epithelial peg although expression was lower in the RA cultures compared to controls (Figure 3.25C,F).

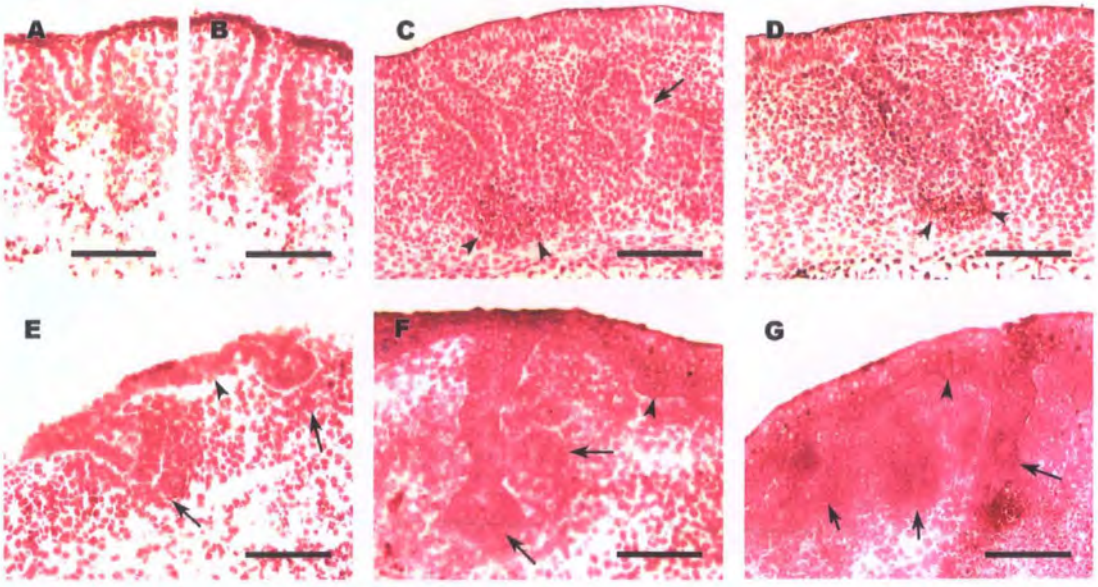

Figure 3.23. Histology of rat mystacial pad cultures.

Haematoxylin and eosin (H&E) stained sections of rat mystacial pad (E13.5 and E14) cultures comparing control (-RA) cultures (A-D) to retinoic acid (+RA) cultures (E-G) at various durations of culture. **Controls** = (A,B) E14 pad, 2.5day; (C,D) E13.5 pad, 4day. **+RA** = (E) E14 pad, 2.5day; (F) E14 pad, 4day; (G) E14 pad, 5day. Scale bar, 100μm, (A-G).

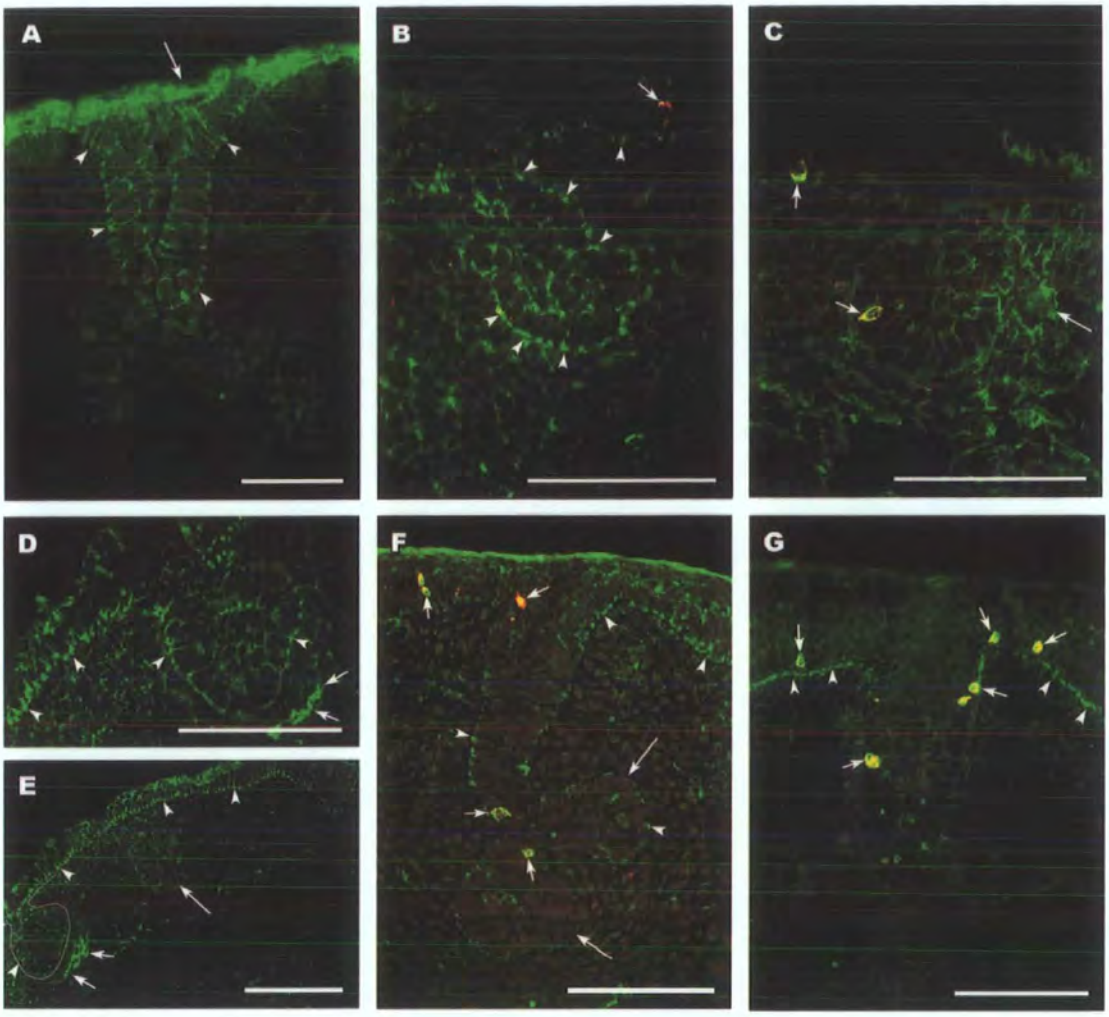

Figure 3.24. Id2 and CK-20 expression in rat mystacial pad cultures.

Id2 (green) and Cytokeratin-20 (red) stained rat mystacial pad (E13.5 and E14) cultures comparing control (-RA) cultures (A-C) to retinoic acid (+RA) cultures (D-G) at various durations of culture. Co-expression of both antibodies (yellow) shows Merkel cells in the epithelium and developing hair peg (B,C,F,G; short arrows). Id2 expression remains polarised in the basal epithelium and hair peg (A-G; arrowheads) in -RA and +RA cultures but after 5 days in E14 pads, expression in the hair peg has diminished (C,G). Id2 expression in the basal epithelium was absent in E14 4day controls but was still there in 4 and 5 day +RA cultures (C,F,G). **Controls** = (A) E14 pad, 2.5day; (B) E13.5 pad, 4day; (C) E14 pad, 4day. **+RA** = (D,E) E14 pad, 2.5day; (F) E14 pad, 4day; (G) E14 pad, 5day. Scale bar, 100μm, (A-G).

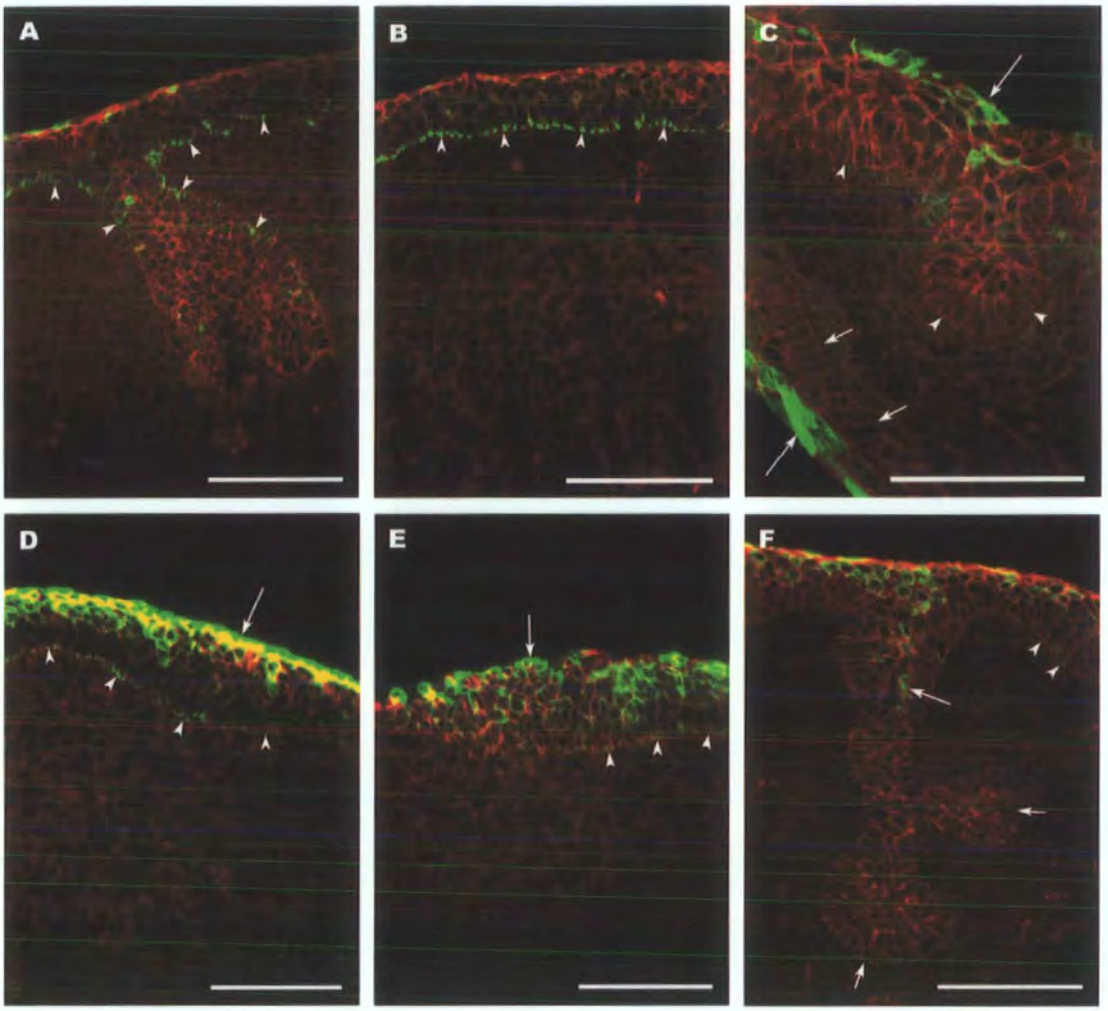

Figure 3.25. Id3 and β-catenin expression in rat mystacial pad cultures.
Id3 (green) and β-catenin (red) stained rat mystacial pad (E13.5 and E14) cultures comparing control (-RA) cultures (A-C) to retinoic acid (+RA) cultures (D-F) at various durations of culture. In E13.5 pad cultures, Id3 expression was polarised to the basal epithelium in -RA and +RA cultures (A,B,D,E; arrowheads). In E14 pads, there was no Id3 expression in the basal epithelium in -RA and +RA cultures (E,F) except for occasional weak staining in +RA cultures (F; arrowheads). **Controls** = (A,B) E13.5 pad, 4day; (C) E14 pad, 4day. **+RA** = (D,E) E13.5 pad, 5day; (F) E14 pad, 4day. Scale bar, 100μm, (A-F).

3.6 Analysis of Gene Expression by RT-PCR

3.6.1 Quality of Isolated RNA

Semi-quantitative PCR was chosen to investigate gene expression in adult vibrissae follicles of both rat and mouse. The follicles selected were those staged as being in mid-anagen where the follicles are growing most rapidly. Because of the nature of vibrissae this stage of the cycle was definable by comparing the length of the growing hair to the club hair, illustrated in Figure 3.26, and ensured the material collected was at a similar stage of the cycle. The follicles were dissected into three sections, upper follicle (UF), mid-follicle (MF) and end bulb (EB) and RNA was extracted. From each sample, a small aliquot was taken to assess to quality of the extracted RNA and was resolved on an agarose gel. The gel showed prominent 28S and 18S rRNA bands indicating good quality RNA, although this is difficult to see in the mouse RNA due to the photograph (Figure 3.26). Most samples showed the presence of genomic DNA contamination, shown on the gel as high molecular weight material. All RNA samples were DNase treated to reduce contamination to undetectable levels.

3.6.2 RT-PCR with GAPDH

RT-PCR was performed using primers specific for the house keeping gene GAPDH using 0.5µl and 1.0µl cDNA samples to check for accurate loading. The controls contained RNA that had not been reverse-transcribed (-RT) to check for any remaining genomic DNA contamination. Expression of GAPDH was equal both in rat and mouse cDNA with 0.5µl samples showing reactions still in the exponential phase, and therefore a good measure of loading. The -RT lanes gave negative results indicating no genomic DNA contamination was detected (Figure 3.27).

3.6.3 Semi-quantitative PCR for Genes of Interest

Once equal loading was established and samples were free from contamination, RT-PCR was performed with primers for genes of interest (Table 2.3). Positive controls used in the experiments consisted of bone marrow and embryonic stem (ES) cells (Figure 3.28). All genes showed differential expression in the controls. The genes BCRP and MRP1 were chosen because of their role in multidrug resistance and potential role in stem cells. Id2 and Id3 were chosen because of their important role in control of the cell cycle and proliferation and differentiation. RT-PCR results for these genes are shown in Figure 3.29. Expression of BCRP in rat was higher in the MF than UF and EB sections, although expression in these samples was still quite high. Comparing this to the mouse, BCRP was still expressed highest in the MF but very low expression was found in the EB, in contrast to the rat EB. MRP1 in rat was equally highly expressed in the MF and EB with low expression in the UF. Similarly, expression in mouse was low in the UF and highest in the MF, but MRP1 expression was absent in the EB, again in contrast to the results for rat cDNA. Expression of Id2 in rat was high in all segments, with possibly higher expression in the MF. In mouse, Id2 was expressed highest in the MF, again with UF and EB showing similar expression. Id3 expression in rat was highest in MF, with a similar level in EB and less in UF. Comparing this to mouse Id3, a similar level of expression was seen in EB, however the UF showed highest expression of Id3 with the MF lowest. This was the opposite of that seen in rat RT-PCR.

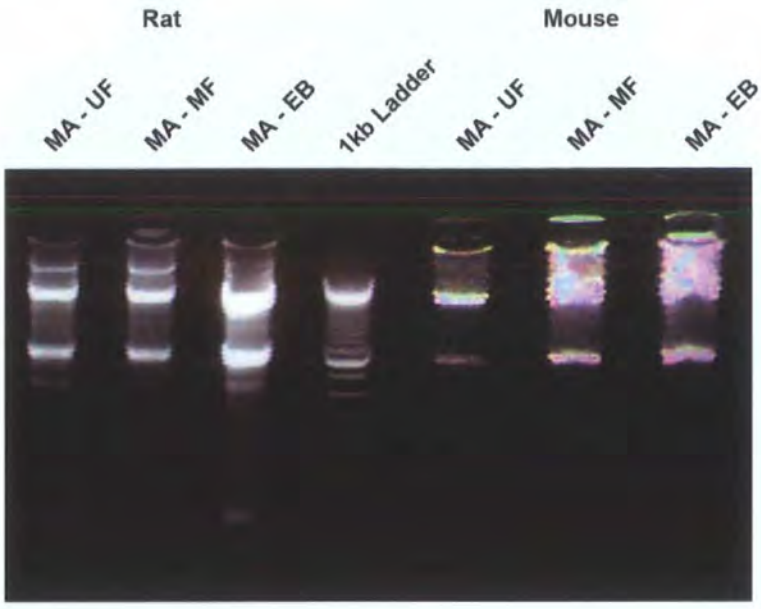

Figure 3.26. RNA extraction.

The RNA gel shows the overall quality of the total RNA for both rat and mouse isolate RNA. For both sets the 28S and 18S rRNA bands are clearly visible and well defined. Some genomic DNA contamination was detected, indicated by the presence of high molecular weight material. This was subsequently removed by DNase treatment. The mouse RNA was kindly provided by Dr. Gavin Richardson.

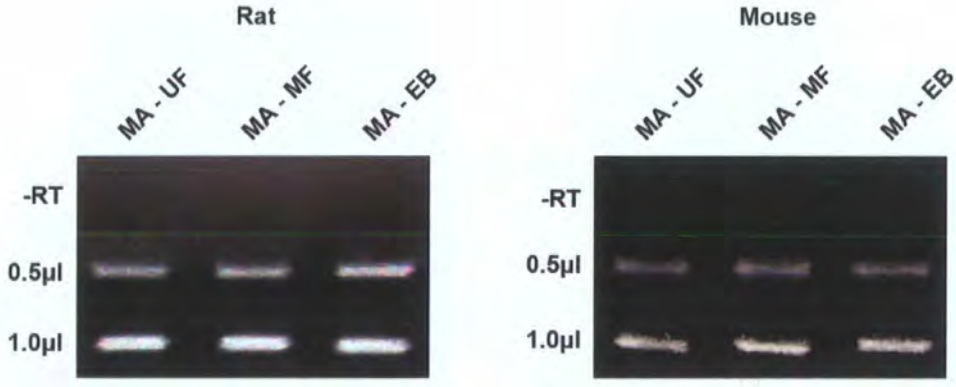

Figure 3.27. RT-PCR with GAPDH.

The DNase treated RNA was subjected to reverse-transcriptase and a PCR run with 0.5µl and 1.0µl of the house keeping gene, GAPDH, for both rat and mouse material to check for equal loading. The -RT lanes were not treated with reverse-transcriptase and show no detectable genomic contamination. Comparisons of the 0.5µl lanes show approximately equal amounts of product. The PCR's were run for 25 cycles.

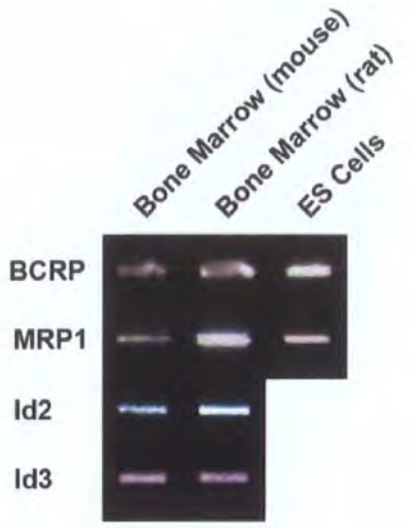

Figure 3.28. RT-PCR positive controls.
Positive controls were used to ensure the PCR had worked and to provide a reference for expression in the other lanes. The cDNA samples of bone marrow and ES cells were kindly provided by Jenna Whitehouse.

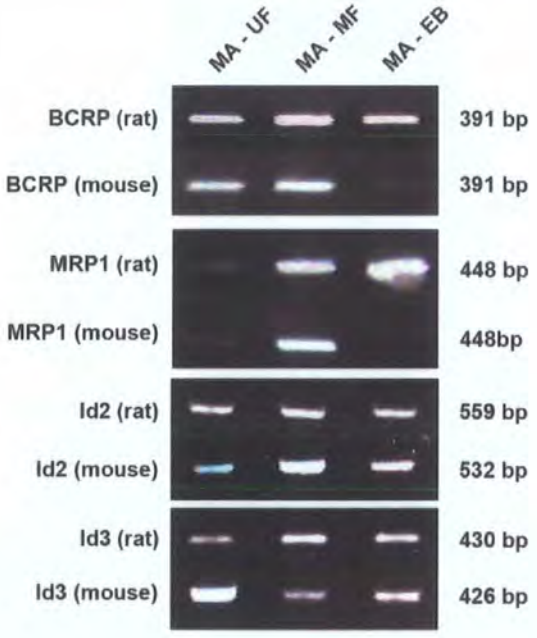

Figure 3.29. Semi-quantitative PCR analysis of genes of interest.
RT-PCR was carried out for the genes BCRP, MRP1, Id2 and Id3 using cDNA of mid-anagen vibrissae follicles dissected into upper follicle (UF), mid-follicle (MF) and end bulb (EB). BCRP was expressed highest in the MF of both rat and mouse. MRP1 showed a similar expression profile in rat and mouse but in contrast to rat EB, mouse EB showed no expression of MRP1. Id2 showed similar expression in both rat and mouse, whereas contrasting expression profiles were seen in Id3. The PCR's were run for 30 cycles except Id2 and Id3 PCR's which were run for 25 cycles to ensure the reaction products were still in the exponential phase due to abundance of Id2 and Id3 mRNA.

4.0 Discussion

4.1 Id2 Expression and Merkel Cells

In this study, immunohistochemical analysis of the protein Id2 was performed on mystacial pads of rats covering the first stages of vibrissae morphogenesis in embryos to cycling in adult follicles. In the developing embryo, Id2 expression was generally quite low in the epidermis but at sites of placode formation high levels of Id2 were seen in the cytoplasm of the developing epithelium. Not only was the staining cytoplasmic, but it also appeared to be preferentially located to the basement membrane of basal epithelial cells in direct contact with the underlying mesenchyme. At sites other than follicle morphogenesis, elevated levels of cytoplasmic Id2 were seen in some cells of the epidermis but it was more pronounced in developing follicles. Later in follicle development (stages 3+), Id2 was lost from epithelial cells at the epithelial-mesenchymal border. Consistent with Id2 expression in the developing follicle, Id proteins are known to be associated with sites of active epithelial-mesenchymal transitions (Jen *et al*, 1996).

Due to the nature of Id proteins acting as inhibitors of DNA binding, they are generally considered to be active when present in the nucleus, actively sequestering bHLH proteins. The presence of high levels of Id2 in the cytoplasm in these cells is interesting as it suggests either Id2 is not involved in blocking transcription of genes promoting differentiation or is involved in other regulatory mechanisms outside of the nucleus.

Kurooka and Yokota (Kurooka and Yokota, 2005) have recently proposed a novel mechanism for the regulation of Id2, finding evidence that Id2 has the ability to shuttle between the nucleus and the cytoplasm, due to the presence of nuclear export signals (NES) in the C-terminal domain. They also found the HLH domain contains a nuclear localisation signal (NLS), but nuclear export is dominant due to the NES, mediated by chromosome region maintenance protein 1 (CRM1). This method of regulation may be employed in specific tissues in addition to other regulatory mechanisms. It is interesting to note that due to the size of Id2 (14 kDa) the protein is capable of passive diffusion (Kurooka and Yokota, 2005), a process which needs to be strictly regulated at the post-translational level due to the multiple functions of Ids.

It is well known that Ids can form transcriptionally inactive complexes in the nucleus, thereby influencing gene expression, but what role do the Id proteins play in the cytoplasm? Work by Samanta and Kessler has highlighted the possibility of a mechanism whereby Ids, namely Id2 and Id4, can sequester bHLH proteins in the cytoplasm thereby preventing them entering the nucleus and activating gene transcription (Samanta and Kessler, 2004). More specifically, Id2 and Id4 were found to bind directly to Olig1/2 (bHLH transcription factors important for oligodendrogenesis) in oligodendrocyte precursors, inhibiting oligodendroglial lineage commitment and instead promoting generation of astrocytes (Samanta and Kessler, 2004). Such a mechanism employing bHLH factors specific to epithelial tissues may well be involved in the epithelial-mesenchymal transitions during follicle development.

At stage 2-3 of follicle development (E16), single cells located in the basal epithelium of the developing hair peg were strongly immunoreactive for Id2. Again staining was restricted to the cytoplasm of these cells. In E18 mystacial pads, very specific Id2 cellular staining was seen in cells populating the bulge region and rete ridge collar of developing vibrissae. The same cytoplasmic expression was also seen in cells in the basal epidermis. This is in contrast to work by Langlands and colleagues who found Id2 predominantly nuclear in proliferating human adult epidermis (Langlands *et al*, 2000). This discrepancy could be due to differences in roles of Ids between developing and adult skin. However, nuclear Id2 expression was seen in cells lining the mesenchymal capsule down one side of the follicle only, the opposite side to DVN entry. This expression of Id2 was first seen in E18 mystacial pads.

To elucidate if the specific Id2 expressing cells were neural in nature, as suspected by their location in the follicle, sections were double stained with the pre-synaptic vesicle marker, Synaptophysin. This molecule is ubiquitously expressed in all neurons and many endocrine cells. Synaptophysin expression revealed the innervation of the developing follicle by the DVN as early as stage 3 and also neural networks spanning the epithelium and mesenchyme of the skin. Double staining revealed co-localisation of both antibodies to the cells in question and sometimes co-expression in the cells reactive in the basal epithelium and bulge region of vibrissae. In the cells lining the mesenchymal capsule, the highly expressing Id2 cells were closely associated with cells expressing Synaptophysin and were never co-expressed. Taken together, this would suggest that the Id2 positive cells are of neural lineage.

However, expression of both antibodies was not found in all nerves as the main DVN showed no Id2 immunoreactivity.

Analysis of mystacial pad serial sections revealed the Id2 expressing cells lining the mesenchymal capsule were part of a structure which projected down from the skin rostrally at approximately 60^{0} to wrap around the rostral side of each vibrissa, acting as a sling (Dörfl, 1982). These are the intrinsic follicular muscles (also referred to as vibrissal capsular muscles) which when contracted cause protraction (forward movement) of vibrissae (Carvell *et al*, 1991; Berg and Kleinfeld, 2003). These muscles are involved in repetitive bouts of protractions and retractions at high speed, known as whisking (Welker *et al*, 1964) and are used by mammals as a means to explore their environment. They are known to be composed of mostly myosin heavy chain type 2b fibers (fast fibers), distinct from skeletal muscle, consistent with their role in fast-scanning of the sensory environment (Jin *et al*, 2004). It is likely Id2 is acting here to inhibit muscle differentiation by binding muscle specific bHLH transcription factors (such as MyoD) in the nucleus thereby promoting proliferation and preventing premature muscle differentiation. Indeed, Langlands and colleagues (Langlands *et al*, 1997) found that Id2 binds strongly to MyoD but less so to myogenin, produced as a result of MyoD transcription.

Vibrissae are responsive in the first week postnatally (Landers and Sullivan, 1999) but whisking is only possible around age P12 (Welker *et al*, 1964). Id2 was still expressed in the same cells at age P1 although the proportion of cells expressing Id2 was less. It is likely these cells are proliferating at E18 and some still at P1, supporting Id2 acting as inhibiting muscle differentiation. Further research into

mystacial pads aged P12 and beyond would confirm if Id2 shows the same expression pattern in differentiated intrinsic muscles.

It was suspected the Id2 reactive cells in the basal epidermis and the ORS of the hair follicle were Merkel cells (MCs). Double immunolabelling was performed with the MC specific antibody, Cytokeratin-20 and Id2. Staining with CK-20 revealed co-expression in Id2 positive cells only, confirming these cells as MCs. However, the Id2 expressing cells lining the mesenchymal capsule showed no immunoreactivity for the low molecular weight keratin. The earliest sign of MCs was in stage 2-3 follicles and epidermis of E16 mystacial pads, but they were present in very low numbers. Analysis of later developmental stages confirmed co-expression of Id2 and CK-20 was still present in neonates and the adult follicular cycle in the ORS of the follicle, rete ridge collar and basal epidermis. MC numbers did seem depleted in the basal epidermis in neonates compared to a typical 18 day embryo sample, but this could be because of the rapid growth and expansion of the skin between these ages, spreading MCs throughout the epidermis giving the impression of reduced numbers.

The presence of high Id2 expression in the cytoplasm of MCs is intriguing. Not only does this expression appear to be postmitotic and highly specific, it persists in MCs from embryonic skin into adults. This is surprising since Ids are generally considered to have temporal and spatial expression patterns (Jen *et al*, 1997). Persistent postmitotic Id expression has also been observed in spermatogenesis (Sablitzky *et al*, 1998). Wang and colleagues (Wang *et al*, 2001) discovered that Id2 has a vital role to play in oligodendrocyte (OL) differentiation. They reported that just before oligodendrocyte precursors (OLPs) start to differentiate, expression of Id2

changed from being nuclear to cytoplasmic. This is consistent with the possibility that Id2 plays a role in controlling the timing or ability of OLPs to differentiate (Wang *et al*, 2001). Therefore, it is reasonable to speculate Id2 may have a similar role to play in MC lineage commitment, translocating out of the nucleus to allow specific MC gene transcription. Furthermore, the persistence of Id2 in the cytoplasm may also serve to sequester bHLH proteins to the cytoplasm as reported earlier, providing another level of regulation (Samanta and Kessler, 2005).

Many bHLH transcription factors have been found expressed specifically in neural progenitors and differentiated neural cells. Interestingly, one of these factors, Math1, has been found expressed in specific neuroendocrine cell populations of the nervous system including cerebellar granule cells (Ben-Arie et al, 1997), hair cells of the inner ear (Bermingham *et al*, 1999; Chen *et al*, 2002), the developing retina (Lumpkin *et al*, 2003) and MCs (Ben-Arie et al., 2000; Helms *et al*, 2000). Id2 may be a target of Math1 in the nucleus, therefore may be involved in suppressing the proneural genes in MC precursors, and upon translocation out of the nucleus this inhibition would be removed leading to appropriate timing of neural differentiation. If this hypothesis is correct, Id2 expression in other Math1 expressing cells would be expected. Consistent with this theory, high cytoplasmic Id2 expression was seen in the developing retina in E16 head samples. In view of this I would also expect similar Id2 expression in similar specialised sensory and neuroendocrine cells, in particular the hair cells of the inner ear. However, it may be that Id2 interacts with other bHLH neural differentiation transcription factors such as NeuroD1, NeuroD2 or Math2, or even an unknown bHLH protein specific to MC differentiation. However, Leonard and co-workers postulate that the POU-IV family member Brn-3c

(now designated Pou4f3) is responsible for maintaining the neuroendocrine phenotype of MCs (Leonard *et al*, 2002). Indeed, Pou4f3 is also known to play major roles in retinal ganglion development (Liu *et al*, 2000) and the maturation and survival of hair cells of the inner ear (Keithley *et al*, 1999).

In addition to the mechanisms of regulation already mentioned, Id2 is unique amongst the Ids in that it binds to the retinoblastoma (Rb) family of tumour suppressor proteins (pRb, p107, p130) demonstrating important implications for cell cycle progression and tumourigenesis (Iaverone *et al*, 1994; Lasorella *et al*, 1996; 2000). The Rb family members, also known as 'pocket proteins', provide a crucial cell cycle checkpoint for proliferation (Weinberg, 1995). Id2, when promoting proliferation, binds to various bHLH transcription factors inhibiting transcription of genes driving differentiation. Conversely, the pocket proteins bind Id2 in a cell cycle regulated manner, removing the inhibition of bHLH factors and allowing differentiation to progress. Although Id2 persists, the block on the cell cycle is reinforced by Rb gene expression, maintaining Rb in its active, hyperphosphorylated form (Iaverone and Lasorella, 2004).

In many tumours, Id proteins have been found to be overexpressed (Kleef *et al*, 1998; Rockman *et al*, 2001; Lasorella *et al*, 2002). When Id2 is overexpressed, the Rb pathway is effectively overridden depriving cells of the most important cell cycle checkpoint leading to uncontrolled proliferation (Iaverone and Lasorella, 2004). In support of this, abnormal levels of Id1 have also been found to block transcription of pocket proteins (Ohtani *et al*, 2001) leading to inactivation of the Rb pathway. Merkel Cell Carcinoma (MCC) is a particularly rare and aggressive cancer of

neuroendocrine origin, thought to develop from MCs in the basal epithelium (Poulsen, 2004). In light of the persistently high expression of Id2 in differentiated MCs and the role of deregulated Id proteins in tumourigenesis, it seems highly plausible that Id proteins may play a vital role in MCC, an area which is yet to be investigated. It would be very interesting to examine whether Ids, in particular Id2, were overexpressed in MCC, and if so whether level of expression related to aggressiveness and an indication of prognosis, as seen in neuroblastomas (Lasorella *et al*, 2002).

MCs were found in two prominent locations in the follicle, the rete ridge collar and the ORS at the level of the bulge. Given the ability of pluripotent stem cells to emigrate out of the follicular bulge in newborn mouse skin (Taylor *et al*, 2000) and that MCs are of neural crest origin which invade the epidermis (Sieber-Blum *et al*, 2004), it may be that MCs have the ability to migrate out of the follicle and repopulate the epidermis. Indeed it has been suggested that MCs can detach from the epithelium and emigrate (Moll *et al*, 1986), fuelling speculation these cells or their progenitors may emigrate out of the follicle as an epithelial sheet with other stem cells.

4.2 Id3 Expression

As for Id2 and CK-20, immunohistochemical analysis of Id3 was performed on mystacial pads of rats covering the first stages of vibrissae morphogenesis in embryos to cycling in adult follicles. At the first stages of placode and hair bud formation, Id3 expression was absent in the mesenchyme but very high in the basal epithelium of both the developing hair bud and the epidermis. This expression was cytoplasmic but interestingly was asymmetrical and predominantly expressed at the

epithelial-mesenchymal border. Although Id2 was also expressed at a similar stage of development, the Id3 expression pattern was very distinctive. Only cells at the epithelial-mesenchymal border of stage 1-4 follicles expressed high levels of Id3, whereas cells in middle of the developing hair peg showed much lower Id3 immunoreactivity.

Double staining with β-catenin, which shows the antibody targeted to the cell membranes, helped to ascertain the localisation of Id3. In stage 4 follicles, the same polarised cytoplasmic staining was experienced in the basal epithelium but some cells inside the developing hair peg showed peri-nuclear Id3 expression. The immediately surrounding mesenchymal cells also showed weak peri-nuclear Id3 expression. This cytoplasmic staining is interesting as the main role of Ids is believed to be in blocking transcription in the nucleus. Id3 does not contain an NES and research has shown that their subcellular localisation is dependent on passive diffusion (Kurooka and Yokota, 2005) and occasionally interaction with E-protein (Deed *et al*, 1996). Indeed, the ubiquitously expressed E-protein, E47, contains an NLS and has been shown to chaperone Id3 to the nucleus (Deed *et al*, 1996). Id3 obviously isn't being regulated in that manner here, but likewise there must be some signal which is keeping Id3 restricted to the cytoplasm otherwise Id3 would be diffused throughout the cytoplasm and not targeted towards the epithelial-mesenchymal border.

It is highly likely the expression pattern seen is as result of epithelial-mesenchymal interactions which are at the heart of the developing hair follicle. However, the nature of the signal and more specifically, the interaction of Id3 at the cell membrane

is unknown. Because of the preferential location of Id3 to the epithelial-mesenchymal border, it is plausible Id3 is involved in a signalling cascade as a result of cell-cell signalling with the surrounding mesenchyme. The notch-delta pathway, important in cell-cell signalling, has been implicated in the control of transcription of Id3 in *Xenopus* (Reynaud-Deonauth *et al*, 2002) and is also known to play a role in cell fate in hair follicle morphogenesis (Kopan and Weintraub, 1993; Favier *et al*, 2000).

Secreted signalling factors such as the bone morphogenetic protein (BMP) family have been shown to be a target of Id3 and induce expression during epithelial-mesenchymal interactions (O'Shaughnessy *et al*, 2004). Alternatively, Kondo and colleagues have shown that Ids play a role in TGF-β induced epithelial-mesenchymal transdifferentiation. They reported that Id proteins interacted with E2A proteins and antagonized E2A-dependent suppression of the E-cadherin promoter. Upon stimulation with TGF-β, E2A is in molar excess and EMT is induced (Kondo *et al*, 2004). TGF-β2 has been found to be both a required and sufficient inducer of murine hair follicle morphogenesis (Foitzik *et al*, 1999). Whatever the target of Id3 in the cytoplasm it is clear elucidation of this mechanism will reveal a great deal about signalling in the epithelial-mesenchymal transitions.

Between stages 4 and 6 of follicle development, there was a dramatic change in expression of Id3. The distinctive cytoplasmic Id3 staining in the basal epithelium and epidermis had changed to being completely nuclear. Indeed, all the cells in the developing mystacial pad now reflected nuclear Id3 expression to varying levels, both epithelial and mesenchymal. Noticeably higher Id3 expression was seen in the

DP, DS, ORS at the bulge region and the rete ridge collar of vibrissae in E18 mystacial pads. This localised high expression was still present in neonates. Neonatal mystacial pads also showed developed pelage follicles displaying high nuclear expression of Id3 in the DP, lower DS, and interestingly in the bulge region.

Immunohistochemical studies by other research groups using the proliferation marker Ki67 (Magerl *et al*, 2001; Xu *et al*, 2003) have shown the DP to be a non-proliferating population. Indeed, during hair follicle morphogenesis and cycling, the epithelial cells of the hair peg and matrix cells respectively, are highly proliferative. The DS and ORS have also been reported to show localised proliferation (Magerl *et al*, 2001). Ids are generally known to inhibit differentiation and promote proliferation but this does not appear to be the case in the hair follicle. Ids are known to be involved in epithelial-mesenchymal transitions (Jen *et al*, 1996) and it has been suggested that epithelial-mesenchymal crosstalk between the matrix cells and DP respectively, keeps nuclear Id3 levels high in the DP, which in turn produces signals to induce the proliferating matrix cells to differentiate into their many lineages (O'Shaughnessy *et al*, 2004). Indeed, further work by this group demonstrated that loss of the specialised extracellular matrix by passaging of cultured DP explants resulted in loss of Id3 expression supporting the idea that Id3 is interaction and signal dependent (O'Shaughnessy *et al*, 2004). As discussed earlier, BMPs have been implicated in the control of this induction (O'Shaughnessy *et al*, 2004).

Id3 immunoreactivity was consistently higher in cells of the ORS at the bulge region both in pelage and vibrissa follicles. This region has long been associated as being the site of hair follicle stem cells (Cotsarelis *et al*, 1990; Kobayashi *et al*, 1993) due

to research into label retaining and clonogenicity of the bulge cells. Because of the Id proteins general role in promoting proliferation, it is tempting to speculate Id3 may play a role in the slow-cycling nature of these cells. Futhermore, it may be more likely to find Id3 upregulated in their highly proliferative transit-amplifying progeny, which may explain the number of highly expressing Id3 cells in this region. In support of this, Id3 (and Id1 and Id4) have been implicated in negatively regulating hematopoetic differentiation of ES cells (Nogueira *et al*, 2000), such a mechanism may be present in adult stem cells. However, in vibrissa follicles higher Id3 expression was seen at the rete ridge collar, a region not known to harbour stem cells. Due to the location, it may be that upregulated Id3 is also a feature of MCs as was seen with Id2. Further work would be required to ascertain this.

In adult follicles, high Id3 expression was seen in the DP and ORS especially in the trichilemmal sac. During the anagen stage of the adult hair cycle, much higher Id3 expression was seen around the lower end of the club hair. This is significant as it may have implications for the anchorage of the club hair, and therefore influence the timing of exogen. Overexpression studies on Id3 have shown this Id protein to promote apoptosis in various cells (Norton and Atherton, 1998; Koyama *et al*, 2004). This phenomenon was however rescued by the E-protein, E47 (Norton and Atherton, 1998).

During the adult cycle, consistent high expression of nuclear Id3 was seen in the trichilemmal sac of the ORS. Id3 was also very high in the DP during anagen and was still present in catagen but at lower levels. O'Shaughnessy and colleagues found that Id3 was absent during catagen (O'Shaughnessy *et al*, 2004), which did not

appear to be the case with my results. It could be that the follicles designated as catagen in my study are very late anagen or late catagen/early telogen which may explain the discrepancy.

4.3 Retinoic Acid Glandular Morphogenesis

After the work of Hardy and colleagues over the past 30 thirty years, the effect of excess vitamin A on the developing hair follicle has been well documented (Hardy, 1968, 1989; Hardy *et al*, 1990; Viallet *et al,* 1991; Viallet and Dhouailly, 1994). Organ culture of embryo mystacial pads treated with excess retinoids produced glandular morphogenesis of developing vibrissae (Hardy, 1968). This phenomenon was shown to be stage-dependent, time-dependent, and irreversible (Hardy *et al*, 1990) with all-*trans* retinoic acid (tRA) being the active metabolite involved in this morphogenetic program (Dhouailly *et al*, 1980). It was established that excess tRA was acting on the mesenchyme rather than the epithelium at a specific stage of development, resulting in a different dermal message being sent to the developing epithelial peg (Hardy *et al*, 1990).

In this study, E13.5 and E14 rat mystacial pads were cultured for 2.5, 4 and 5 days in culture medium containing tRA with complimentary pads set up in control culture medium. After organ culture, the mystacial pads were removed and immunohistochemical analysis of the Id proteins (Id2 and Id3) was conducted to investigate the effect of this morphogen on the expression pattern of these multi-functional proteins. The existence of MCs was also investigated due to earlier work highlighting the specific, high expression of Id2 in these specialised sensory cells.

4.3.1 Histology

Staining of mystacial pads for H&E showed cultures incubated in tRA had evidence of epithelial metaplasia, consistent with tRA acting as a morphogen. This was most obvious comparing the 2.5day cultures where RA cultures showed an increased epithelial thickening compared to a relatively undifferentiated, primitive epithelium in control cultures. After 4days of culture, both control and RA cultures were coping well in the culture conditions, displaying a multilayered epithelium and elongating epithelial pegs. In the RA cultures, clear glandular morphogenesis had occurred showing elaborate branching structures, no internal differentiation and rounded epithelial pegs, consistent with earlier work (Hardy, 1990). These glands were classified as Grade II, after Bellows and Hardy (Bellows and Hardy, 1977). No evidence of a lumen was found in these structures. The complimentary control culture showed evidence of cell death at the site of the dermal condensation, both in 4 and 5day cultures. In 5day RA cultures this was very apparent. This cell death may be indicative of the control cultures inability to progress past stage 3 of development. No internal differentiation of developing follicles or a fully formed, integrated DP was observed.

4.3.2 Id2 Expression and Merkel Cells

After 2.5days of culture, controls showed Id2 expression in developing epithelial pegs was cytoplasmic and mostly polarised to the basal membrane. This staining was similar to that seen *in vivo* in E16 mystacial pads. However, the equivalent RA cultures displayed much higher levels of cytoplasmic Id2, strongly polarised to the basal epidermis and basal epithelium of stage 2 follicles. The expression pattern observed was very similar to Id3 in E16 mystacial pads. Curiously, very high expression of Id2 was seen below 2 developing follicles, resembling a nerve -like

morphology. Further analysis would need to be carried out to elucidate if this was indeed nerve, such as the DVN. If so it would be very surprising as Id2 was restricted to specific neural lineages *in vivo* with the DVN showing no Id2 immunoreactivity. No MCs were detected in the mystacial pads after 2.5days of culture, using the antibody CK-20, whereas in follicles of a similar developmental stage *in vivo* a few MCs were present.

In E13.5 mystacial pad controls (4day), expression of Id2 was cytoplasmic and polarised but all E14 controls (4day) showed none of this characteristic staining, with high expression restricted to MCs in the basal epidermis and developing follicular epithelium, shown by double labelling with CK-20. This is consistent with expression seen *in vivo*, where cytoplasmic Id2 staining was seen in early developing follicles but this was absent as the follicle progressed to later developmental stages. In E14 RA mystacial pads, MCs were found in the glandular structures indicating the epithelial peg started to form a hair follicle, but changed developmental pathways. MCs have no known function in these glands. Id2 expression was still polarised to the epithelial-mesenchymal border, but was greatly reduced in the epithelial peg. After 5days of RA culture, MCs were still prevalent but Id2 expression was absent from the epithelial peg, but curiously still present in the cytoplasm of the basal epidermis. This could be a direct result of differentiation and cessation of epithelial-mesenchymal interactions. Id2 is known to be down-regulated in tRA culture of monocytic leukaemia cells, consistent with RA inducing differentiation and suppression of Id2 leading to reduced proliferation (Wagsater *et al*, 2003). Id2 is also known to be a retinoic acid responsive gene (Nigten *et al*, 2005). Although tRA

appeared to influence Id2 expression during early follicle development, the expression in MCs did not change.

4.3.3 Id3 and β-catenin Expression

E13.5 and E14 mystacial pads were stained for Id3 to investigate its expression and also β-catenin to visualise the cells as it is known to be important during follicle morphogenesis (Huelsken *et al*, 2001). Id3 expression in E13.5 mystacial pads after 4days of culture was as expected showing basal epithelial, polarised staining preferentially towards the epithelial-mesenchymal border, consistent with expression seen *in vivo* in E16 mystacial pads. Abnormal epithelial pegs in control cultures showed reduced Id3 expression but this may be as a consequence of the abnormal development. β-catenin expression was higher in the epithelial pegs consistent with previous reports (Huelskin *et al*, 2001). In complimentary RA cultures, E13.5 mystacial pads also showed the same Id3 expression but levels were much lower than those seen in control cultures. This may be as a result of tRA promoting differentiation. In RA cultures, the stratum corneum stained strongly for both Id3 and β-catenin but it is believed this is not positive staining due to the keratinised nature of these cells.

Interestingly in E14 mystacial pad cultures, both controls and RA, the characteristic Id3 staining seen in E13.5 mystacial pads was absent from both developing epithelial pegs and basal epidermis. *In vivo*, this loss of cytoplasmic Id3 expression was accompanied by nuclear Id3 staining throughout the mystacial pad, but this was not the case in the cultures. Throughout this study, cytoplasmic Id3 expression in the basal epithelium has been associated with epithelial-mesenchymal interactions (Jen *et al*, 1996) in the developing follicle. The lack of expression is similar to that seen

with Id2, indicating differentiating cells. However, the lack of nuclear Id3 seen widespread in mystacial pads of a similar age *in vivo* is confusing. I can only speculate that culture conditions kept nuclear Id3 levels low, whilst cytoplasmic Id3 is regulated by a different mechanism.

4.4 Gene Expression by RT-PCR

The genes chosen for RT-PCR were selected based on their potential role in stem cells and their TA population and on their influence on the cell cycle regulation and proliferation. The BCRP RT-PCR profile in rat showed expression throughout the follicle but highest in the MF, leading to speculation of a possible cell population enriched for BCRP here. The same was true for mouse but interestingly there was very low expression in the EB. I can only speculate at the apparent difference between rat and mouse BCRP, such as BCRP expression may be linked to the hair follicle cycle. Even though all follicles chosen were in mid-anagen, some variation between the stages of follicle growth is inevitable. No further experimental procedures were carried out to assess if mRNA expression matched the protein expression in the follicle.

Expression of MRP1 was similar in rat and mouse, with very high expression in the MF. Interestingly, MRP1 was absent from mouse EB but very highly expressed in rat EB, a similar situation to that of BCRP. Again it is unknown why the expression should be so different in rat and mouse. Because of the differential expression seen with MRP1, immunocytochemistry was performed on adult follicles with an MRP1 antibody to assess the protein expression profile. The results (not shown) were inconclusive showing high expression in the proliferating matrix cells and the hair shaft but largely matched the mRNA expression.

Id2 and Id3 mRNA expression was as expected, present at high levels throughout the follicle. Id2 showed high expression in rat in all segments but possibly higher expression in the MF. This was much more conclusive in mouse, showing much higher expression in the MF. Immunocytochemistry of adult follicles showed MCs were stained for Id2 in the bulge region of the ORS, and this would appear to correlate with the higher mRNA expression in the MF. Id3 showed contrasting mRNA expression, being highest in the MF and UF for rat and mouse, respectively. Immunocytochemistry of adult follicles with Id3 showed ubiquitous expression of Id3, with possibly higher expression seen around the club hair and in the ORS at the level of the isthmus.

It is important to remember with RT-PCR, the results are semi-quantitative and levels of mRNA may not accurately reflect expression at the protein level. This is illustrated by a recent study by Kowanetz and colleagues. They found that TGF-β could transiently induce Id2 and Id3 mRNA but not protein expression in certain cells types (Kowanetz *et al*, 2004).

4.5 Summary

In summary, Id2 expression was investigated during hair follicle morphogenesis and the adult hair cycle. During the early stages of morphogenesis, Id2 expression was restricted to specific cells in the basal epidermis, rete ridge collar and ORS at the bulge level of the follicle. These cells were identified as Merkel cells (MCs) by double immunolabelling Id2 with CK-20, and also with Syp. These Id2 reactive cells were still present in neonatal mystacial pads and in adult follicles. It is interesting to find that expression of Id2 in MCs was post-mitotic and persisted throughout their

life, leading to speculation that Id2 may have a protective role in the survival of these specialised cells. This finding may also have implications for the rare cancer believed to form from these cells, Merkel Cell Carcinoma.

Cells lining the mesenchymal capsule, first seen in stage 5-6 follicles, displayed high Id2 immunoreactivity but were not MCs. Other cells in very close proximity showed Syp expression leading to speculation these cells may be neural. Further analysis revealed these cells to be part of the intrinsic follicular muscles, used for protracting the follicle in a process known as 'whisking'. As these cells may well be proliferating until fully differentiated in P12, Id2 may be acting classically to inhibit muscle differentiation and promote proliferation.

In mystacial pad cultures, treatment with tRA induced glandular morphogenesis in some cultures, as expected. Immunostaining with Id2 showed a basally polarised expression pattern in the epithelial peg and basal epidermis, not seen in untreated, frozen mystacial pads. This effect was much more apparent in +RA cultures. However, Id2 expression seemed to be lost from the epithelial peg in cultures incubated for 5 days. MCs were present both in +RA and -RA cultures. Id3 expression was investigated during the same stages of morphogenesis through to neonatal and the adult hair cycle. Distinctive cytoplasmic, basally polarised expression was seen in the epithelial peg of follicles up to stage 4. After this stage, Id3 staining in the follicle was peri-nuclear with expression in most cell types except the proliferating matrix cells of the end bulb. The cytoplasmic, basally polarised staining is very interesting as Id3 is classically involved in the nucleus influencing the cell cycle amongst other functions. Elucidation of this pathway in the cytoplasm

and its influence on hair follicle morphogenesis, and possibly pattern formation will offer a valuable insight into this complex and poorly understood phenomenon.

After the switch of Id3 expression from cytoplasmic to nuclear, high expression was seen at the rete ridge collar and ORS at the bulge level. Because of the location, Id3 may also be highly expressed in MCs. However, high Id3 expression was seen in the bulge of developing pelage follicles, suggesting that this may be a feature of the putative bulge epithelial stem cells. High Id3 expression was also seen around the club hair of adult follicles and may have a role in the exogen stage of the cycle.

Analysis of Id3 staining in mystacial pad cultures revealed an interesting pattern. E13.5 cultures showed cytoplasmic, basally polarised expression in the epithelial cells, as seen in cryostat frozen sections. However, E14 mystacial pad cultures displayed none of this distinctive staining. The explanation for this 'switch' is unknown but may be an effect of the culture not providing a specific molecular signal.

4.6 Further Work

This study into the molecular expression in vibrissa follicle development and differentiation has revealed novel expression patterns of Id genes in this fascinating appendage. As a result, it has highlighted new research opportunities which merit further investigation:

1) The significance of high levels of post-mitotic Id2 expression in MCs needs to be addressed, elucidating the molecular pathways involved.

2) High Id2 expression in MCs may have implications for the rare aggressive cancer, Merkel Cell Carcinoma (MCC). Expression of Id2 has not been

examined in such a cancer and represents a new avenue to explore in the understanding and treatment of MCC.

3) Id2 was restricted in the mystacial pad to specialised neuroendocrine cells. It would be interesting to investigate the potential role of Id2 in other neuroendocrine cells, such as the hair cells of the inner ear and the developing retina.

4) Id2 knockout mice have been generated and have been found to lack NK cells, Langerhans' cells, Peyer's patches and peripheral lymph nodes (Yokota *et al*, 1999). The effect of $Id2^{-/-}$ on MCs does not appear to have been investigated and may provide vital clues to its role in MC development and differentiation.

5) Id3 expression in the early stages (1-4) of morphogenesis revealed cytoplasmic, basally polarised expression in epithelial cells. The molecular basis of this signalling, possibly at the cell membrane will provide further insights into the molecular events occurring during hair follicle morphogenesis and its effect, if any, on pattern formation.

6) High Id3 expression was seen around club hairs in adult follicles. Id3 may have a role in the shedding phase of the cycle, exogen, and will require further investigation.

7) Id3 expression was also elevated in the bulge of pelage follicles, at the rete ridge and ORS of stage 6+ vibrissa follicles. Further investigation will be required to understand the significance of this expression, especially in relation to putative stem cells in the bulge region.

8) BCRP expression was found throughout the hair follicle according to RT-PCR data. This molecule has recently been found expressed in stem cells and SP cells of the heart and skeletal muscle. Immunocytochemical analysis in vibrissa and pelage follicles may reveal a role for BCRP in the multiple stem cell and SPs of the hair follicle.

5.0 Appendix

5.1 General Solutions and Culture Medium

5.1.1 Phosphate Buffered Saline

The following reagents were accurately weighed out and then made up to 5 litres using distilled water. The solution was mixed using a magnetic stirrer until fully dissolved. The pH was adjusted to 7.4 using conc. HCl. Before being used for immunohistochemistry the solution was paper filtered.

40.0g NaCl
9.03g $Na_2HP0_4 \cdot 2H_20$
1.45g KH_2P0_4
1.00g KCl

5.1.2 Mowiol

The reagents below were mixed together in a falcon tube and left for several hours with periodic mixing. 12ml of 0.2M Tris-HCl (pH 8.5) was added and incubated at 50°C in a water bath for 30mins, mixing occasionally. The mixture was centrifuged at 5000g for 15mins and the supernatant aliquoted into 1.5ml mini-centrifuge tubes and stored at -20°C.

6.0ml dH_20
6.0g Glycerol (analytical grade)
2.4g Mowiol 4.88 (Calbiochem)
2.5% DABCO (Diazobicyclo-octane)

5.1.3 Poly-l-lysine

The stock (P8920, Sigma) was diluted 1:10 using filtered PBS, mixed well and stored at 4°C. To coat slides the solution was brought to room temperature and clean slides (Superfrost, VWR) were submerged in poly-l-lysine held by glass slide holders. The

slides were incubated for 30mins then transferred to a hot oven for drying. Once dry the slides were ready to use.

5.1.4 Blocking Buffer

Filtered PBS was supplemented with 0.2% fish skin gelatin (FSG; Sigma) and used as a blocking reagent in immunocytochemistry.

5.1.5 EMEM Culture Medium

EMEM medium (Sigma, UK) containing 50μg/ml Fungicide and Gentamycin was supplemented with 20% FCS (Sigma). To 10ml of this medium, 0.1ml of all-*trans* retinoic acid (tRA) (500μg/ml dissolved in absolute ethanol) was added, or for the control medium 0.1ml absolute ethanol. This medium was used for culture of rat mystacial face pads investigating the effect of RA on follicle morphogenesis.

8ml EMEM
2ml FCS
0.1ml RA (500μg/ml) or absolute ethanol

5.1.6 DEPC Treated Water

Distilled water was treated with 0.1% diethylpyrocarbonate (DEPC), an RNase inhibitor. The water was left to mix overnight in glass bottles and then autoclaved.

5.1.7 Agarose Gel Electrophoresis

Products of PCR were electrophoresed on a 2% agarose gel containing ethidium bromide (0.1μg/ml) in 1X Tris-Acetate-EDTA (TAE) buffer (0.04M Tris-acetate, 0.001M EDTA, pH 7.6). This was done to ensure the amplified fragment was the correct length, check the level of expression in the cDNA samples as part of semi-quantitative PCR and that the samples were free from contamination. 2μl of 6X DNA loading buffer was added to each sample and mixed, then 20μl of each PCR amplified

product was loaded onto the gel along with 5µl of 1kb Molecular Marker (Invitrogen) in a separate well. It was run at 90 volts until the loading buffer had moved 4-5 cm down the gel giving sufficient resolution of product. The gels were photographed using a Gel Doc 2000 transilluminator (Bio-Rad, UK) running Quantity One software.

6.0 Bibliography

Allikmets, R., Schriml, L.M., Hutchinson, A., Romano-Spica, V., and Dean, M. (1998). A human placenta-specific ATP-binding cassette gene (ABCP) on chromosome 4q22 that is involved in multidrug resistance. Cancer Res **58,** 5337-5339.

Alway, S.E., Martyn, J.K., Ouyang, J., Chaudhrai, A., and Murlasits, Z.S. (2003). Id2 expression during apoptosis and satellite cell activation in unloaded and loaded quail skeletal muscles. Am J Physiol Regul Integr Comp Physiol **284,** R540-549.

Andres, K.H. (1966). Uber die Feinstrukter der Rezeptoren an Sinushaaren. Z. Zellforsch **75,** 339-365.

Auber, L. (1952). The anatomy of follicles producing wool-fibers, with special reference to keratinization. Trans Roy Soc Edin **62,** 191-254.

Bain, G., Cravatt, C.B., Loomans, C., Alberola-Ila, J., Hedrick, S.M., and Murre, C. (2001). Regulation of the helix-loop-helix proteins, E2A and Id3, by the Ras-ERK MAPK cascade. Nat Immunol **2,** 165-171.

Bakos, E., Evers, R., Szakacs, G., Tusnady, G.E., Welker, E., Szabo, K., de Haas, M., van Deemter, L., Borst, P., Varadi, A., and Sarkadi, B. (1998). Functional multidrug resistance protein (MRP1) lacking the N-terminal transmembrane domain. J Biol Chem **273,** 32167-32175.

Balmer, J.E., and Blomhoff, R. (2005). A robust characterization of retinoic acid response elements based on a comparison of sites in three species. J Steroid Biochem Mol Biol **96,** 347-354.

Barsh, G. (1999). Of ancient tales and hairless tails. Nat Genet **22,** 315-316.

Belletti, B., Prisco, M., Morrione, A., Valentinis, B., Navarro, M., and Baserga, R. (2001). Regulation of Id2 gene expression by the insulin-like growth factor I receptor requires signaling by phosphatidylinositol 3-kinase. J Biol Chem **276,** 13867-13874.

Bellows, C.G., and Hardy, M.H. (1977). Histochemical evidence of mucosubstances in the metaplastic epidermis and hair follicles produced in vitro in the presence of excess vitamin A. Anat Rec **187,** 257-271.

Ben-Arie, N., Bellen, H.J., Armstrong, D.L., McCall, A.E., Gordadze, P.R., Guo, Q., Matzuk, M.M., and Zoghbi, H.Y. (1997). Math1 is essential for genesis of cerebellar granule neurons. Nature **390,** 169-172.

Ben-Arie, N., Hassan, B.A., Bermingham, N.A., Malicki, D.M., Armstrong, D., Matzuk, M., Bellen, H.J., and Zoghbi, H.Y. (2000). Functional conservation of atonal and Math1 in the CNS and PNS. Development **127,** 1039-1048.

Benezra, R., Rafii, S., and Lyden, D. (2001). The Id proteins and angiogenesis. Oncogene **20,** 8334-8341.

Berg, R.W., and Kleinfeld, D. (2003). Vibrissa movement elicited by rhythmic electrical microstimulation to motor cortex in the aroused rat mimics exploratory whisking. J Neurophysiol **90,** 2950-2963.

Bermingham, N.A., Hassan, B.A., Price, S.D., Vollrath, M.A., Ben-Arie, N., Eatock, R.A., Bellen, H.J., Lysakowski, A., and Zoghbi, H.Y. (1999). Math1: an essential gene for the generation of inner ear hair cells. Science **284,** 1837-1841.

Bitgood, M.J., and McMahon, A.P. (1995). Hedgehog and Bmp genes are coexpressed at many diverse sites of cell-cell interaction in the mouse embryo. Dev Biol **172,** 126-138.

Blanpain, C., Lowry, W.E., Geoghegan, A., Polak, L., and Fuchs, E. (2004). Self-renewal, multipotency, and the existence of two cell populations within an epithelial stem cell niche. Cell **118,** 635-648.

Blom, B., Heemskerk, M.H., Verschuren, M.C., van Dongen, J.J., Stegmann, A.P., Bakker, A.Q., Couwenberg, F., Res, P.C., and Spits, H. (1999). Disruption of alpha beta but not of gamma delta T cell development by overexpression of the helix-loop-helix protein Id3 in committed T cell progenitors. Embo J **18,** 2793-2802.

Borst, P., Evers, R., Kool, M., and Wijnholds, J. (2000). A family of drug transporters: the multidrug resistance-associated proteins. J Natl Cancer Inst **92,** 1295-1302.

Breathnach, A.S. (1980). Branched cells in the epidermis: an overview. J Invest Dermatol **75,** 6-11.

Bunting, K.D. (2002). ABC transporters as phenotypic markers and functional regulators of stem cells. Stem Cells **20,** 11-20.

Cai, J., Cheng, A., Luo, Y., Lu, C., Mattson, M.P., Rao, M.S., and Furukawa, K. (2004). Membrane properties of rat embryonic multipotent neural stem cells. J Neurochem **88,** 212-226.

Cai, J., Wu, Y., Mirua, T., Pierce, J.L., Lucero, M.T., Albertine, K.H., Spangrude, G.J., and Rao, M.S. (2002). Properties of a fetal multipotent neural stem cell (NEP cell). Dev Biol **251,** 221-240.

Carvell, G.E., Simons, D.J., Lichtenstein, S.H., and Bryant, P. (1991). Electromyographic activity of mystacial pad musculature during whisking behavior in the rat. Somatosens Mot Res **8,** 159-164.

Cauna, N. (1963). Functional Significance of the Submicroscopical, Histochemical and Microscopical Organization of the Cutaneous Receptor Organs. Verh Anat Ges **57,** 181-197.

Chambon, P. (1996). A decade of molecular biology of retinoic acid receptors. Faseb J **10,** 940-954.

Chan, L.M., Lowes, S., and Hirst, B.H. (2004). The ABCs of drug transport in intestine and liver: efflux proteins limiting drug absorption and bioavailability. Eur J Pharm Sci **21,** 25-51.

Chase, H.B., Rauch, R., and Smith, V.W. (1951). Critical stages of hair development and pigmentation in the mouse. Physiol Zool **24,** 1-8.

Chase, H.B., Montagna, W., and Malone, J.D. (1953). Changes in the skin in relation to the hair growth cycle. Anat Rec **116,** 75-81.

Chase, H.B. (1954). Growth of the hair. Physiol Rev **34,** 113-126.

Chen, P., Johnson, J.E., Zoghbi, H.Y., and Segil, N. (2002). The role of Math1 in inner ear development: Uncoupling the establishment of the sensory primordium from hair cell fate determination. Development **129,** 2495-2505.

Cheng-Chew, S.B., and Leung, P.Y. (1994). Ultrastructural study of the Merkel cell and its expression of met-enkephalin immunoreactivity during fetal and postnatal development in mice. J Anat **185 (Pt 3),** 511-520.

Cheng-Chew, S.B., and Leung, P.Y. (1996). Localisation of VIP-and CGRP-like substances in the skin and sinus hair follicles of various mammalian species. Histochem Cell Biol **105,** 443-452.

Chew, S.B., and Leung, P.Y. (1991). Immunocytochemical evidence of a met-enkephalin-like substance in the dense-core granules of mouse Merkel cells. Cell Tissue Res **265,** 611-614.

Chuong, C.M., Widelitz, R.B., Ting-Berreth, S., and Jiang, T.X. (1996). Early events during avian skin appendage regeneration: dependence on epithelial-mesenchymal interaction and order of molecular reappearance. J Invest Dermatol **107,** 639-646.

Cole, S.P., Bhardwaj, G., Gerlach, J.H., Mackie, J.E., Grant, C.E., Almquist, K.C., Stewart, A.J., Kurz, E.U., Duncan, A.M., and Deeley, R.G. (1992). Overexpression of a transporter gene in a multidrug-resistant human lung cancer cell line. Science **258,** 1650-1654.

Coppe, J.P., Smith, A.P., and Desprez, P.Y. (2003). Id proteins in epithelial cells. Exp Cell Res **285,** 131-145.

Cotsarelis, G., Sun, T.T., and Lavker, R.M. (1990). Label-retaining cells reside in the bulge area of pilosebaceous unit: implications for follicular stem cells, hair cycle, and skin carcinogenesis. Cell **61,** 1329-1337.

Cronk, K.M., Wilkinson, G.A., Grimes, R., Wheeler, E.F., Jhaveri, S., Fundin, B.T., Silos-Santiago, I., Tessarollo, L., Reichardt, L.F., and Rice, F.L. (2002). Diverse dependencies of developing Merkel innervation on the trkA and both full-length and truncated isoforms of trkC. Development **129,** 3739-3750.

Dahmane, N., Lee, J., Robins, P., Heller, P., and Ruiz i Altaba, A. (1997). Activation of the transcription factor Gli1 and the Sonic hedgehog signalling pathway in skin tumours. Nature **389,** 876-881.

DasGupta, R., and Fuchs, E. (1999). Multiple roles for activated LEF/TCF transcription complexes during hair follicle development and differentiation. Development **126,** 4557-4568.

de Paiva, C.S., Chen, Z., Corrales, R.M., Pflugfelder, S.C., and Li, D.Q. (2005). ABCG2 transporter identifies a population of clonogenic human limbal epithelial cells. Stem Cells **23,** 63-73.

De Weert, J., Kint, A., and Geerts, M.L. (1982). Morphological changes in the proximal area of the rat's hair follicle during early catagen. An electron-microscopic study. Arch Dermatol Res **272,** 79-92.

Deed, R.W., Armitage, S., and Norton, J.D. (1996). Nuclear localization and regulation of Id protein through an E protein-mediated chaperone mechanism. J Biol Chem **271,** 23603-23606.

Deed, R.W., Hara, E., Atherton, G.T., Peters, G., and Norton, J.D. (1997). Regulation of Id3 cell cycle function by Cdk-2-dependent phosphorylation. Mol Cell Biol **17,** 6815-6821.

Dhouailly, D. (1973). Dermo-epidermal interactions between birds and mammals: differentiation of cutaneous appendages. J Embryol Exp Morphol **30,** 587-603.

Dhouailly, D., and Sengel, P. (1975). [Feather- and hair-forming properties of dermal cells of glabrous skin from bird and mammals]. C R Acad Sci Hebd Seances Acad Sci D **281,** 1007-1010.

Dhouailly, D. (1978). Feather-forming capacities of the avian extra-embryonic somatopleure. J Embryol Exp Morphol **43,** 279-287.

Dhouailly, D., Hardy, M.H., and Sengel, P. (1980). Formation of feathers on chick foot scales: a stage-dependent morphogenetic response to retinoic acid. J Embryol Exp Morphol **58,** 63-78.

Dorfl, J. (1982). The musculature of the mystacial vibrissae of the white mouse. J Anat **135,** 147-154.

Dörfl, J. (1985). The innervation of the mystacian region of the white mouse. A topographical study. J Anat **142,** 173-184.

Doyle, L.A., Yang, W., Abruzzo, L.V., Krogmann, T., Gao, Y., Rishi, A.K., and Ross, D.D. (1998). A multidrug resistance transporter from human MCF-7 breast cancer cells. Proc Natl Acad Sci U S A **95,** 15665-15670.

Dry, F.W. (1926). The coat of the mouse (Mus musculum). J. Genet. **16,** 287-340.

Duncan, M., DiCicco-Bloom, E.M., Xiang, X., Benezra, R., and Chada, K. (1992). The gene for the helix-loop-helix protein, Id, is specifically expressed in neural precursors. Dev Biol **154,** 1-10.

Durward, A., and Rudall, K.M. (1949). Studies on hair growth in the rat. J Anat **83,** 325-335, 324 pl.

Ekholm, E., and Egelrud, T. (1998). The expression of stratum corneum chymotryptic enzyme in human anagen hair follicles: further evidence for its involvement in desquamation-like processes. Br J Dermatol **139,** 585-590.

Ellmeier, W., and Weith, A. (1995). Expression of the helix-loop-helix gene Id3 during murine embryonic development. Dev Dyn **203,** 163-173.

Favier, B., Fliniaux, I., Thelu, J., Viallet, J.P., Demarchez, M., Jahoda, C.A., and Dhouailly, D. (2000). Localisation of members of the notch system and the differentiation of vibrissa hair follicles: receptors, ligands, and fringe modulators. Dev Dyn **218,** 426-437.

Foitzik, K., Paus, R., Doetschman, T., and Dotto, G.P. (1999). The TGF-beta2 isoform is both a required and sufficient inducer of murine hair follicle morphogenesis. Dev Biol **212,** 278-289.

Fong, S., Debs, R.J., and Desprez, P.Y. (2004). Id genes and proteins as promising targets in cancer therapy. Trends Mol Med **10,** 387-392.

Forrest, S.T., Taylor, A.M., Sarembock, I.J., Perlegas, D., and McNamara, C.A. (2004). Phosphorylation regulates Id3 function in vascular smooth muscle cells. Circ Res **95,** 557-559.

Fuchs, E., Merrill, B.J., Jamora, C., and DasGupta, R. (2001). At the roots of a never-ending cycle. Dev Cell **1,** 13-25.

Gilliam, A.C., Kremer, I.B., Yoshida, Y., Stevens, S.R., Tootell, E., Teunissen, M.B., Hammerberg, C., and Cooper, K.D. (1998). The human hair follicle: a reservoir of CD40+ B7-deficient Langerhans cells that repopulate epidermis after UVB exposure. J Invest Dermatol **110,** 422-427.

Gleichmann, M., Buchheim, G., El-Bizri, H., Yokota, Y., Klockgether, T., Kugler, S., Bahr, M., Weller, M., and Schulz, J.B. (2002). Identification of inhibitor-of-differentiation 2 (Id2) as a modulator of neuronal apoptosis. J Neurochem **80,** 755-762.

Goodell, M.A., Rosenzweig, M., Kim, H., Marks, D.F., DeMaria, M., Paradis, G., Grupp, S.A., Sieff, C.A., Mulligan, R.C., and Johnson, R.P. (1997). Dye efflux studies suggest that hematopoietic stem cells expressing low or undetectable levels of CD34 antigen exist in multiple species. Nat Med **3,** 1337-1345.

Gottesman, M.M., Pastan, I., and Ambudkar, S.V. (1996). P-glycoprotein and multidrug resistance. Curr Opin Genet Dev **6,** 610-617.

Haeberle, H., Fujiwara, M., Chuang, J., Medina, M.M., Panditrao, M.V., Bechstedt, S., Howard, J., and Lumpkin, E.A. (2004). Molecular profiling

reveals synaptic release machinery in Merkel cells. Proc Natl Acad Sci U S A **101,** 14503-14508.

Halata, Z. (1975). The mechanoreceptors of the mammalian skin ultrastructure and morphological classification. Adv Anat Embryol Cell Biol **50,** 3-77.

Halata, Z., and Sames, K. (2002). Merkel Nerve Endings in Sinus Hairs of Young and Aged Rats.

Halata, Z., Grim, M., and Bauman, K.I. (2003). Friedrich Sigmund Merkel and his "Merkel cell", morphology, development, and physiology: review and new results. Anat Rec A Discov Mol Cell Evol Biol **271,** 225-239.

Hara, E., Hall, M., and Peters, G. (1997). Cdk2-dependent phosphorylation of Id2 modulates activity of E2A-related transcription factors. Embo J **16,** 332-342.

Hardy, M.H. (1949). The development of mouse hair in vitro with some observations on pigmentation. J Anat **83,** 364-384, 363 pl.

Hardy, M.H. (1951). The development of pelage hairs and vibrissae from skin in tissue culture. Ann N Y Acad Sci **53,** 546-561.

Hardy, M.H. (1968). Glandular metaplasia of hair follicles and other responses to vitamin A excess in cultures of rodent skin. J Embryol Exp Morphol **19,** 157-180.

Hardy, M.H. (1969). The differentiation of hair follicles and hairs in organ culture. In Advances in Biology of Skin, Vol. IX Hair Growth (Eds W. Montagna & R. L. Dobson) Pergamon Press, Oxford, 35-60.

Hardy, M.H. (1989). The use of retinoids as probes for analyzing morphogenesis of glands from epithelial tissues. In Vitro Cell Dev Biol **25,** 454-459.

Hardy, M.H. (1992). The secret life of the hair follicle. Trends Genet **8,** 55-61.

Hardy, M.H., and Vielkind, U. (1996). Changing patterns of cell adhesion molecules during mouse pelage hair follicle development. 1. Follicle morphogenesis in wild-type mice. Acta Anat (Basel) **157,** 169-182.

Hardy, M.H., Dhouailly, D., Torma, H., and Vahlquist, A. (1990). Either chick embryo dermis or retinoid-treated mouse dermis can initiate glandular morphogenesis from mammalian epidermal tissue. J Exp Zool **256,** 279-289.

Hartschuh, W., and Weihe, E. (1988). Multiple messenger candidates and marker substance in the mammalian Merkel cell-axon complex: a light and electron microscopic immunohistochemical study. Prog Brain Res **74,** 181-187.

Hartschuh, W., Weihe, E., and Reinecke, M. (1986). The Merkel cell. Biology of the Integument 2, 605-620.

Hartschuh, W., Weihe, E., and Egner, U. (1990). Electron microscopic immunogold cytochemistry reveals chromogranin A confined to secretory granules of porcine Merkel cells. Neurosci Lett **116,** 245-249.

Hashimoto, K., and Shibazaki, S. (1976). Ultrastructural study on differentiation and funtion of hair. Biology and Disease of the Hair. University Park Press, Baltimore., 23-57.

Heemskerk, M.H., Blom, B., Nolan, G., Stegmann, A.P., Bakker, A.Q., Weijer, K., Res, P.C., and Spits, H. (1997). Inhibition of T cell and promotion of natural killer cell development by the dominant negative helix loop helix factor Id3. J Exp Med **186,** 1597-1602.

Helms, A.W., Abney, A.L., Ben-Arie, N., Zoghbi, H.Y., and Johnson, J.E. (2000). Autoregulation and multiple enhancers control Math1 expression in the developing nervous system. Development **127,** 1185-1196.

Hollnagel, A., Oehlmann, V., Heymer, J., Ruther, U., and Nordheim, A. (1999). Id genes are direct targets of bone morphogenetic protein induction in embryonic stem cells. J Biol Chem **274,** 19838-19845.

Huelsken, J., Vogel, R., Erdmann, B., Cotsarelis, G., and Birchmeier, W. (2001). beta-Catenin controls hair follicle morphogenesis and stem cell differentiation in the skin. Cell **105,** 533-545.

Iavarone, A., and Lasorella, A. (2004). Id proteins in neural cancer. Cancer Lett **204,** 189-196.

Iavarone, A., Garg, P., Lasorella, A., Hsu, J., and Israel, M.A. (1994). The helix-loop-helix protein Id-2 enhances cell proliferation and binds to the retinoblastoma protein. Genes Dev **8,** 1270-1284.

Iggo, A., and Findlater, G.S. (1984). A Review of Merkel cell mechanisms. Sensory Receptor Mechanisms **World Scientific Publications, Singapore,** 117-131.

Ikawa, T., Fujimoto, S., Kawamoto, H., Katsura, Y., and Yokota, Y. (2001). Commitment to natural killer cells requires the helix-loop-helix inhibitor Id2. Proc Natl Acad Sci U S A **98,** 5164-5169.

Ikeda, I., Yamashita, Y., Ono, T., and Ogawa, H. (1994). Selective phototoxic destruction of rat Merkel cells abolishes responses of slowly adapting type I mechanoreceptor units. J Physiol **479 (Pt 2),** 247-256.

Ito, M., Kizawa, K., Hamada, K., and Cotsarelis, G. (2004). Hair follicle stem cells in the lower bulge form the secondary germ, a biochemically distinct but functionally equivalent progenitor cell population, at the termination of catagen. Differentiation **72,** 548-557.

Jahoda, C.A. (1992). Induction of follicle formation and hair growth by vibrissa dermal papillae implanted into rat ear wounds: vibrissa-type fibres are specified. Development **115,** 1103-1109.

Jahoda, C.A., and Oliver, R.F. (1984a). Vibrissa dermal papilla cell aggregative behaviour in vivo and in vitro. J Embryol Exp Morphol **79,** 211-224.

Jahoda, C.A., and Oliver, R.F. (1984b). Observations on the relationship between nerve supply and hair positioning in the rat vibrissa follicle. J Anat **139 (Pt 2),** 333-339.

Jahoda, C.A., Horne, K.A., and Oliver, R.F. (1984). Induction of hair growth by implantation of cultured dermal papilla cells. Nature **311,** 560-562.

Jahoda, C.A., Mauger, A., Bard, S., and Sengel, P. (1992). Changes in fibronectin, laminin and type IV collagen distribution relate to basement membrane restructuring during the rat vibrissa follicle hair growth cycle. J Anat **181 (Pt 1),** 47-60.

Jen, Y., Manova, K., and Benezra, R. (1996). Expression patterns of Id1, Id2, and Id3 are highly related but distinct from that of Id4 during mouse embryogenesis. Dev Dyn **207,** 235-252.

Jen, Y., Manova, K., and Benezra, R. (1997). Each member of the Id gene family exhibits a unique expression pattern in mouse gastrulation and neurogenesis. Dev Dyn **208,** 92-106.

Jin, T.E., Witzemann, V., and Brecht, M. (2004). Fiber types of the intrinsic whisker muscle and whisking behavior. J Neurosci **24,** 3386-3393.

Karlsson, L., Bondjers, C., and Betsholtz, C. (1999). Roles for PDGF-A and sonic hedgehog in development of mesenchymal components of the hair follicle. Development **126,** 2611-2621.

Kee, B.L., Rivera, R.R., and Murre, C. (2001). Id3 inhibits B lymphocyte progenitor growth and survival in response to TGF-beta. Nat Immunol **2,** 242-247.

Keithley, E.M., Erkman, L., Bennett, T., Lou, L., and Ryan, A.F. (1999). Effects of a hair cell transcription factor, Brn-3.1, gene deletion on homozygous and heterozygous mouse cochleas in adulthood and aging. Hear Res **134,** 71-76.

Kim, D.K., and Holbrook, K.A. (1995). The appearance, density, and distribution of Merkel cells in human embryonic and fetal skin: their relation to sweat gland and hair follicle development. J Invest Dermatol **104,** 411-416.

Kinkelin, I., Stucky, C.L., and Koltzenburg, M. (1999). Postnatal loss of Merkel cells, but not of slowly adapting mechanoreceptors in mice lacking the neurotrophin receptor p75. Eur J Neurosci **11,** 3963-3969.

Kleeff, J., Ishiwata, T., Friess, H., Buchler, M.W., Israel, M.A., and Korc, M. (1998). The helix-loop-helix protein Id2 is overexpressed in human pancreatic cancer. Cancer Res **58,** 3769-3772.

Klein, I., Sarkadi, B., and Varadi, A. (1999). An inventory of the human ABC proteins. Biochim Biophys Acta **1461,** 237-262.

Kligman, A.M. (1961). Pathologic dynamics of human hair loss. I. Telogen effuvium. Arch Dermatol **83,** 175-198.

Kobayashi, K., Rochat, A., and Barrandon, Y. (1993). Segregation of keratinocyte colony-forming cells in the bulge of the rat vibrissa. Proc Natl Acad Sci U S A **90,** 7391-7395.

Kondo, M., Cubillo, E., Tobiume, K., Shirakihara, T., Fukuda, N., Suzuki, H., Shimizu, K., Takehara, K., Cano, A., Saitoh, M., and Miyazono, K. (2004). A role for Id in the regulation of TGF-beta-induced epithelial-mesenchymal transdifferentiation. Cell Death Differ **11,** 1092-1101.

Kopan, R., and Weintraub, H. (1993). Mouse notch: expression in hair follicles correlates with cell fate determination. J Cell Biol **121,** 631-641.

Kowanetz, M., Valcourt, U., Bergstrom, R., Heldin, C.H., and Moustakas, A. (2004). Id2 and Id3 define the potency of cell proliferation and differentiation responses to transforming growth factor beta and bone morphogenetic protein. Mol Cell Biol **24,** 4241-4254.

Koyama, T., Suzuki, H., Imakiire, A., Yanase, N., Hata, K., and Mizuguchi, J. (2004). Id3-mediated enhancement of cisplatin-induced apoptosis in a sarcoma cell line MG-63. Anticancer Res **24,** 1519-1524.

Kurooka, H., and Yokota, Y. (2005). Nucleo-cytoplasmic shuttling of Id2, a negative regulator of basic helix-loop-helix transcription factors. J Biol Chem **280,** 4313-4320.

Landers, M.S., and Sullivan, R.M. (1999). Vibrissae-evoked behavior and conditioning before functional ontogeny of the somatosensory vibrissae cortex. J Neurosci **19,** 5131-5137.

Langlands, K., Down, G.A., and Kealey, T. (2000). Id proteins are dynamically expressed in normal epidermis and dysregulated in squamous cell carcinoma. Cancer Res **60,** 5929-5933.

Langlands, K., Yin, X., Anand, G., and Prochownik, E.V. (1997). Differential interactions of Id proteins with basic-helix-loop-helix transcription factors. J Biol Chem **272,** 19785-19793.

Lasorella, A., Iavarone, A., and Israel, M.A. (1996). Id2 specifically alters regulation of the cell cycle by tumor suppressor proteins. Mol Cell Biol **16,** 2570-2578.

Lasorella, A., Boldrini, R., Dominici, C., Donfrancesco, A., Yokota, Y., Inserra, A., and Iavarone, A. (2002). Id2 is critical for cellular proliferation and is the oncogenic effector of N-myc in human neuroblastoma. Cancer Res **62,** 301-306.

Lavker, R.M., and Sun, T.T. (1982). Heterogeneity in epidermal basal keratinocytes: morphological and functional correlations. Science **215,** 1239-1241.

Lavker, R.M., and Sun, T.T. (2000). Epidermal stem cells: properties, markers, and location. Proc Natl Acad Sci U S A **97,** 13473-13475.

Lavker, R.M., Risse, B., Brown, H., Ginsburg, D., Pearson, J., Baker, M.S., and Jensen, P.J. (1998). Localization of plasminogen activator inhibitor type 2 (PAI-2) in hair and nail: implications for terminal differentiation. J Invest Dermatol **110,** 917-922.

Lindner, G., Botchkarev, V.A., Botchkareva, N.V., Ling, G., van der Veen, C., and Paus, R. (1997). Analysis of apoptosis during hair follicle regression (catagen). Am J Pathol **151,** 1601-1617.

Lindner, G., Menrad, A., Gherardi, E., Merlino, G., Welker, P., Handjiski, B., Roloff, B., and Paus, R. (2000). Involvement of hepatocyte growth factor/scatter factor and met receptor signaling in hair follicle morphogenesis and cycling. Faseb J **14,** 319-332.

Litman, T., Druley, T.E., Stein, W.D., and Bates, S.E. (2001). From MDR to MXR: new understanding of multidrug resistance systems, their properties and clinical significance. Cell Mol Life Sci **58,** 931-959.

Liu, W., Khare, S.L., Liang, X., Peters, M.A., Liu, X., Cepko, C.L., and Xiang, M. (2000). All Brn3 genes can promote retinal ganglion cell differentiation in the chick. Development **127,** 3237-3247.

Longley, D.B., and Johnston, P.G. (2005). Molecular mechanisms of drug resistance. J Pathol **205,** 275-292.

Lyden, D., Young, A.Z., Zagzag, D., Yan, W., Gerald, W., O'Reilly, R., Bader, B.L., Hynes, R.O., Zhuang, Y., Manova, K., and Benezra, R. (1999). Id1 and Id3 are required for neurogenesis, angiogenesis and vascularization of tumour xenografts. Nature **401,** 670-677.

Lyle, S., Christofidou-Solomidou, M., Liu, Y., Elder, D.E., Albelda, S., and Cotsarelis, G. (1998). The C8/144B monoclonal antibody recognizes cytokeratin 15 and defines the location of human hair follicle stem cells. J Cell Sci **111 (Pt 21),** 3179-3188.

Ma, D.R., Yang, E.N., and Lee, S.T. (2004). A review: the location, molecular characterisation and multipotency of hair follicle epidermal stem cells. Ann Acad Med Singapore **33,** 784-788.

Magerl, M., Tobin, D.J., Muller-Rover, S., Hagen, E., Lindner, G., McKay, I.A., and Paus, R. (2001). Patterns of proliferation and apoptosis during murine hair follicle morphogenesis. J Invest Dermatol **116,** 947-955.

Maklad, A., Fritzsch, B., and Hansen, L.A. (2004). Innervation of the maxillary vibrissae in mice as revealed by anterograde and retrograde tract tracing. Cell Tissue Res **315,** 167-180.

Martin, C.M., Meeson, A.P., Robertson, S.M., Hawke, T.J., Richardson, J.A., Bates, S., Goetsch, S.C., Gallardo, T.D., and Garry, D.J. (2004). Persistent expression of the ATP-binding cassette transporter, Abcg2, identifies cardiac SP cells in the developing and adult heart. Dev Biol **265,** 262-275.

Martinsen, B.J., and Bronner-Fraser, M. (1998). Neural crest specification regulated by the helix-loop-helix repressor Id2. Science **281,** 988-991.

Martinsen, B.J., Frasier, A.J., Baker, C.V., and Lohr, J.L. (2004). Cardiac neural crest ablation alters Id2 gene expression in the developing heart. Dev Biol **272,** 176-190.

Matzuk, M.M., Kumar, T.R., and Bradley, A. (1995). Different phenotypes for mice deficient in either activins or activin receptor type II. Nature **374,** 356-360.

Meeson, A.P., Hawke, T.J., Graham, S., Jiang, N., Elterman, J., Hutcheson, K., Dimaio, J.M., Gallardo, T.D., and Garry, D.J. (2004). Cellular and molecular regulation of skeletal muscle side population cells. Stem Cells **22,** 1305-1320.

Melnikova, I.N., and Christy, B.A. (1996). Muscle cell differentiation is inhibited by the helix-loop-helix protein Id3. Cell Growth Differ **7,** 1067-1079.

Merkel, F.S. (1875). Tastzellen und Tastkörperchen bei den Haustieren und beim Menschen. Arch. Mikrosk. Anat. **11,** 636-652.

Millar, S.E. (2002). Molecular mechanisms regulating hair follicle development. J Invest Dermatol **118,** 216-225.

Mills, L.R., and Diamond, J. (1995). Merkel cells are not the mechanosensory transducers in the touch dome of the rat. J Neurocytol **24,** 117-134.

Miner, J.H. (2001). Mystery solved: discovery of a novel integrin ligand in the developing kidney. J Cell Biol **154,** 257-259.

Miyake, K., Mickley, L., Litman, T., Zhan, Z., Robey, R., Cristensen, B., Brangi, M., Greenberger, L., Dean, M., Fojo, T., and Bates, S.E. (1999). Molecular cloning of cDNAs which are highly overexpressed in mitoxantrone-resistant cells: demonstration of homology to ABC transport genes. Cancer Res **59,** 8-13.

Moll, I., Moll, R., and Franke, W.W. (1986). Formation of epidermal and dermal Merkel cells during human fetal skin development. J Invest Dermatol **87,** 779-787.

Morris, R.J., and Potten, C.S. (1999). Highly persistent label-retaining cells in the hair follicles of mice and their fate following induction of anagen. J Invest Dermatol **112,** 470-475.

Morris, R.J., Liu, Y., Marles, L., Yang, Z., Trempus, C., Li, S., Lin, J.S., Sawicki, J.A., and Cotsarelis, G. (2004). Capturing and profiling adult hair follicle stem cells. Nat Biotechnol **22,** 411-417.

Müller, M. (2001). 48 Human ATP-Binding Cassette Transporters. http://www.nutrigene.4t.com/humanabc.htm.

Muller-Rover, S., Handjiski, B., van der Veen, C., Eichmuller, S., Foitzik, K., McKay, I.A., Stenn, K.S., and Paus, R. (2001). A comprehensive guide for the accurate classification of murine hair follicles in distinct hair cycle stages. J Invest Dermatol **117,** 3-15.

Munger, B.L. (1965). The intraepidermal innervation of the snout skin of the opossum. A light and electron microscope study, with observations on the nature of Merkel's Tastzellen. J Cell Biol **26,** 79-97.

Munger, B.L., and Rice, F.L. (1986). Sequential maturation of cutaneous receptors in the rat mystacial pad. J. Comp. Neurol. **252,** 404-411.

Navarro, M., Valentinis, B., Belletti, B., Romano, G., Reiss, K., and Baserga, R. (2001). Regulation of Id2 gene expression by the type 1 IGF receptor and the insulin receptor substrate-1. Endocrinology **142,** 5149-5157.

Nishimura, E.K., Jordan, S.A., Oshima, H., Yoshida, H., Osawa, M., Moriyama, M., Jackson, I.J., Barrandon, Y., Miyachi, Y., and Nishikawa, S. (2002). Dominant role of the niche in melanocyte stem-cell fate determination. Nature **416,** 854-860.

Nogueira, M.M., Mitjavila-Garcia, M.T., Le Pesteur, F., Filippi, M.D., Vainchenker, W., Dubart Kupperschmitt, A., and Sainteny, F. (2000). Regulation of Id gene expression during embryonic stem cell-derived hematopoietic differentiation. Biochem Biophys Res Commun **276,** 803-812.

Noramly, S., Freeman, A., and Morgan, B.A. (1999). beta-catenin signaling can initiate feather bud development. Development **126,** 3509-3521.

Norton, J.D. (2000). ID helix-loop-helix proteins in cell growth, differentiation and tumorigenesis. J Cell Sci **113 (Pt 22),** 3897-3905.

Norton, J.D., and Atherton, G.T. (1998). Coupling of cell growth control and apoptosis functions of Id proteins. Mol Cell Biol **18,** 2371-2381.

Ogawa, H. (1996). The Merkel cell as a possible mechanoreceptor cell. Prog Neurobiol **49,** 317-334.

Ohtani, N., Zebedee, Z., Huot, T.J., Stinson, J.A., Sugimoto, M., Ohashi, Y., Sharrocks, A.D., Peters, G., and Hara, E. (2001). Opposing effects of Ets and Id proteins on p16INK4a expression during cellular senescence. Nature **409,** 1067-1070.

Oliver, R.F. (1966a). Regeneration of dermal papillae in rat vibrissae. J Invest Dermatol **47,** 496-497.

Oliver, R.F. (1966b). Histological studies of whisker regeneration in the hooded rat. J Embryol Exp Morphol **16,** 231-244.

Oliver, R.F. (1966c). Whisker growth after removal of the dermal papilla and lengths of follicle in the hooded rat. J Embryol Exp Morphol **15,** 331-347.

Oliver, R.F. (1969). The vibrissa dermal papilla and its influcnce on epidermal tissues. Br J Dermatol **81,** Suppl 3:55+.

Olivera-Martinez, I., Viallet, J.P., Michon, F., Pearton, D.J., and Dhouailly, D. (2004). The different steps of skin formation in vertebrates. Int J Dev Biol **48,** 107-115.

Orwin, D.F. (1979). The cytology and cytochemistry of the wool follicle. Int Rev Cytol **60,** 331-374.

Osada, A., Kiyozumi, D., Tsutsui, K., Ono, Y., Weber, C.N., Sugimoto, N., Imai, T., Okada, A., and Sekiguchi, K. (2005). Expression of MAEG, a novel basement membrane protein, in mouse hair follicle morphogenesis. Exp Cell Res **303,** 148-159.

O'Shaughnessy, R.F., Christiano, A.M., and Jahoda, C.A. (2004). The role of BMP signalling in the control of ID3 expression in the hair follicle. Exp Dermatol **13,** 621-629.

Pallavicini, M.G., Summers, L.J., Dean, P.N., and Gray, J.W. (1985). Enrichment of murine hemopoietic clonogenic cells by multivariate analyses and sorting. Exp Hematol **13,** 1173-1181.

Parakkal, P.F. (1969). Ultrastructural changes of the basal lamina during the hair growth cycle. J Cell Biol **40,** 561-564.

Parker, B.W., Kaur, G., Nieves-Neira, W., Taimi, M., Kohlhagen, G., Shimizu, T., Losiewicz, M.D., Pommier, Y., Sausville, E.A., and Senderowicz, A.M.

(1998). Early induction of apoptosis in hematopoietic cell lines after exposure to flavopiridol. Blood **91,** 458-465.

Pasche, F., Merot, Y., Carraux, P., and Saurat, J.H. (1990). Relationship between Merkel cells and nerve endings during embryogenesis in the mouse epidermis. J Invest Dermatol **95,** 247-251.

Paus, R., and Cotsarelis, G. (1999). The biology of hair follicles. N Engl J Med **341,** 491-497.

Paus, R., and Foitzik, K. (2004). In search of the "hair cycle clock": a guided tour. Differentiation **72,** 489-511.

Paus, R., Muller-Rover, S., and Botchkarev, V.A. (1999a). Chronobiology of the hair follicle: hunting the " hair cycle clock". J Investig Dermatol Symp Proc **4,** 338-345.

Paus, R., Muller-Rover, S., Van Der Veen, C., Maurer, M., Eichmuller, S., Ling, G., Hofmann, U., Foitzik, K., Mecklenburg, L., and Handjiski, B. (1999b). A comprehensive guide for the recognition and classification of distinct stages of hair follicle morphogenesis. J Invest Dermatol **113,** 523-532.

Peters, E.M., Tobin, D.J., Botchkareva, N., Maurer, M., and Paus, R. (2002). Migration of melanoblasts into the developing murine hair follicle is accompanied by transient c-Kit expression. J Histochem Cytochem **50,** 751-766.

Philpott, M.P., Sanders, D., Westgate, G.E., and Kealey, T. (1994). Human hair growth in vitro: a model for the study of hair follicle biology. J Dermatol Sci **7 Suppl,** S55-72.

Pinkus, H. (1958). Embryology of hair. The Biology of Hair Growth. New York, Academic Press, 18.

Pinkus, H. (1978). Epithelial-mesodermal interaction in normal hair growth, alopecia, and neoplasia. J Dermatol **5,** 93-101.

Ploemacher, R.E., and Brons, N.H. (1985). The relative spatial distribution of CFU-S in the mouse spleen. Exp Hematol **13,** 1068-1072.

Poulsen, M. (2004). Merkel-cell carcinoma of the skin. Lancet Oncol **5,** 593-599.

Prisco, M., Peruzzi, F., Belletti, B., and Baserga, R. (2001). Regulation of Id gene expression by type I insulin-like growth factor: roles of Stat3 and the tyrosine 950 residue of the receptor. Mol Cell Biol **21,** 5447-5458.

Rawles, M.E. (1947). Origin of pigment cells from the neural crest in the mouse embryo. Physiol. Zool. **20,** 248-266.

Reynaud-Deonauth, S., Zhang, H., Afouda, A., Taillefert, S., Beatus, P., Kloc, M., Etkin, L.D., Fischer-Lougheed, J., and Spohr, G. (2002). Notch signaling is involved in the regulation of Id3 gene transcription during Xenopus embryogenesis. Differentiation **69,** 198-208.

Reynolds, A.J., Lawrence, C., Cserhalmi-Friedman, P.B., Christiano, A.M., and Jahoda, C.A. (1999). Trans-gender induction of hair follicles. Nature **402,** 33-34.

Rice, F.L., Mance, A., and Munger, B.L. (1986). A comparative light microscopic analysis of the sensory innervation of the mystacial pad. I. Innervation of vibrissal follicle-sinus complexes. J Comp Neurol **252,** 154-174.

Roberts, V.J., and Barth, S.L. (1994). Expression of messenger ribonucleic acids encoding the inhibin/activin system during mid- and late-gestation rat embryogenesis. Endocrinology **134,** 914-923.

Rockman, S.P., Currie, S.A., Ciavarella, M., Vincan, E., Dow, C., Thomas, R.J., and Phillips, W.A. (2001). Id2 is a target of the beta-catenin/T cell factor pathway in colon carcinoma. J Biol Chem **276,** 45113-45119.

Ros, J.E., Libbrecht, L., Geuken, M., Jansen, P.L., and Roskams, T.A. (2003). High expression of MDR1, MRP1, and MRP3 in the hepatic progenitor cell compartment and hepatocytes in severe human liver disease. J Pathol **200,** 553-560.

Ruberte, E., Dolle, P., Krust, A., Zelent, A., Morriss-Kay, G., and Chambon, P. (1990). Specific spatial and temporal distribution of retinoic acid receptor gamma transcripts during mouse embryogenesis. Development **108,** 213-222.

Sablitzky, F., Moore, A., Bromley, M., Deed, R.W., Newton, J.S., and Norton, J.D. (1998). Stage- and subcellular-specific expression of Id proteins in male germ and Sertoli cells implicates distinctive regulatory roles for Id proteins during meiosis, spermatogenesis, and Sertoli cell function. Cell Growth Differ **9,** 1015-1024.

Samanta, J., and Kessler, J.A. (2004). Interactions between ID and OLIG proteins mediate the inhibitory effects of BMP4 on oligodendroglial differentiation. Development **131,** 4131-4142.

Sarkadi, B., Ozvegy-Laczka, C., Nemet, K., and Varadi, A. (2004). ABCG2 - a transporter for all seasons. FEBS Lett **567,** 116-120.

Scharenberg, C.W., Harkey, M.A., and Torok-Storb, B. (2002). The ABCG2 transporter is an efficient Hoechst 33342 efflux pump and is preferentially expressed by immature human hematopoietic progenitors. Blood **99,** 507-512.

Schmidt-Ullrich, R., and Paus, R. (2005). Molecular principles of hair follicle induction and morphogenesis. Bioessays **27,** 247-261.

Sengel, P. (1971). The organogenesis and arrangement of cutaneous appendages in birds. Adv Morphog **9,** 181-230.

Sengel, P. (1975). Feather pattern development. Ciba Found Symp **0,** 51-70.

Sengel, P. (1976). Morphogenesis of skin. Cambridge University Press, Cambridge and London.

Sieber-Blum, M., Grim, M., Hu, Y.F., and Szeder, V. (2004). Pluripotent neural crest stem cells in the adult hair follicle. Dev Dyn **231,** 258-269.

Silver, A.F., and Chase, H.B. (1970). DNA synthesis in the adult hair germ during dormancy (telogen) and activation (early anagen). Dev Biol **21,** 440-451.

Slack, J.M. (1991). The nature of the mesoderm-inducing signal in Xenopus: a transfilter induction study. Development **113,** 661-669.

Spangrude, G.J., and Johnson, G.R. (1990). Resting and activated subsets of mouse multipotent hematopoietic stem cells. Proc Natl Acad Sci U S A **87,** 7433-7437.

Sperling, L.C. (1991). Hair anatomy for the clinician. J Am Acad Dermatol **25,** 1-17.

Spits, H., Couwenberg, F., Bakker, A.Q., Weijer, K., and Uittenbogaart, C.H. (2000). Id2 and Id3 inhibit development of CD34(+) stem cells into predendritic cell (pre-DC)2 but not into pre-DC1. Evidence for a lymphoid origin of pre-DC2. J Exp Med **192,** 1775-1784.

Staricco, R.G. (1963). Amelanotic melanocytes in the outer sheath of the human hair follicle and their role in the repigmentation of regenerated epidermis. Ann N Y Acad Sci **100,** 239-255.

Stenn, K.S., and Paus, R. (1999). What controls hair follicle cycling? Exp Dermatol **8,** 229-233; discussion 233-226.

Stenn, K.S., and Paus, R. (2001). Controls of hair follicle cycling. Physiol Rev **81,** 449-494.

St-Jacques, B., Dassule, H.R., Karavanova, I., Botchkarev, V.A., Li, J., Danielian, P.S., McMahon, J.A., Lewis, P.M., Paus, R., and McMahon, A.P. (1998). Sonic hedgehog signaling is essential for hair development. Curr Biol **8,** 1058-1068.

Stohr, P. (1903). Textbook of Histology. P. Blakiston's Son and Co., Philadelphia, Pennsylvania.

Storms, R.W., Goodell, M.A., Fisher, A., Mulligan, R.C., and Smith, C. (2000). Hoechst dye efflux reveals a novel CD7(+)CD34(-) lymphoid progenitor in human umbilical cord blood. Blood **96,** 2125-2133.

Sugai, M., Gonda, H., Kusunoki, T., Katakai, T., Yokota, Y., and Shimizu, A. (2003). Essential role of Id2 in negative regulation of IgE class switching. Nat Immunol **4,** 25-30.

Szeder, V., Grim, M., Halata, Z., and Sieber-Blum, M. (2003). Neural crest origin of mammalian Merkel cells. Dev Biol **253,** 258-263.

Tachibana, T. (1995). The Merkel cell: recent findings and unresolved problems. Arch Histol Cytol **58,** 379-396.

Tachibana, T., and Nawa, T. (2002). Recent progress in studies on Merkel cell biology. Anat Sci Int **77,** 26-33.

Tachibana, T., Kamegai, T., Takahashi, N., and Nawa, T. (1998). Evidence for polymorphism of Merkel cells in the adult human oral mucosa. Arch Histol Cytol **61,** 115-124.

Tachibana, T., Yamamoto, H., Takahashi, N., Kamegai, T., Shibanai, S., Iseki, H., and Nawa, T. (1997). Polymorphism of Merkel cells in the rodent palatine mucosa: immunohistochemical and ultrastructural studies. Arch Histol Cytol **60,** 379-389.

Tanaka, Y., Yoshikawa, M., Kobayashi, Y., Kuroda, M., Kaito, M., Shiroi, A., Yamao, J., Fukui, H., Ishizaka, S., and Adachi, Y. (2003). Expressions of hepatobiliary organic anion transporters and bilirubin-conjugating enzyme in differentiating embryonic stem cells. Biochem Biophys Res Commun **309,** 324-330.

Taylor, G., Lehrer, M.S., Jensen, P.J., Sun, T.T., and Lavker, R.M. (2000). Involvement of follicular stem cells in forming not only the follicle but also the epidermis. Cell **102,** 451-461.

Toma, J.G., El-Bizri, H., Barnabe-Heider, F., Aloyz, R., and Miller, F.D. (2000). Evidence that helix-loop-helix proteins collaborate with retinoblastoma tumor suppressor protein to regulate cortical neurogenesis. J Neurosci **20,** 7648-7656.

Tumbar, T., Guasch, G., Greco, V., Blanpain, C., Lowry, W.E., Rendl, M., and Fuchs, E. (2004). Defining the epithelial stem cell niche in skin. Science **303,** 359-363.

Valcourt, U., Kowanetz, M., Niimi, H., Heldin, C.H., and Moustakas, A. (2005). TGF-{beta} and the Smad Signaling Pathway Support Transcriptomic Reprogramming during Epithelial-Mesenchymal Cell Transition. Mol Biol Cell.

van Tellingen, O., Buckle, T., Jonker, J.W., van der Valk, M.A., and Beijnen, J.H. (2003). P-glycoprotein and Mrp1 collectively protect the bone marrow from vincristine-induced toxicity in vivo. Br J Cancer **89,** 1776-1782.

Vanscott, E.J., Ekel, T.M., and Auerbach, R. (1963). Determinants of Rate and Kinetics of Cell Division in Scalp Hair. J Invest Dermatol **41,** 269-273.

Wagsater, D., Sirsjo, A., and Dimberg, J. (2003). Down-regulation of ID2 by all-trans retinoic acid in monocytic leukemia cells (THP-1). J Exp Clin Cancer Res **22,** 471-475.

Wang, S., Sdrulla, A., Johnson, J.E., Yokota, Y., and Barres, B.A. (2001). A role for the helix-loop-helix protein Id2 in the control of oligodendrocyte development. Neuron **29,** 603-614.

Watt, F.M., and Hogan, B.L. (2000). Out of Eden: stem cells and their niches. Science **287,** 1427-1430.

Weedon, D., Searle, J., and Kerr, J.F. (1979). Apoptosis. Its nature and implications for dermatopathology. Am J Dermatopathol **1,** 133-144.

Weihe, E., Hartschuh, W., and Nohr, D. (1991). Light microscopic immunoenzyme and electron microscopic immunogold cytochemistry reveal tachykinin immunoreactivity in Merkel cells of pig skin. Neurosci Lett **124,** 260-263.

Weinberg, R.A. (1995). The retinoblastoma protein and cell cycle control. Cell **81,** 323-330.

Welker, W.I., Johnson, J.I., Jr., and Pubols, B.H., Jr. (1964). Some Morphological and Physiological Characteristics of the Somatic Sensory System in Raccoons. Am Zool **136,** 75-94.

Whitear, M. (1989). Merkel cells in lower vertebrates. Arch Histol Cytol **52 Suppl,** 415-422.

Whitehouse, C.J., Huckle, J.W., Demarchez, M., Reynolds, A.J., and Jahoda, C.A. (2002). Genes that are differentially expressed in rat vibrissa follicle germinative epithelium in vivo show altered expression patterns after extended organ culture. Exp Dermatol **11,** 542-555.

Williams, D., and Stenn, K.S. (1994). Transection level dictates the pattern of hair follicle sheath growth in vitro. Dev Biol **165,** 469-479.

Wilson, C.L., Sun, T.T., and Lavker, R.M. (1994). Cells in the bulge of the mouse telogen follicle give rise to the lower anagen follicle. Skin Pharmacol **7,** 8-11.

Winkelmann, R.K., and Breathnach, A.S. (1973). The Merkel cell. J Invest Dermatol **60,** 2-15.

Xu, X., Lyle, S., Liu, Y., Solky, B., and Cotsarelis, G. (2003). Differential expression of cyclin D1 in the human hair follicle. Am J Pathol **163,** 969-978.

Yokota, Y. (2001). Id and development. Oncogene **20,** 8290-8298.

Yokota, Y., Mansouri, A., Mori, S., Sugawara, S., Adachi, S., Nishikawa, S., and Gruss, P. (1999). Development of peripheral lymphoid organs and natural killer cells depends on the helix-loop-helix inhibitor Id2. Nature **397,** 702-706.

Young, R.D., and Oliver, R.F. (1976). Morphological changes associated with the growth cycle of vibrissal follicles in the rat. J Embryol Exp Morphol **36,** 597-607.

Zebedee, Z., and Hara, E. (2001). Id proteins in cell cycle control and cellular senescence. Oncogene **20,** 8317-8325.

Zhou, S., Schuetz, J.D., Bunting, K.D., Colapietro, A.M., Sampath, J., Morris, J.J., Lagutina, I., Grosveld, G.C., Osawa, M., Nakauchi, H., and Sorrentino, B.P. (2001). The ABC transporter Bcrp1/ABCG2 is expressed in a wide variety of stem cells and is a molecular determinant of the side-population phenotype. Nat Med **7**, 1028-1034.